UNIVERSITY OF CALIFORNIA, SAN DIEGO

Characterization of the ER stress checkpoint in mammalian cells

A dissertation submitted in partial satisfaction of the

requirements for the degree of Doctor of Philosophy

in

Molecular Pathology

by

Meifan Chen

Committee in charge:

Professor Ze'ev Ronai, Chair
Professor Mark Kamps, Co-Chair
Professor Arshad Desai
Professor Daniel Donoghue
Professor Randolph Hampton
Professor Bruce Torbett

2011

The Dissertation of Meifan Chen is approved, and it is acceptable in quality and form for publication on microfilm and electronically:

_____

_____

_____

_____

_____

Co-Chair

_____

Chair

University of California, San Diego

2011

DEDICATION

To my mom and dad, for giving me the freedom and unconditional support to pursue my interests.

To Gary, for making me laugh and think.

TABLE OF CONTENTS

Signature Page iii

Dedication iv

Table of Contents v

List of Figures vii

Acknowledgements viii

Vita ix

Abstract of the Dissertation x

Chapter 1 : Introduction 1

The cell division cycle, an overview 2

Cell cycle control by cyclin-dependent kinases 2

Cell cycle control by the ubiquitin proteasome system 5

Cell cycle checkpoints 11

Endoplasmic reticulum stress 13

An emerging ER stress checkpoint 15

Figures 21

References 24

Chapter 2 : Ubiquitin-recognition protein Ufd1 couples the endoplasmic reticulum (ER) stress response to cell cycle control 31

Abstract 32

Introduction 33

Results 34

Discussion 41

Figures 43

Materials and Methods 67

Acknowledgements 76

References 76

Chapter 3 : APC/C^{Cdh1} regulates ER stress-dependent G1 delay 79

Abstract 80

Introduction 80

Results 82

Discussion 85

Figures 87

Materials and Methods 92

Acknowledgements 94

References 94

Chapter 4 : Conclusions and implications 97

References 100

LIST OF FIGURES

Figure 1-1: Cyclin-Cdk complexes and checkpoints regulating the cell cycle. 21

Figure 1-2: Activities and substrates of SCF^{Skp2} and APC/C in the cell cycle. 22

Figure 1-3: Pathways regulating the ER stress checkpoint in G1 in mammalian cells. 23

Figure 2-1: Prolonged ER stress downregulates Ufd1 and depletion of Ufd1 by RNAi affects cell cycle progression. 43

Figure 2-2: Ufd1 interferes with the ubiquitination of Skp2 in vivo. 45

Figure 2-3: Ufd1 interferes with the ubiquitination of Skp2 by recruiting the deubiquitinating enzyme USP13. 47

Figure 2-4: USP13 controls Skp2 levels via deubiquitination. 49

Figure 2-5: ER stress regulates the Ufd1-Cdh1-Skp2-p27 axis to delay progression through G1. 50

Figure 2-6: Validation of Ufd1-knockdown in HeLa cells by qRT-PCR and immunoblotting. 52

Figure 2-7: Ufd1 affects Skp2 protein levels and ubiquitination. 54

Figure 2-8: Ufd1 with internal deletion of amino acids 261-280 does not bind USP13 *in vivo*. 55

Figure 2-9: USP13 exhibits DUB acitivity towards K48-linked di-ubiquitins. 57

Figure 2-10: ER stress-dependent regulation of Ufd1-Skp2 and G1 cell cycle progression. 59

Figure 2-11: APC/C^{Cdh1} mediates ER stress-dependent Skp2 degradation and subsequent p27 stabilization. 61

Figure 2-12: Cyclin D1 overexpression does not overcome tunicamycin-induced G1 cell cycle delay in HeLa cells. 63

Figure 2-13: Enhanced clearance of NHK and CFTR in G1. 64

Figure 2-14: Increased G1 and hypersensitivity to tunicamycin in cells from cystic fibrosis-affected individual. 66

Figure 3-1: ER stress activates APC/C^{Cdh1} 87

Figure 3-2: Depletion of Cdh1 overcomes ER stress-induced G1 delay. 88

Figure 3-3: ER stress promotes binding of Cdh1 to the APC/C core. 90

Figure 3-4: ER stress downregulates the APC/C inhibitor Emi1. 91

ACKNOWLEDGEMENTS

This thesis would not have been possible without the help and advice of the past and current members of the Ronai lab. I would like to especially thank Gustavo Gutierrez for guiding me by the hand from day one, for teaching me all the scientific knowledge that I have today without reservation, and for his friendship. I would also like to thank my committee members Arshad Desai, Daniel Donoghue, Randy Hampton, Mark Kamps, and Bruce Torbett for their helpful suggestions and guidance to make this thesis stronger. Finally, I am grateful to my advisor Ze'ev Ronai, who never ceases to challenge me scientifically to help me grow as a researcher. I thank him for the invaluable opportunities to interact with the scientific communities at home and abroad, as well as for his encouragements when needed and words of advice on career development. His mentorship has made graduate training an intellectually stimulating, humbling, and rewarding experience.

Chapter 2, in full, has been accepted for publication of the material as it may appear in Proceedings of the National Academy of Sciences, 2011, Chen, Meifan; Gutierrez, Gustavo J.; Ronai, Ze'ev A. The dissertation author was the primary investigator and author of this work. Specifically, the dissertation author performed experiments and analyzed data.

Chapter 3, in part, is currently being prepared for submission for publication of the material. Chen, Meifan; Gutierrez, Gustavo J.; Ronai, Ze'ev A. The dissertation author was the primary investigator and author of this work. Specifically, the dissertation author performed experiments and analyzed data.

VITA

2005 Bachelor of Arts in Molecular and Cell Biology, University of California, Berkeley

2011 Doctor of Philosophy in Molecular Pathology, University of California, San Diego

PUBLICATIONS

Chen M, Gutierrez GJ, and Ronai ZA. Ubiquitin-recognition protein Ufd1 couples the endoplasmic reticulum (ER) stress response to cell cycle control. PNAS, 2011, in press.

Chen M, Smoke and miRrors: pseudogenes tricking miRNAs. Pigment Cell and Melanoma Research, 2010 Oct; 23(5): 583-4

Gutierrez GJ, Tsuji T, Chen M, Wei Jiang, and Ronai ZA. Interplay between Cdh1 and JNK activity during the cell cycle. Nature Cell Biology, 2010 Jul;12(7):686-95

Li S, Ezhevsky S, Dewing A, Cato MH, Scortegagna M, Bhoumik A, Breitwieser W, Braddock D, Eroshkin A, Qi J, Chen M, Kim JY, Jones S, Jones N, Rickert R, and Ronai ZA. Radiation sensitivity and tumor susceptibility in ATM phospho-mutant ATF2 mice. Genes & Cancer, April 2010, 1: 4: 316-330

Topisirovic I, Gutierrez GJ, Chen M, Appella E, Borden KL, and Ronai ZA. Control of p53 multimerization by Ubc13 is JNK-mediated. Proc Natl Acad Sci USA, 2009 Aug 4;106(31):12676-81

ABSTRACT OF THE DISSERTATION

Characterization of the ER stress checkpoint in mammalian cells

by

Meifan Chen

Doctor of Philosophy in Molecular Pathology

University of California, San Diego, 2011

Professor Ze'ev Ronai, Chair

Professor Mark Kamps, Co-Chair

Progression through the cell cycle adapts to both internal and environmental stimuli to ensure fidelity of cell division. Endoplasmic reticulum (ER) stress arising from an imbalance between cellular demand for protein folding and ER capacity has been described to cause G1 cell cycle arrest. The molecular components of this ER stress checkpoint have just begun to be uncovered. Although evidence emerge to suggest a prosurvival role for the ER stress-induced cell cycle arrest, the functional significance of this checkpoint in mammalian cells largely remains as an open question. Given the implication of ER stress in multiple human diseases like cancer and

neurological disorders, elucidation of the link between ER stress and cell cycle may provide new insights to the pathogenesis and treatment of these diseases.

In Chapter 1, I introduce the principles of cell cycle regulation and checkpoint responses, leading to a discussion on the discoveries that support an emerging ER stress checkpoint in eukaryotic cells. In Chapter 2, I investigate the mechanisms underlying cell cycle delay in G1 in response to ER stress in mammalian cells, showing that ER stress reduces the protein expression of Skp2 by downregulating Ufd1, a protein that stabilizes Skp2 through its ability to recruit the deubiquitinating enzyme USP13. This results in an accumulation of p27 that partly contributes to G1 arrest in ER-stressed cells. In Chapter 3, I identify another regulator of the ER stress checkpoint, APC/C^{Cdh1}, and begin to examine the upstream signals responsible for activating APC/C^{Cdh1} under ER stress conditions. In Chapter 4, I provide a summary of the work and discuss the implications of my findings.

Chapter 1 : Introduction

The cell division cycle, an overview

Cell cycle, the process by which a cell reproduces itself, is fundamentally important in the propagation, growth, and maintenance of all organisms. Regulated cell division is essential from development of the embryo to cell turnover in the adult, whereas uncontrolled cell proliferation contributes to human diseases like cancer.

The basic goal of cell division is to produce two daughter cells genetically identical to the parent. To achieve this, parental DNA has to be faithfully duplicated and equally partitioned between the progeny. These defining events of cell division constitute the S phase (synthesis phase), in which the DNA is replicated, and the M phase (mitosis phase), in which the DNA is segregated, culminating in the separation of the two daughter cells during cytokinesis. In between the S and M phases are two gap phases –G1 before S and G2 between S and M– that prepare the cell for the S and M phases respectively by allowing duplication of proteins and organelles as well as ensuring that conditions are favorable for reproduction (Figure 1-1).

Genetic and biochemical dissections of cell cycle regulatory components in *Saccharomyces cerevisiae*, *Saccharomyces pombe*, and *Xenopus laevis* have precipitated our current understanding that the cell cycle runs on an internal timer that drives sequence-specific events in an unidirectional and irreversible manner, such that DNA duplication occurs before DNA segregation and cytokinesis. Post-translational modifications of cell cycle regulators by phosphorylation and ubiquitination are chiefly responsible for orchestrating the timing and order of events.

Cell cycle control by cyclin-dependent kinases

The cell cycle is in part powered by the cyclin-dependent kinases (Cdks) (Figure 1-1). Owing to the cell cycle phase-specific expression of their activating protein partners –the cyclins, Cdks exhibit oscillating activity towards specific substrates to stimulate entry into and transitions between cell cycle phases. Structural study reveals that cyclin binding activates Cdks via rearrangement of the autoinhibitory T-loop of the kinase that blocks the active site[1]. While association with cyclins is a prerequisite for Cdk activation, the activity of the cyclin-Cdk complexes is tightly controlled through additional mechanisms, such as activator binding, inhibitor binding, and phosphorylation. Cdk complexes are also the ultimate targets of checkpoints, which will be described in the section "Cell cycle checkpoints."

G1/S Cdks

Early G1 is characterized by cell growth and Cdk inactivity. The key decision to commit to cell division is made in response to the availability of growth factors in late G1, at the restriction point in animal cells[2]. Acting as mitogen sensors are the D-type cyclins that initiate cell cycle entry. Mitogenic signaling induces the transcription of cyclin D1 through a cascade involving Ras and mitogen-activated protein kinase while inhibiting the turnover and nuclear export of cyclin D1 through a different cascade of Ras, phosphatidylinositol 3-kinase (PI3K), and Akt[3]. The accumulating cyclin D1 activates the G1-Cdks, Cdk4 and Cdk6, which in turn partially inactivate the retinoblastoma protein (Rb) by phosphorylation. Rb is an inhibitor of E2F – a transcriptional activator of S phase-promoting genes including the E-type cyclins[4]. Priming phosphorylation of Rb by cyclin D-Cdk4 leads to complete phosphorylation of Rb by cyclin E-Cdk2, dissociating Rb from E2F to allow transition into S phase.

In addition to the activation of both the G1- and S-Cdks, G1-S transition also requires removal of Cdk inhibitors. In particular, p27, a member of the Cip/Kip family of Cdk inhibitors, maintains the G1 phase by suppressing cyclinE/A-Cdk2 (S-Cdk). Structural data reveals that p27 inhibits S-Cdk through direct binding to both subunits that disrupts the structure of the Cdk catalytic site[5]. The increase in cyclin E-Cdk2 activity in response to mitogenic signaling

phosphorylates p27 to target it for SCF^{Skp2}-mediated ubiquitination and degradation (described in the section of "Cell cycle control by the ubiquitin proteasome system"), releasing the final brake on S-phase entry[6,7]. Passing the restriction point concludes the mitogen-dependent phase of the cell cycle and commits the cell to go through the cell cycle in the absence of stress signals[8]. Besides phosphorylating Rb, cyclin E-Cdk2 also promotes S phase entry by initiating DNA replication[9]. Once in S phase, cyclin E is degraded by SCF^{Fbxw7} to prevent re-replication. Cyclin A-Cdk2 then drives completion of S phase.

G2/M Cdks

Type A-cyclins persists from S phase to G2 to form complex with Cdk1. cyclin A-Cdk1 continues to inhibit re-replication in G2 through phosphorylation of substrates like the origin recognition complex 1 (Orc1)[10]. Subsequent mitotic entry requires the activity of cyclin B-Cdk1. Association of cyclin B to Cdk1, however, is not sufficient for activation. Full activation of the complex requires an activating phosphorylation of Cdk1 at threonine 161 by the Cdk-activating kinase (CAK), as well as removal of two inhibitory phosphorylations at threonine 14 and tyrosine 15 of Cdk1 by the members of the Cdc25 family of phosphatases. Interestingly in mammals, CAK itself is a Cdk complex: cyclin H-Cdk7, and can activate Cdk2 and Cdk4 as well[11]. The kinase Wee1 is responsible for phosphorylation at tyrosine 15, whereas a separate kinase is suggested to mediate phosphorylation of threonine 14[11]. There are about 300 Cdk1 substrates, ranging from components of the kinetochore and mitotic spindle to proteins regulating translation and cell polarity[12]. Exit from mitosis requires inactivation of Cdk1 complex through degradation of cyclin B, discussed in the section of "Anaphase-promoting complex/cyclosome".

Physiological and pathological importance of Cdk regulation

The exquisite control of Cdk activities by the aforementioned exemplary mechanisms underscores the key role of the Cdks in cell division as well as the importance of keeping cell

division in check. Indeed, the biological significance of Cdks extends from yeasts to mice and humans, as substantiated by genetic analysis in mice and identification of cell cycle aberrations impinging on Cdk activity in human cancers. Mouse genetics highlight the absolute requirement for certain cyclin-Cdks in development and survival of vertebrates while revealing functional redundancy among others. For example, individual deletion of mitotic Cdk1, cyclin B1, or cyclin A2 results in embryonic lethality, demonstrating their irreplaceable role in life. On the other hand, deletion of either of the G1-Cdks –Cdk4 or Cdk6– yielded viable mice; developmental defects and embryonic lethality arose only from their combined ablation. Similarly for the D- and E-type cyclins, multiple members need to be depleted for lethality to occur[13]. The physiological role of these proteins should not be underestimated due to functional redundancy in development, as individual members may be required for stress response.

In humans, as well as in mouse models, the importance of Cdks in cell division manifests in pathological conditions. Aberrant control of Cdks and their regulators is intimately linked to the development of cancer, generally viewed as a disease of deregulated cell proliferation. In human malignancies, the expression of cell cycle proteins that promote Cdk activities, such as Cdk1, D-type cyclins, E-type cyclins, and Cdc25 family of proteins, is often found to be upregulated; whereas the expression of proteins that inhibit Cdk activation like p27 is downregulated (Principles of Molecular Oncology). Given that Cdk activation is the common downstream target of deregulated cell cycle pathways correlated with tumorigenesis, blocking the Cdks seems to be a reasonable strategy for cancer therapy. However, the therapeutic value of direct Cdk inhibition is uncertain because such an approach likely would not be selective towards tumors, unless malignant cells preferentially rely on certain Cdks for survival and proliferation.

Cell cycle control by the ubiquitin proteasome system

While the Cdks present a major force powering the cell cycle, they alone cannot confer directionality and order. In addition to the Cdk machinery that initiates a cell cycle phase, irreversible transition into the next phase requires another machinery to terminate the activities that maintain the current phase. The ubiquitin proteasome system is in charge of this latter arm of negative regulation.

In the cell cycle, the most spectacular example of regulation by the ubiquitin proteasome system is the oscillating levels of cyclins that in turn control the waves of Cdk activities. Like the cyclins, many cell cycle proteins undergo proteasome-mediated destruction. Protein complexes responsible for targeting substrates to the proteasome are integral to the control of proper timing and sequence of cell cycle events.

Ubiquitin proteasome system

The ubiquitin proteasome system (UPS) regulates protein levels in a cell by targeted degradation. It involves tagging of protein substrates with the covalent attachment of multiple ubiquitins, low molecular weight proteins of about 8.5kDa, for degradation by the 26S proteasome. The conjugation of ubiquitin to a target requires the concerted action of three enzymes: a ubiquitin activating enzyme (E1) that uses ATP to form a thiol-ester bond with the carboxy-terminus of ubiquitin, a ubiquitin conjugating enzyme (E2) that accepts the ubiquitin from the E1, and a substrate-specific ubiquitin ligase (E3) that mediates the final transfer of ubiquitin to a lysine residue on the target[14]. Polyubiquitin chains can be formed through isopeptide linkages between a lysine on the ubiquitin and the carboxy terminus of the next ubiquitin to be added. Ubiquitin chains of K48 linkage on a substrate target it to proteasome-mediated degradation[15]. In the regulation of cell division, two ubiquitin ligase complexes belonging to the class of multisubunit Cullin-containing RING ligases (CRLs) are crucial: the Skp1-Cullin-F-box-protein (SCF) and the anaphase promoting complex or cyclosome (APC/C) (Figure 1-2), as detailed in the corresponding sections below.

Like phosphorylation, ubiquitination is dynamic and reversible. Balancing the action of the ubiquitin conjugating system are the deubiquitinating enzymes (DUBs) that edit ubiquitin chains, a common activity with multiple consequences. First, DUBs generate ubiquitin monomers either from unanchored polyubiquitin chains or ubiquitin precursors made as linear polyubiquitins or fused to ribosomal proteins. Second, DUBs antagonize the action of ubiquitin ligases on the substrate. Third, proteasome-bound DUBs remove ubiquitin chains from the substrate before its insertion into the proteasome catalytic chamber, which facilitates proteolysis and recycle ubiquitin molecules[16]. In human, the ubiquitin specific proteases (USPs) represent the largest family of DUBs. USPs are cysteine proteases, some of which harbor additional domains for protein-protein interaction. One example is USP5 that disassembles polyubiquitin chains containing a free carboxy terminus[17]. Binding of the C-terminal Arg-Gly-Gly motif of ubiquitin to the ZnF-UBP domain of USP5 was shown to activate USP5 *in vitro*. Not all ZnF-UBP domains bind ubiquitin, however; some USPs like USP33 and USP22 have mutations in their ZnF-UBP domains suggested to disable their association with ubiquitin[18]. Closely related to USP5 is USP13, a DUB with no previously known substrates and reported to be reactive towards ISG15, a ubiquitin-like modifier whose expression is induced by type I interferon[19]. USP13 also has a ZnF-UBP, but it contains a mutation at a residue predicted to affect ubiquitin binding[18]. In contrast to USP5 that is found throughout the cell, USP13 is localized mainly in the nucleus, suggesting different cellular functions between these two DUBs[19]. In our study, we show that USP13 can hydrolyze K48-linked di-ubiquitins and identify the F-box protein Skp2 as a putative *in vivo* substrate of USP13 (Chapter 2 of dissertation). It is estimated that humans have about 80-100 DUBs, most of which currently have unknown targets and biological roles.

Finally, the destination of K48-linked polyubiquitinated proteins is the 26S proteasome. It is a multisubunit protease consisting of a 20S catalytic core capped at both ends by the 19S regulatory particle. The 19S cap is further divided into the “base” and the “lid”. The lid contains polyubiquitin receptors that recruit polyubiquitinated substrates to the proteasome, as well as deubiquitinating enzymes that remove polyubiquitin chains to facilitate insertion of the substrates

into the proteasome[16]. The base of the 19S contains ATPase activity that helps to unfold and linearize the substrates and channel them into the proteolytic core. Four heptameric rings make up the 20S core: two outer rings of α-subunits that form a pore through which the unfolded polypeptides pass to reach the proteolytic chamber, contained by the two inner rings of β-subunits. In addition to degrading proteins in the cytoplasm and the nucleus, where the proteasomes are localized, proteasomes can also degrade misfolded proteins that are selectively exported from the ER to the cytoplasm (as we will discuss in the section of "ER-associated degradation").

Skp1-Cullin-F-box-protein complex

The SCF is a multisubunit E3 composed of a core platform containing Skp1-Cul1-Rbx1/Roc1 that interacts with the E2 through the RING finger of Rbx1, and a variable substrate recognition subunit containing the F-box that interacts with Skp1. A large group of F-box proteins recognize phospho-degrons in their targets.

Originally thought to primarily control the G1 and S phases, the SCFs are now shown to function throughout the cell cycle owing to the continuous discovery of F-box proteins and substrates. The archetypical SCF regulating the G1-S transition is the one bearing the F-box subunit Skp2. SCF^{Skp2} targets p27 phosphorylated on threonine 187 for degradation, thereby activating the Cdk2 complex to promote S phase entry[7,20]. Particular to SCF^{Skp2}-mediated ubiquitination of p27 is the requirement of the accessory protein Cks1 to promote the binding of phosphorylated p27 to Skp2[21]. Consistent with the negative effect of Skp2 on p27, the levels of these proteins exhibit inverse correlation in the cell cycle: whereas p27 expression is high in G1 and decreases in late G1, Skp2 expression is low in G1 and rises from the G1/S transition to G2[20]. Mouse genetics further confirmed p27 as the major in vivo bona fide substrate of SCF^{Skp2}, as shown by the accumulation of p27 in $Skp2^{-/-}$ mice[22] and the rescue of the $Skp2^{-/-}$ phenotype in $Skp2^{-/-}$ $p27^{-/-}$ double knockout mice[23].

Anaphase-promoting complex/cyclosome

Progression through mitosis and establishment of the subsequent G1 require activation of the E3 anaphase-promoting complex/cyclosome (APC/C). Also a CRL, the APC/C is much more intricate in composition – about a dozen subunits make up the core, including a cullin subunit Apc2 and a RING finger protein Apc11. Through sequential coupling to its two WD40 repeat-containing substrate receptors –Cdc20/Fzy and Cdh1/Fzr, the APC/C is activated in mitosis and G1 respectively. A conserved isoleucine-arginine (IR) tail at the C-terminus of both Cdc20 and Cdh1 mediates binding to the APC/C, specifically to the core proteins containing the tetratrico peptide repeat (TPR) motif[24]. While common recognition motifs of Cdc20 and Cdh1, the destruction box and/or KEN box, can be found on APC/C targets, the code of substrate recognition by the APC/C is a subject of evolving complexity. Accumulating data suggest that core components such as APC10 (yeast Doc1) also contribute to target specificity[25].

As the name implies, APC/C^{Cdc20} promotes anaphase by targeting securin for proteolysis that is required for the separation of sister chromatids[26]. APC/C^{Cdc20} also initiates degradation of mitotic cyclins to enable mitotic exit[27]. Cdc20 is essential to cell division and viability. The cdc20 mutant of budding yeast exhibits mitotic arrest because of failure to execute chromosome segregation[28]. Homozygous Cdc20-deficient mouse embryos die at the 2-cell stage because of permanent metaphase arrest that cannot be rescued by the loss of securin alone[29].

Because APC/C^{Cdc20} controls the critical event of DNA division, formation and activation of the complex are subjected to tight regulation. Rising activity of cyclin B-Cdk1 and polo-like kinase (Plk1) in mitosis promotes the association of Cdc20 to the APC/C core through phosphorylation of the core APC/C components[30]. The assembled complex however remains inactive as a result of inhibitor binding. At least three inhibitors suppress APC/C^{Cdc20} activity. In S and G2, the pseudosubstrate Emi1 antagonizes the activity of both forms of the APC/C by competitive binding[31]. In prometaphase, following degradation of Emi1, RASSF1A restrains APC/C^{Cdc20} independently of and before the spindle assembly checkpoint (SAC) that delays the onset of anaphase until the proper attachment of all sister chromatids to the mitotic spindle[32].

During activation of the SAC, the mitotic checkpoint complex composed of Mad2, Bub3, and BubR1 inhibits APC/C^{Cdc20} [33]. When spindle attachment is complete, APC/C^{Cdc20} becomes fully activated.

The decrease in Cdk1 activity as a result of APC/C^{Cdc20}–mediated proteolysis of cyclin B in turn leads to the assembly of APC/C^{Cdh1}. In contrast to the positive regulatory role of mitotic kinases in the formation of APC/C^{Cdc20}, phosphorylation of Cdh1 by Cdks and other kinases prevents formation of APC/C^{Cdh1} in part by nuclear export of Cdh1[34,35]. The phosphatase Cdc14 counteracts this mode of inhibition in late mitosis[34,36]. Targeting mitotic proteins including Cdc20 and cyclin B for destruction, APC/C^{Cdh1} drives completion of mitosis and establishes G1. One major target of APC/C^{Cdh1} in G1 is the F-box protein Skp2, as mentioned previously. By degrading Skp2, APC/C^{Cdh1} allows the accumulation of p27 that is involved in the maintenance of G1. APC/C^{Cdh1} activity persists throughout G1 although it also autoubiquitinates itself[37]. At the transition of G1-S, cyclin A2-Cdk2 and Emi1 then inactivate APC/C^{Cdh1} [38].

In yeast, Cdh1 is not required for viability[39]. In contrast, homozygous deletion of Cdh1 in mice results in embryonic lethality due to placental defects, which can be bypassed with conditional deletion of Cdh1 in the embryo but not in the placenta[40]. Mouse embryonic fibroblasts from homozygous knockouts are aneuploid, prone to senescence, and have aberrant progression through mitosis[40,41].

The findings that Cdh1 conditional knockout embryos are viable whereas Cdc20 deficiency is embryonically lethal suggest that Cdc20 can compensate for the loss of Cdh1 *in vivo*, but not vice versa. While this may be a result of the inability of Cdh1 to recognize Cdc20 substrates, an alternative explanation is the inability of Cdh1 to access Cdc20 substrates due to suppression of APC/C^{Cdh1} by cyclin B-Cdk1, whose activity sustains in the absence of Cdc20. Developmental-specific regulation of Cdc20 and Cdh1 may also prevent functional overlap of these proteins.

Inter-regulation between SCF and APC/C

The SCF and APC/C also regulate each other. APC/C^{Cdh1} targets Skp2 for degradation from the end of mitosis through G1[42], thereby allowing p27 to accumulate to establish and maintain G1. Evidence for SCF-mediated degradation of Cdh1 has also been provided to account for the downregulation of Cdh1 in S-phase[43]. Interestingly, the APC/C inhibitor Emi1 is an F-box protein originally identified as a Skp1-binding partner[44], although it exerts its inhibitory function as a pseudosubstrate independently of ligase activity or the other subunits of the SCF[31].

Cell cycle checkpoints

While cell cycle events are generally portrayed to proceed in sequence like falling dominoes, the system is more sophisticated than that. Cell cycle progression can adapt to intracellular conditions and extracellular stimuli. Checkpoints are points of surveillance that adjust cell cycle progression according to environmental cues and completion of cell cycle events. When conditions are not ready for continuation or damage is sensed, brakes are applied to delay progression until conditions become favorable or to provide time for repair. The major checkpoints in the cell cycle are situated in G1, where the decision to enter the cell cycle is made depending on environmental conditions; G2, where the fidelity and completion of DNA replication is checked before DNA division; and metaphase, where the attachment of the sister chromatids to the spindle is assessed before chromosome segregation (Figure 1-1). The lack of checkpoint mechanisms could lead to improper cell cycle entry as well as accumulation of damages and mutations that promote tumorigenesis. Here, we focus on the activation of G1 and G2 checkpoints in response to genotoxic stress as examples.

G1 Checkpoint

The G1 checkpoint, activated in response to cellular stress, integrates the stress sensing pathways and the restriction point to cause a G1 arrest. One of the most studied is G1 checkpoint activation by genotoxic agents that prevents replication of damaged DNA. Such a G1 arrest can be p53-dependent or independent[45,46]. Regardless of the dependency on p53, inhibition of G1-S Cdk (cyclin E-Cdk2) leading to the induction of growth suppressive Rb is critical. In the first case, ionizing ratiation (IR) activates the ATM-Chk2 pathway to stabilize p53[47]. p53 then induces the expression of the Cdk inhibitor p21 that selectively inhibits cyclin E-Cdk2 activity to block hyperphosphorylation of Rb, thereby leading to G1 arrest[48]. Because p53-dependent pathway relies on the transcriptional activation of p53 target genes, its response time is slow. Notably, it was observed that even before the expression of p53 target genes, cells can arrest in G1 when exposed to IR, pointing to p53-independent pathways that act in a more immediate manner[49]. One of these pathways, the trigger of which is not clear, acts through the degradation of cyclin D1 that leads to the release of p21 from Cdk4 to inhibit Cdk2 complexes[46]. Another pathway depends on the IR-induced degradation of Cdc25A that requires Chk1, which then reduces the activity of Cdk2 [50]. Although able to arrest cells more rapidly, these latter pathways act only transiently; the sustenance of the G1 arrest requires p53[46].

As the G1 checkpoint guards the gate to cell cycle entry, overriding this checkpoint results in unscheduled cell division that is frequently found in human malignancies. Components that reinforce the checkpoint like p53, Rb –originally identified through its inactivation in retinoblastoma, and p21 are commonly suppressed in cancers[51].

G2 Checkpoint

Activation of the G2 checkpoint arrests cell cycle in G2 by repression of cyclin B-Cdk1. Genotoxic stress-dependent G2 checkpoint inhibits the Cdk1 complex by preventing Cdc25 from removing the inhibitory phosphates from Cdk1. Checkpoint activation can be p53-independent or

dependent. In the former pathway, Chk1 phosphorylates Cdc25C on serine 216, creating a binding site for 14-3-3σ that sequesters the phosphatase in the cytoplasm[52]. In the latter pathway, p53 transcriptionally induces 14-3-3σ, which reinforces the inactivation of Cdc25C by cytoplasmic localization[52,53]. Although the G2 checkpoint can be initiated in the absence of p53, p53 and its target gene p21 are required to maintain G2 arrest in response to DNA damage through direct inhibition of cyclin B-Cdk1 by p21[54]. 14-3-3σ is also required to sustain G2 checkpoint activation that prevents mitotic cell death in the presence of genotoxic stress[55].

Overall, checkpoints confer adaptability of the cell cycle to internal and external stimuli. While not required for normal cell cycle progression, they are important quality control mechanisms that ensure the fidelity of cell division. Premature progression into the next cell cycle stage under unfavorable conditions or while bearing cellular damage due to checkpoint defects may compromise the survival of the organism. Understanding the mechanisms underlying the loss of checkpoint response to various stress signals frequently observed in human cancer and how these cells cope with stress in the absence of checkpoints may help to devise strategies to selectively target cancer cells.

Endoplasmic reticulum stress

The endoplasmic reticulum (ER) is the cellular organelle that produces transmembrane/secretory proteins and lipids. To ensure proper protein folding within the ER, the state of this organelle is closely monitored. Under conditions of ER stress that upset homeostasis in the ER, which may be caused by physiological fluctuations in protein synthesis or pathological accumulation of misfolded proteins, the cell activates a coordinated program called the unfolded protein response (UPR) to facilitate the restoration of ER homeostasis[56]. Three transmembrane proteins act as sensors to initiate the UPR: IRE1, ATF6, and the ER stress-activated PKR-like ER kinase (PERK). Under unperturbed conditions, these transmembrane proteins are kept inactive

through inhibitory binding of the chaperone BiP/GRP78 to the luminal domains. Upon ER stress, misfolded proteins sequester BiP/GRP78, activating these sensors. The major outcomes of the UPR are: 1) transcriptional induction of chaperones that enhance protein folding, mediated by ATF6 and XBP1 whose activation requires IRE-1; 2) global translational repression, mediated by PERK-dependent inactivation of the eukaryotic initiation factor 2α (eIF2α); and 3) cell death if ER stress cannot be resolved. In addition, the UPR also coordinates induction of genes essential for the removal of misfolded proteins by ER-associated degradation[57].

ER-associated degradation

During ER stress, ER-associated degradation (ERAD) complements the UPR to reduce the load of misfolded proteins in the ER; however, ERAD substrates also include wildtype proteins that cannot be easily folded or undergo regulated degradation[58]. ERAD is a multi-step process involving substrate recognition, substrate export from the ER to the cytosol, and finally degradation by 26S proteasomes. Substrate recognition is a critical but poorly understood step in ERAD. Detection of exposed hydrophobic patches on improperly folded proteins by chaperones may serve as a general mechanism of sensing ERAD substrate selection. For example, the luminal chaperone BiP/GRP78/Kar2 of the 70kD heat shock protein family is required for ERAD of soluble substrates[59], while a cytosolic Hsp70 mediates degradation of the integral membrane substrate cystic fibrosis transmembrane conductance regulator (CFTR)[60]. Substrate selection involving glycosylation status and enzymes catalyzing disulfide bond formation has also been proposed[61]. ERAD substrates are then targeted to cross the ER membrane through putative protein conducting channels suggested to contain the Sec61 complex or Derlin1[62]. As substrates emerge from the ER, they are polyubiquitinated on the cytosolic side by ER-associated E3 ligase. In yeast, the ubiquitin ligases Doa10 and Hrd1 ubiquitinate ERAD substrate with the E2 Ubc6, a ER membrane protein, and Ubc7, which is anchored to the ER membrane by its partner Cue1[63]. In mammals, E3s implicated in ERAD also includes GP78, RMA1/RNF5, CHIP, parkin, and SCF^{FBX2} [61]. While it was reported that the proteasome itself could localize to the ER on the

cytosolic side through association with the ER resident JNK-associated membrane protein (JAMP)[64] and directly pull the polyubiquitinated ERAD substrates out of the channel for degradation[65], a complex containing the AAA-ATPase Cdc48/p97 and its cofactors Ufd1-Npl4 also plays a role in the extraction and degradation of ERAD substrates[66]. It was suggested that p97 and Ufd1 recognize ubiquitin chains on ERAD substrates and carry out extraction in an ATP-dependent manner. Finally, degradation by the proteasome follows the release of polyubiquitinated proteins into the cytosol. Much remains to be learned about the components and regulation of each step in ERAD. It is unlikely that the degradation of all ERAD substates follow the general scheme above. For example, some luminal substrates have been reported to take a detour to the Golgi to become "ERAD-competent"[58]. In the presence of large protein aggregates that cannot be processed by the ERAD machinery, the cell utilizes the alternative strategy of autophagy to remove misfolded proteins[67].

An emerging ER stress checkpoint

ER stress activates the UPR that in turn reinforces ERAD. Slowly coming into focus is another biological outcome of ER stress: alteration in cell cycle progression. When it was first described, it was uncertain whether cell cycle arrest is merely a bystander effect of ER stress or whether it plays an active role in cellular adaptation to ER stress. Since the initial documentation of ER stress-dependent G1 checkpoint in mammalian cells about a decade ago[68], the molecular determinants and the biological significance of such an arrest are beginning to be elucidated, revealing a pro-survival function of cell cycle delay induced by ER stress. In addition to providing time to resolve stress as hypothesized, cell cycle arrest also provides an environment that is favorable for clearance of misfolded proteins (unpublished data from our lab, Chapter 2 of dissertation), as well as preventing the deleterious effects of cell division bearing stressed

organelles[69]. ER stress causes an arrest in G1 or G2 in mammalian cells, whereas it prevents cytokinesis in yeast.

Cyclin D1-dependent ER stress checkpoint response

In mammalian cells, pharmacological induction of ER stress –such as by tunicamycin that inhibits N-linked glycosylation or thapsigargin that disrupts ER calcium influx– and the physiological induction of ER stress by glucose deprivation impinge on the G1 checkpoint to delay cell cycle progression into S phase. ER stress engages the G1 checkpoint by inactivation of the G1- and G1/S-Cdks via multiple signaling pathways (Figure 1-3). PERK-mediated translational repression of cyclin D1, a G1-cyclin, represents one such pathway. This places cyclin D1 as a cell cycle receptor of the ER stress signal responsible for initiating the propagation of this signal to the downstream cell cycle effector proteins that execute G1 arrest. Specifically, activation of PERK under ER stress phosphorylates eIF2α on serine 51 to inhibit mRNA translation, including that of cyclin D1. The decrease in cyclin D1 expression mobilizes p21 and p27, whose protein levels were shown to be constant or decreased after induction of ER stress, from cyclin D-Cdk4 complexes for incorporation into cyclin E/A-Cdk2 complexes. This leads to the inactivation of both Cdk4 and Cdk2, resulting in Rb-mediated G1 arrest[68,70,71]. Of note, this ER stress-dependent G1 arrest is not a consequence of ER stress-induced improper maturation of mitogen receptors, as the mitogenic activation of ERK appeared intact.

A couple of clues point to additional mechanisms regulating cyclin D1 levels under such conditions. First, although expression of the dominant negative PERK mutant lacking the kinase domain could attenuate the decline of cyclin D1 upon ER stress, it is unable to overcome cyclin D1 downregulation[70]. Second, ER stress-induced cyclin D1 downregulation in PERK null fibroblasts occurs as in wildtype fibroblasts. It was then found that another eIF2α kinase, GCN2, can mediate the repression of cyclin D1 translation in the absence of PERK; however, its role in mediating translational inhibition in PERK-intact cells is suggested to be marginal[71]. Curiously, even in fibroblasts deficient in all three eIF2α kinases (PKR, PERK, and GCN2), tunicamycin can

still trigger translational repression, indicating the existence of other compensatory pathways regulating protein synthesis in ER stressed-cells yet to be identified. Ubiquitin proteasome-mediated degradation has also been reported to contribute to the downregulation of cyclin D1 under ER stress, through a pathway requiring PERK-mediated phosphorylation of eIF2α[72]. Notably, phosphorylated eIF2α becomes dispensable in the downregulation of cyclin D1 in extended ER stress induction, indicating that the maintenance of cyclin D1 downregulation involves other inputs. The immediate question in this case concerns the identity of the E3 ligase targeting cyclin D1 for degradation. Findings from the same study suggest that phosphorylation at threonine 286, previously shown to be the recognition site of SCF^{Fbx4}, is not required for the observed degradation[73]. While it is proposed that eIF2α directly promotes proteasome-dependent proteolysis of specific proteins in addition to regulating global translation, it is also possible that eIF2α regulates the translation of a protein that stabilizes cyclin D1.

p53-dependent ER stress checkpoint response

Cyclin D1 is not the only transducer of the ER stress signal to the cell cycle machinery; p53 is also employed as a messenger to signal cell cycle arrest. The dual role of p53 in regulating both G1 and G2 arrests in response to DNA damage also holds true under ER stress[74,75]. p53-mediated G1 arrest occurs through PERK-dependent stabilization of p53 that transcriptionally induces p21 to inhibit the Cdk2 complexes (Figure 1-3). PERK-mediated translational repression is thought to increase free ribosomal proteins that sequester Hdm2, an E3 of p53[76], thereby releasing its inhibition on p53. Inactivation of Hdm2 by translocation to the nucleolus upon ER stress was also observed; however, whether such nucleolar translocation of Hdm2 occurs independently of PERK and its association with ribosomal subunits remains to be tested. In addition, the relative contribution of p53 induction and cyclin D1 repression to G1 arrest upon ER stress has not been directly compared in cells with intact p53 function, although the depletion of

p53 or the overexpression of cyclin D1 individually appeared adequate to overcome ER stress-dependent G1 arrest[68,74].

Seemingly contradictory to the requirement of p53 in establishing G1 arrest mentioned above is a report suggesting ER stress-mediated p53 inhibition by degradation and cytoplasmic translocation[77]. This discrepancy may be attributed to a biphasic regulation of p53 that determines survival based on the duration of ER stress: p53 may be inactivated to promote survival upon short exposure to ER stress (as are the experimental conditions used in that study[77]), whereas p53 may be activated to arrest the cell cycle or even promote cell death[78] over an extended period of ER stress induction (as are the experimental conditions used in[74]).

Intriguingly, whereas the wildtype p53 is dedicated to activate the ER stress G1 checkpoint, an isoform of p53 called p53/47 controls the G2 checkpoint[75]. p53/47 contains an internal ribosome entry site-like sequence that allows cap-independent translation, enabling ER stress induction via PERK[75,79]. Structurally, p53/47 lacks the Hdm2 binding site and the first transactivation domain. It forms oligomers that are proposed to be biochemically distinct from the wildtype counterpart. Specific to p53/47 is its ability to dramatically upregulate the transcription of 14-3-3σ upon ER stress, which is critical in establishing the G2 arrest, presumably by preventing Cdc25C-mediated activation of Cdk1 under these conditions. p53/47-dependent G2 arrest is demonstrated to be dominant over p53-dependent G1 arrest, which raises the question of what conditions would allow ER stress to induce G1 arrest via wildtype p53, as shown in the previous studies. In line with this, it would be of interest to identify the determinants for G1 versus G2 arrest in cells with functional p53.

Cyclin D1- and p53-independent ER stress checkpoint response

Given the importance of p53 in the activation of the ER stress G1 checkpoint, it was curious to observe that ER stress is able to induce G1 arrest in HeLa cells, a cervical carcinoma cell line bearing p53 inactivated by the human papilloma virus (unpublished data, Chapter 2 of dissertation). In addition, while cyclin D1 expression is repressed in ER stressed-HeLa cells, it

does not contribute to G1 arrest in these cells. This suggests the existence of alternative cyclin D1- and p53-independent pathways that control the ER stress checkpoint in HeLa cells. We have identified one such pathway requiring the induction of p27, an inhibitor of the Cdk2 complexes, which occurs both transcriptionally and posttranslationally. While it is currently unclear how p27 is transcriptionally activated, we have elucidated the mechanism that stabilizes p27 protein levels in response to ER stress. We found that ER stress accelerates APC/C^{Cdh1}-mediated ubiquitination of Skp2, the F-box protein of SCF^{Skp2} that targets p27 for degradation, as a result of a decline in the nuclear expression of Ufd1–an adaptor that recruits the deubiquitinating enzyme USP13 specifically to Skp2 (unpublished data, Chapter 2 of dissertation) (Figure 1-3). While necessary for delaying G1 progression, this pathway only partially accounts for the ability of p53-deficient cells to activate the ER stress G1 checkpoint, which we found also depends on the hyperactivation of APC/C^{Cdh1} (unpublished data, Chapter 3 of dissertation) (Figure 1-3). Furthermore, supporting the hypothesis of ER stress-induced cell cycle arrest enabling restoration of homeostasis is our observation that clearance of misfolded proteins is more efficient in G1 phase of the cell cycle (unpublished data, Chapter 2 of dissertation). This suggests enhanced activity of the degradation machinery in G1, possibly due to cell cycle-dependent regulation of the machinery or the low metabolic demand of G1 that allows energy and resources to be devoted to regain ER homeostasis.

ER stress surveillance

In *Saccharomyces cerevisiae*, there is an ER stress checkpoint preceding cytokinesis. Induction of the UPR either by use of the mutant carrying the temperature-sensitive allele of ero1-1 encoding the ER oxidoreductin protein essential for oxidative protein folding[80] or tunicamycin in G1-synchronized cells delays cytokinesis. Defective cytokinesis results in a multibudded morphology containing polyploidy[69,81]. Intriguingly, not only do UPR-deficient cells exhibit cytokinetic defects in a normal division, cytokinetic mutants have heightened basal UPR, suggesting the requirement for higher ER functionality to complete cytokinesis[81].

Further investigation revealed that an UPR-independent ER stress surveillance system (ERSU) in yeast involving the Pkc1-Slt2 MAPK pathway is responsible for preventing cytokinesis through control of the septin ring and for retaining specifically the cortical ER in the mother[69]. Genetic abrogation of ERSU allows formation of a normal septin ring and transmission of the cortical ER to the daughter cell under ER stress; however, this leads to cell death, demonstrating the critical role of ERSU in preventing the inheritance of stressed ER that would otherwise compromise the survival of both mother and daughter cells.

Interestingly in budding yeast, heat shock, which generates misfolded or aggregated proteins, leads to G1 delay in temperature sensitive mutants of Cdc48/p97, Npl4, and Ufd1[82]. This observation parallels our finding in mammalian cells that ER stress induces G1 delay through downregulation of Ufd1 (Chapter 2 of dissertation). Cell cycle delay of the Cdc48, Npl4, and Ufd1 yeast mutants is independent of these proteins' function in ERAD and was proposed to be the result of cell wall defect.

Emanating from the simple observation that ER stress alters cell cycle progression is a complex and expanding network of signal sensors and effectors that coordinate the ER stress checkpoint, accompanied by a growing list of questions on how distinct checkpoint responses are orchestrated. Given that ER stress is implicated in a number of pathologies like neurodegenerative diseases[83], cancer[84], and viral infection[85], our current knowledge in the link between ER stress and the cell cycle raises the possibility that ER stress may contribute to pathogenesis through its effect on the cell cycle. This suggests that it may be possible to treat ER stress-related diseases by targeting the cell cycle machinery. In line with this idea, alterations in stress sensing and cell cycle response may allow cell survival and proliferation under constant ER stress in pathological conditions such as cancer. Understanding how these cells overcome checkpoint-induced growth arrest would provide therapeutic interventions that promote cell survival in neurodegenerative diseases and repress cell proliferation in cancer.

Figures

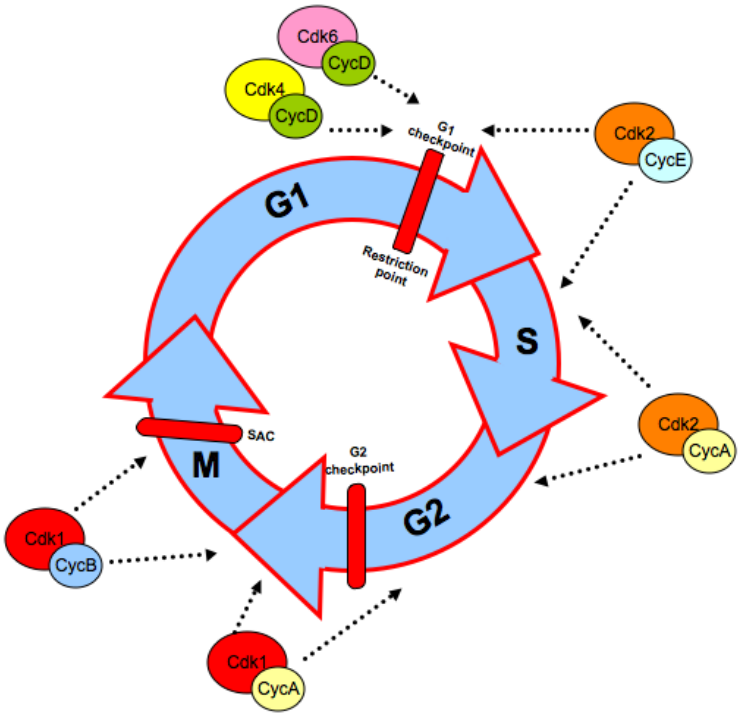

Figure 1-1: Cyclin-Cdk complexes and checkpoints regulating the cell cycle.

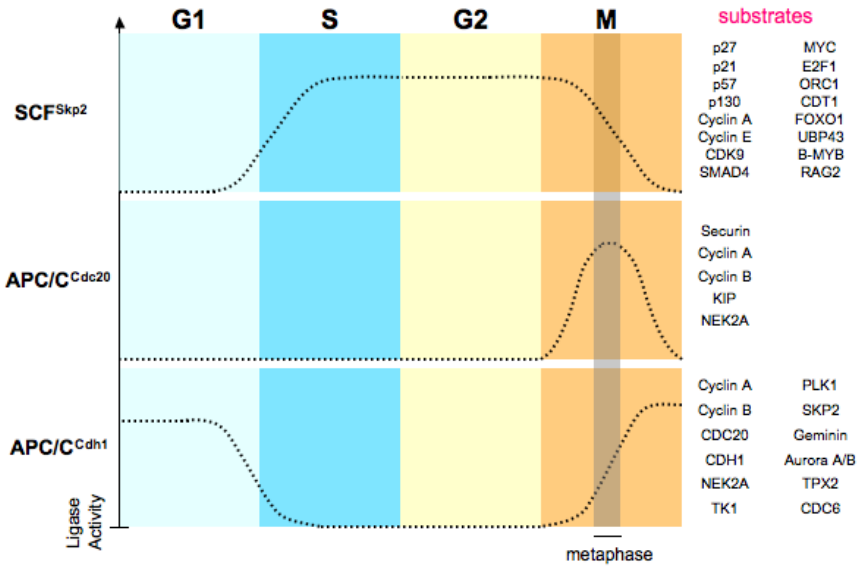

Figure 1-2: Activities and substrates of SCF^{Skp2} and APC/C in the cell cycle.

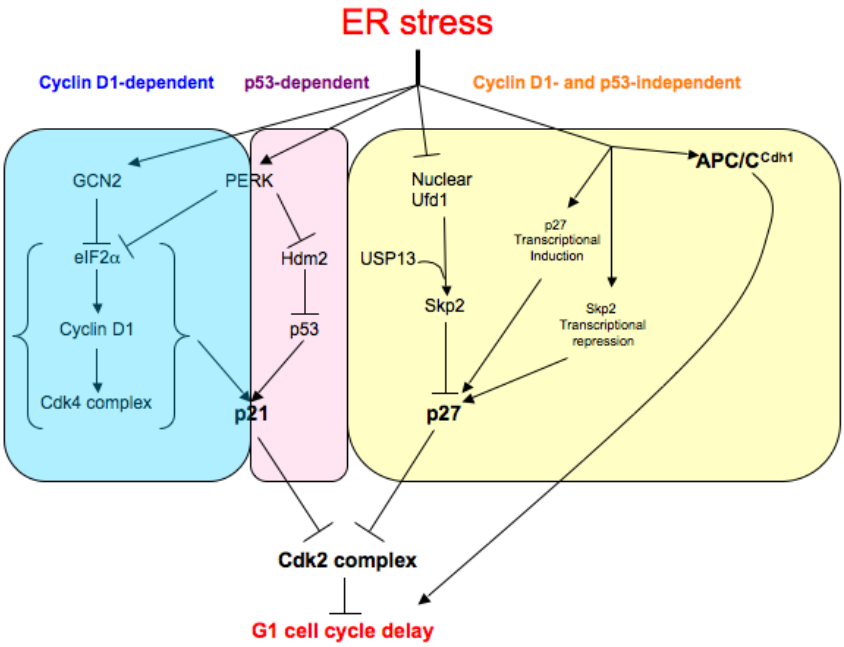

Figure 1-3: Pathways regulating the ER stress checkpoint in G1 in mammalian cells.

References

[1] De Bondt, H. L. et al., Crystal structure of cyclin-dependent kinase 2. *Nature* **363** (6430), 595 (1993).

[2] Pardee, A. B., A restriction point for control of normal animal cell proliferation. *Proc Natl Acad Sci U S A* **71** (4), 1286 (1974).

[3] Sherr, C. J., Mammalian G1 cyclins. *Cell* **73** (6), 1059 (1993).

[4] Ezhevsky, S. A. et al., Hypo-phosphorylation of the retinoblastoma protein (pRb) by cyclin D:Cdk4/6 complexes results in active pRb. *Proc Natl Acad Sci U S A* **94** (20), 10699 (1997); Lundberg, A. S. and Weinberg, R. A., Functional inactivation of the retinoblastoma protein requires sequential modification by at least two distinct cyclin-cdk complexes. *Mol Cell Biol* **18** (2), 753 (1998); Chellappan, S. P. et al., The E2F transcription factor is a cellular target for the RB protein. *Cell* **65** (6), 1053 (1991); Harbour, J. W. and Dean, D. C., The Rb/E2F pathway: expanding roles and emerging paradigms. *Genes Dev* **14** (19), 2393 (2000).

[5] Russo, A. A. et al., Crystal structure of the p27Kip1 cyclin-dependent-kinase inhibitor bound to the cyclin A-Cdk2 complex. *Nature* **382** (6589), 325 (1996).

[6] Sheaff, R. J. et al., Cyclin E-CDK2 is a regulator of p27Kip1. *Genes Dev* **11** (11), 1464 (1997).

[7] Sutterluty, H. et al., p45SKP2 promotes p27Kip1 degradation and induces S phase in quiescent cells. *Nat Cell Biol* **1** (4), 207 (1999).

[8] Planas-Silva, M. D. and Weinberg, R. A., The restriction point and control of cell proliferation. *Curr Opin Cell Biol* **9** (6), 768 (1997).

[9] Woo, R. A. and Poon, R. Y., Cyclin-dependent kinases and S phase control in mammalian cells. *Cell Cycle* **2** (4), 316 (2003).

[10] Li, C. J., Vassilev, A., and DePamphilis, M. L., Role for Cdk1 (Cdc2)/cyclin A in preventing the mammalian origin recognition complex's largest subunit (Orc1) from binding to chromatin during mitosis. *Mol Cell Biol* **24** (13), 5875 (2004).

[11] Morgan, D. O., Principles of CDK regulation. *Nature* **374** (6518), 131 (1995).

[12] Ubersax, J. A. et al., Targets of the cyclin-dependent kinase Cdk1. *Nature* **425** (6960), 859 (2003); Holt, L. J. et al., Global analysis of Cdk1 substrate phosphorylation sites provides insights into evolution. *Science* **325** (5948), 1682 (2009).

[13] Malumbres, M. and Barbacid, M., Cell cycle, CDKs and cancer: a changing paradigm. *Nat Rev Cancer* **9** (3), 153 (2009).

[14] Pickart, C. M., Mechanisms underlying ubiquitination. *Annu Rev Biochem* **70**, 503 (2001).

[15] Chau, V. et al., A multiubiquitin chain is confined to specific lysine in a targeted short-lived protein. *Science* **243** (4898), 1576 (1989).

[16] Reyes-Turcu, F. E., Ventii, K. H., and Wilkinson, K. D., Regulation and cellular roles of ubiquitin-specific deubiquitinating enzymes. *Annu Rev Biochem* **78**, 363 (2009).

[17] Reyes-Turcu, F. E. et al., The ubiquitin binding domain ZnF UBP recognizes the C-terminal diglycine motif of unanchored ubiquitin. *Cell* **124** (6), 1197 (2006).

[18] Bonnet, J., Romier, C., Tora, L., and Devys, D., Zinc-finger UBPs: regulators of deubiquitylation. *Trends Biochem Sci* **33** (8), 369 (2008).

[19] Catic, A. et al., Screen for ISG15-crossreactive deubiquitinases. *PLoS One* **2** (7), e679 (2007).

[20] Carrano, A. C., Eytan, E., Hershko, A., and Pagano, M., SKP2 is required for ubiquitin-mediated degradation of the CDK inhibitor p27. *Nat Cell Biol* **1** (4), 193 (1999).

[21] Ganoth, D. et al., The cell-cycle regulatory protein Cks1 is required for SCF(Skp2)-mediated ubiquitinylation of p27. *Nat Cell Biol* **3** (3), 321 (2001).

[22] Nakayama, K. et al., Targeted disruption of Skp2 results in accumulation of cyclin E and p27(Kip1), polyploidy and centrosome overduplication. *EMBO J* **19** (9), 2069 (2000).

[23] Nakayama, K. et al., Skp2-mediated degradation of p27 regulates progression into mitosis. *Dev Cell* **6** (5), 661 (2004).

[24] Vodermaier, H. C. et al., TPR subunits of the anaphase-promoting complex mediate binding to the activator protein CDH1. *Curr Biol* **13** (17), 1459 (2003).

[25] Wang, Q., Carroll, J. S., and Brown, M., Spatial and temporal recruitment of androgen receptor and its coactivators involves chromosomal looping and polymerase tracking. *Mol Cell* **19** (5), 631 (2005); Passmore, L. A. and Barford, D., Coactivator functions in a stoichiometric complex with anaphase-promoting complex/cyclosome to mediate substrate recognition. *EMBO Rep* **6** (9), 873 (2005); Yamano, H., Gannon, J., Mahbubani, H., and Hunt, T., Cell cycle-regulated recognition of the destruction box of cyclin B by the APC/C in Xenopus egg extracts. *Mol Cell* **13** (1), 137 (2004); Carroll, C. W. and Morgan, D. O., The Doc1 subunit is a processivity factor for the anaphase-promoting complex. *Nat Cell Biol* **4** (11), 880 (2002).

[26] Funabiki, H. et al., Cut2 proteolysis required for sister-chromatid seperation in fission yeast. *Nature* **381** (6581), 438 (1996); Cohen-Fix, O., Peters, J. M., Kirschner, M. W., and Koshland, D., Anaphase initiation in Saccharomyces cerevisiae is controlled by the APC-dependent degradation of the anaphase inhibitor Pds1p. *Genes Dev* **10** (24), 3081 (1996).

[27] Pines, J., Mitosis: a matter of getting rid of the right protein at the right time. *Trends Cell Biol* **16** (1), 55 (2006).

[28] Hartwell, L. H., Mortimer, R. K., Culotti, J., and Culotti, M., Genetic Control of the Cell Division Cycle in Yeast: V. Genetic Analysis of cdc Mutants. *Genetics* **74** (2), 267 (1973).

[29] Li, M., York, J. P., and Zhang, P., Loss of Cdc20 causes a securin-dependent metaphase arrest in two-cell mouse embryos. *Mol Cell Biol* **27** (9), 3481 (2007).

[30] Rudner, A. D. and Murray, A. W., Phosphorylation by Cdc28 activates the Cdc20-dependent activity of the anaphase-promoting complex. *J Cell Biol* **149** (7), 1377 (2000); Kramer, E. R. et al., Mitotic regulation of the APC activator proteins CDC20 and CDH1. *Mol Biol Cell* **11** (5), 1555 (2000).

[31] Reimann, J. D. et al., Emi1 is a mitotic regulator that interacts with Cdc20 and inhibits the anaphase promoting complex. *Cell* **105** (5), 645 (2001); Miller, J. J. et al., Emi1 stably binds and inhibits the anaphase-promoting complex/cyclosome as a pseudosubstrate inhibitor. *Genes Dev* **20** (17), 2410 (2006).

[32] Song, M. S. et al., The tumour suppressor RASSF1A regulates mitosis by inhibiting the APC-Cdc20 complex. *Nat Cell Biol* **6** (2), 129 (2004).

[33] Musacchio, A. and Salmon, E. D., The spindle-assembly checkpoint in space and time. *Nat Rev Mol Cell Biol* **8** (5), 379 (2007).

[34] Jaspersen, S. L., Charles, J. F., and Morgan, D. O., Inhibitory phosphorylation of the APC regulator Hct1 is controlled by the kinase Cdc28 and the phosphatase Cdc14. *Curr Biol* **9** (5), 227 (1999).

[35] Zhou, Y., Ching, Y. P., Chun, A. C., and Jin, D. Y., Nuclear localization of the cell cycle regulator CDH1 and its regulation by phosphorylation. *J Biol Chem* **278** (14), 12530 (2003); Crasta, K. et al., Inactivation of Cdh1 by synergistic action of Cdk1 and polo kinase is necessary for proper assembly of the mitotic spindle. *Nat Cell Biol* **10** (6), 665 (2008); Gutierrez, G. J. et al., Interplay between Cdh1 and JNK activity during the cell cycle. *Nat Cell Biol* **12** (7), 686.

[36] Visintin, R. et al., The phosphatase Cdc14 triggers mitotic exit by reversal of Cdk-dependent phosphorylation. *Mol Cell* **2** (6), 709 (1998).

[37] Listovsky, T. et al., Mammalian Cdh1/Fzr mediates its own degradation. *EMBO J* **23** (7), 1619 (2004).

[38] Hsu, J. Y. et al., E2F-dependent accumulation of hEmi1 regulates S phase entry by inhibiting APC(Cdh1). *Nat Cell Biol* **4** (5), 358 (2002); Lukas, C. et al., Accumulation of cyclin B1 requires E2F and cyclin-A-dependent rearrangement of the anaphase-promoting complex. *Nature* **401** (6755), 815 (1999).

[39] Schwab, M., Lutum, A. S., and Seufert, W., Yeast Hct1 is a regulator of Clb2 cyclin proteolysis. *Cell* **90** (4), 683 (1997); Visintin, R., Prinz, S., and Amon, A., CDC20 and CDH1: a family of substrate-specific activators of APC-dependent proteolysis. *Science* **278** (5337), 460 (1997); Kitamura, K., Maekawa, H., and Shimoda, C., Fission yeast Ste9, a homolog of Hct1/Cdh1 and Fizzy-related, is a novel negative regulator of cell cycle progression during G1-phase. *Mol Biol Cell* **9** (5), 1065 (1998).

[40] Garcia-Higuera, I. et al., Genomic stability and tumour suppression by the APC/C cofactor Cdh1. *Nat Cell Biol* **10** (7), 802 (2008).

[41] Li, M. et al., The adaptor protein of the anaphase promoting complex Cdh1 is essential in maintaining replicative lifespan and in learning and memory. *Nat Cell Biol* **10** (9), 1083 (2008).

[42] Bashir, T. et al., Control of the SCF(Skp2-Cks1) ubiquitin ligase by the APC/C(Cdh1) ubiquitin ligase. *Nature* **428** (6979), 190 (2004).

[43] Benmaamar, R. and Pagano, M., Involvement of the SCF complex in the control of Cdh1 degradation in S-phase. *Cell Cycle* **4** (9), 1230 (2005).

[44] Regan-Reimann, J. D., Duong, Q. V., and Jackson, P. K., Identification of novel F-box proteins in Xenopus laevis. *Curr Biol* **9** (20), R762 (1999).

[45] Kastan, M. B. et al., A mammalian cell cycle checkpoint pathway utilizing p53 and GADD45 is defective in ataxia-telangiectasia. *Cell* **71** (4), 587 (1992).

[46] Agami, R. and Bernards, R., Distinct initiation and maintenance mechanisms cooperate to induce G1 cell cycle arrest in response to DNA damage. *Cell* **102** (1), 55 (2000).

[47] Shieh, S. Y., Ikeda, M., Taya, Y., and Prives, C., DNA damage-induced phosphorylation of p53 alleviates inhibition by MDM2. *Cell* **91** (3), 325 (1997); Shieh, S. Y. et al., The human homologs of checkpoint kinases Chk1 and Cds1 (Chk2) phosphorylate p53 at multiple DNA damage-inducible sites. *Genes Dev* **14** (3), 289 (2000).

[48] Gu, Y., Turck, C. W., and Morgan, D. O., Inhibition of CDK2 activity in vivo by an associated 20K regulatory subunit. *Nature* **366** (6456), 707 (1993); Harper, J. W. et al., The p21 Cdk-interacting protein Cip1 is a potent inhibitor of G1 cyclin-dependent kinases. *Cell* **75** (4), 805 (1993); Poon, R. Y., Jiang, W., Toyoshima, H., and Hunter, T., Cyclin-dependent kinases are inactivated by a combination of p21 and Thr-14/Tyr-15 phosphorylation after UV-induced DNA damage. *J Biol Chem* **271** (22), 13283 (1996); Brugarolas, J. et al., Inhibition of cyclin-dependent kinase 2 by p21 is necessary for retinoblastoma protein-mediated G1 arrest after gamma-irradiation. *Proc Natl Acad Sci U S A* **96** (3), 1002 (1999).

[49] Lee, H., Larner, J. M., and Hamlin, J. L., A p53-independent damage-sensing mechanism that functions as a checkpoint at the G1/S transition in Chinese hamster ovary cells. *Proc Natl Acad Sci U S A* **94** (2), 526 (1997).

[50] Mailand, N. et al., Rapid destruction of human Cdc25A in response to DNA damage. *Science* **288** (5470), 1425 (2000).

[51] Weinberg, R. A., The retinoblastoma gene and gene product. *Cancer Surv* **12**, 43 (1992); Abukhdeir, A. M. and Park, B. H., P21 and p27: roles in carcinogenesis and drug resistance. *Expert Rev Mol Med* **10**, e19 (2008); Kuerbitz, S. J., Plunkett, B. S., Walsh, W. V., and Kastan, M. B., Wild-type p53 is a cell cycle checkpoint determinant following irradiation. *Proc Natl Acad Sci U S A* **89** (16), 7491 (1992); Hahn, W. C. and Weinberg, R. A., Rules for making human tumor cells. *N Engl J Med* **347** (20), 1593 (2002).

[52] Peng, C. Y. et al., Mitotic and G2 checkpoint control: regulation of 14-3-3 protein binding by phosphorylation of Cdc25C on serine-216. *Science* **277** (5331), 1501 (1997).

[53] Hermeking, H. et al., 14-3-3 sigma is a p53-regulated inhibitor of G2/M progression. *Mol Cell* **1** (1), 3 (1997).

[54] Bunz, F. et al., Requirement for p53 and p21 to sustain G2 arrest after DNA damage. *Science* **282** (5393), 1497 (1998).

[55] Chan, T. A. et al., 14-3-3Sigma is required to prevent mitotic catastrophe after DNA damage. *Nature* **401** (6753), 616 (1999).

[56] Ron, D. and Walter, P., Signal integration in the endoplasmic reticulum unfolded protein response. *Nat Rev Mol Cell Biol* **8** (7), 519 (2007).

[57] Travers, K. J. et al., Functional and genomic analyses reveal an essential coordination between the unfolded protein response and ER-associated degradation. *Cell* **101** (3), 249 (2000).

[58] Hampton, R. Y., ER-associated degradation in protein quality control and cellular regulation. *Curr Opin Cell Biol* **14** (4), 476 (2002).

[59] Chen, Y., Le Caherec, F., and Chuck, S. L., Calnexin and other factors that alter translocation affect the rapid binding of ubiquitin to apoB in the Sec61 complex. *J Biol Chem* **273** (19), 11887 (1998); Brodsky, J. L. et al., The requirement for molecular chaperones during endoplasmic reticulum-associated protein degradation demonstrates that protein export and import are mechanistically distinct. *J Biol Chem* **274** (6), 3453 (1999); Knittler, M. R., Dirks, S., and Haas, I. G., Molecular chaperones involved in protein degradation in the endoplasmic reticulum: quantitative interaction of the heat shock cognate protein BiP with partially folded immunoglobulin light chains that are degraded in the endoplasmic reticulum. *Proc Natl Acad Sci U S A* **92** (5), 1764 (1995).

[60] Zhang, Y. et al., Hsp70 molecular chaperone facilitates endoplasmic reticulum-associated protein degradation of cystic fibrosis transmembrane conductance regulator in yeast. *Mol Biol Cell* **12** (5), 1303 (2001).

[61] Vembar, S. S. and Brodsky, J. L., One step at a time: endoplasmic reticulum-associated degradation. *Nat Rev Mol Cell Biol* **9** (12), 944 (2008).

[62] Wiertz, E. J. et al., Sec61-mediated transfer of a membrane protein from the endoplasmic reticulum to the proteasome for destruction. *Nature* **384** (6608), 432 (1996); Lilley, B. N. and Ploegh, H. L., A membrane protein required for dislocation of misfolded proteins from the ER. *Nature* **429** (6994), 834 (2004).

[63] Bays, N. W. et al., Hrd1p/Der3p is a membrane-anchored ubiquitin ligase required for ER-associated degradation. *Nat Cell Biol* **3** (1), 24 (2001); Ravid, T., Kreft, S. G., and Hochstrasser, M., Membrane and soluble substrates of the Doa10 ubiquitin ligase are degraded by distinct pathways. *EMBO J* **25** (3), 533 (2006).

[64] Tcherpakov, M. et al., JAMP optimizes ERAD to protect cells from unfolded proteins. *Mol Biol Cell* **19** (11), 5019 (2008).

[65] Mayer, T. U., Braun, T., and Jentsch, S., Role of the proteasome in membrane extraction of a short-lived ER-transmembrane protein. *EMBO J* **17** (12), 3251 (1998); Lee, R. J. et al., Uncoupling retro-translocation and degradation in the ER-associated degradation of a soluble protein. *EMBO J* **23** (11), 2206 (2004).

[66] Ye, Y., Meyer, H. H., and Rapoport, T. A., The AAA ATPase Cdc48/p97 and its partners transport proteins from the ER into the cytosol. *Nature* **414** (6864), 652 (2001); Jarosch, E. et al., Protein dislocation from the ER requires polyubiquitination and the AAA-ATPase Cdc48. *Nat Cell Biol* **4** (2), 134 (2002); Bays, N. W. et al., HRD4/NPL4 is required for the proteasomal processing of ubiquitinated ER proteins. *Mol Biol Cell* **12** (12), 4114 (2001).

[67] Yorimitsu, T., Nair, U., Yang, Z., and Klionsky, D. J., Endoplasmic reticulum stress triggers autophagy. *J Biol Chem* **281** (40), 30299 (2006).

[68] Brewer, J. W., Hendershot, L. M., Sherr, C. J., and Diehl, J. A., Mammalian unfolded protein response inhibits cyclin D1 translation and cell-cycle progression. *Proc Natl Acad Sci U S A* **96** (15), 8505 (1999).

[69] Babour, A., Bicknell, A. A., Tourtellotte, J., and Niwa, M., A surveillance pathway monitors the fitness of the endoplasmic reticulum to control its inheritance. *Cell* **142** (2), 256.

[70] Brewer, J. W. and Diehl, J. A., PERK mediates cell-cycle exit during the mammalian unfolded protein response. *Proc Natl Acad Sci U S A* **97** (23), 12625 (2000).

[71] Hamanaka, R. B., Bennett, B. S., Cullinan, S. B., and Diehl, J. A., PERK and GCN2 contribute to eIF2alpha phosphorylation and cell cycle arrest after activation of the unfolded protein response pathway. *Mol Biol Cell* **16** (12), 5493 (2005).

[72] Raven, J. F. et al., PKR and PKR-like endoplasmic reticulum kinase induce the proteasome-dependent degradation of cyclin D1 via a mechanism requiring eukaryotic initiation factor 2alpha phosphorylation. *J Biol Chem* **283** (6), 3097 (2008).

[73] Lin, D. I. et al., Phosphorylation-dependent ubiquitination of cyclin D1 by the SCF(FBX4-alphaB crystallin) complex. *Mol Cell* **24** (3), 355 (2006).

[74] Zhang, F. et al., Ribosomal stress couples the unfolded protein response to p53-dependent cell cycle arrest. *J Biol Chem* **281** (40), 30036 (2006).

[75] Bourougaa, K. et al., Endoplasmic reticulum stress induces G2 cell-cycle arrest via mRNA translation of the p53 isoform p53/47. *Mol Cell* **38** (1), 78.

[76] Haupt, Y., Maya, R., Kazaz, A., and Oren, M., Mdm2 promotes the rapid degradation of p53. *Nature* **387** (6630), 296 (1997).

[77] Qu, L. et al., Endoplasmic reticulum stress induces p53 cytoplasmic localization and prevents p53-dependent apoptosis by a pathway involving glycogen synthase kinase-3beta. *Genes Dev* **18** (3), 261 (2004); Pluquet, O., Qu, L. K., Baltzis, D., and Koromilas, A. E., Endoplasmic reticulum stress accelerates p53 degradation by the cooperative actions of Hdm2 and glycogen synthase kinase 3beta. *Mol Cell Biol* **25** (21), 9392 (2005); Baltzis, D. et al., The eIF2alpha kinases PERK and PKR activate glycogen synthase kinase 3 to promote the proteasomal degradation of p53. *J Biol Chem* **282** (43), 31675 (2007).

[78] Li, J., Lee, B., and Lee, A. S., Endoplasmic reticulum stress-induced apoptosis: multiple pathways and activation of p53-up-regulated modulator of apoptosis (PUMA) and NOXA by p53. *J Biol Chem* **281** (11), 7260 (2006).

[79] Candeias, M. M. et al., Expression of p53 and p53/47 are controlled by alternative mechanisms of messenger RNA translation initiation. *Oncogene* **25** (52), 6936 (2006).

[80] Frand, A. R. and Kaiser, C. A., The ERO1 gene of yeast is required for oxidation of protein dithiols in the endoplasmic reticulum. *Mol Cell* **1** (2), 161 (1998); Pollard, M. G., Travers, K. J., and Weissman, J. S., Ero1p: a novel and ubiquitous protein with an essential role in oxidative protein folding in the endoplasmic reticulum. *Mol Cell* **1** (2), 171 (1998).

[81] Bicknell, A. A., Babour, A., Federovitch, C. M., and Niwa, M., A novel role in cytokinesis reveals a housekeeping function for the unfolded protein response. *J Cell Biol* **177** (6), 1017 (2007).

[82] Hsieh, M. T. and Chen, R. H., Cdc48 and Cofactors Npl4-Ufd1 Are Important for G1 Progression during Heat Stress by Maintaining Cell Wall Integrity in Saccharomyces cerevisiae. *PLoS One* **6** (4), e18988.

[83] Lindholm, D., Wootz, H., and Korhonen, L., ER stress and neurodegenerative diseases. *Cell Death Differ* **13** (3), 385 (2006).

[84] Ma, Y. and Hendershot, L. M., The role of the unfolded protein response in tumour development: friend or foe? *Nat Rev Cancer* **4** (12), 966 (2004).

[85] He, B., Viruses, endoplasmic reticulum stress, and interferon responses. *Cell Death Differ* **13** (3), 393 (2006).

Chapter 2 : Ubiquitin-recognition protein Ufd1 couples the endoplasmic reticulum (ER) stress response to cell cycle control

Abstract

The ubiquitin-recognition protein Ufd1 facilitates clearance of misfolded proteins through the endoplasmic reticulum-associated degradation (ERAD) pathway. Here we report that prolonged ER stress represses Ufd1 expression to trigger cell cycle delay that contributes to ERAD. Remarkably, downregulation of Ufd1 enhances ubiquitination and destabilization of Skp2 mediated by the Anaphase-Promoting Complex or Cyclosome bound to Cdh1 (APC/C^{Cdh1}), resulting in an accumulation of the cyclin-dependent kinase inhibitor p27 and a concomitant cell cycle delay during G1 phase that enables more efficient clearance of misfolded proteins. Mechanistically, nuclear Ufd1 recruits the deubiquitinating enzyme USP13 to counteract APC/C^{Cdh1}-mediated ubiquitination of Skp2. Our data identify coordinated cell cycle response to prolonged ER stress through regulation of the Cdh1-Skp2-p27 axis by Ufd1 and USP13.

Introduction

Regulated protein degradation by the ubiquitin-proteasome system (UPS) plays a central role in diverse cellular processes. In an effort to dissect this proteolytic system in *Saccharomyces cerevisiae*, Ufd1 was discovered in a genetic screen for mutations in the ubiquitin fusion degradation (UFD) pathway responsible for degradation of a synthetic substrate N-terminally fused to one ubiquitin moiety (1). Functional and structural evidence suggest that Ufd1 acts as an ubiquitin-recognition protein with putative mono- and poly-ubiquitin binding sites (2).

To date, Ufd1 is best characterized as an adaptor protein that together with Npl4 confer the AAA-ATPase Cdc48/p97/VCP specific activity in ER-associated degradation (ERAD) (3), a process constitutively functioning to export misfolded proteins from the ER to the cytosol for UPS-dependent degradation. ERAD is part of the unfolded protein response (UPR) that is critical for the restoration of homeostasis in the ER when its function is perturbed, such as by the accumulation of misfolded proteins. Analyses of ERAD primarily performed in yeast suggest a role for the Ufd1-Npl4-p97 complex in the recognition and extraction of polyubiquitinated misfolded proteins from the ER through ATP hydrolysis to promote their degradation by cytosolic proteasomes. Intriguingly, in mammalian cells, Ufd1 has also been reported to directly enhance the activity of GP78, an ubiquitin ligase involved in ERAD, independently of p97 and Npl4 (4). Studies in yeast reported impaired degradation of the ER proteins HMG-CoA reductase, H-2Kb (major histocompatibility complex class I heavy chain), and CPY* (an aberrant form of carboxypeptidase Y) in the Ufd1 mutant –which suggests an essential role of Ufd1 in promoting ERAD (3, 5). However, RNAi-mediated depletion of Ufd1 in mammalian cells has yielded opposite results. While some reported impaired ERAD in Ufd1-depleted cells (6, 7), others showed accelerated degradation of classical ERAD substrates such as cholera toxin and the TCR (T-cell receptor) (8, 9). Although these seemingly contradictory observations may stem from the use of distinct cellular systems, they point to greater complexity in the regulation and function of Ufd1 that impinge on the ER stress response.

Furthermore, Ufd1-Npl4-p97 has been found to regulate cell cycle progression. In *Xenopus laevis* egg extracts, Ufd1-Npl4-p97 promotes chromatin decondensation by dissociating polyubiquitinated Aurora B from chromatin (10) and regulates spindle disassembly by removing the spindle assembly factors XMAP215 and TPX2 from microtubules (11).

In this study, we reveal the function of Ufd1 in maintaining the steady-state levels of Skp2 (the F-box adaptor of the E3 ubiquitin ligase SCF^{Skp2}) in mammalian cells by regulating its ubiquitination. We report that Ufd1 acts as a scaffold for Skp2 and the deubiquitinating enzyme USP13 to antagonize APC/C^{Cdh1}-mediated ubiquitination of Skp2. Our findings also show that prolonged ER stress downregulates Ufd1 levels, triggering Skp2 destabilization and accumulation of p27 that contributes to delayed progression through G1. Further, we show facilitated degradation of misfolded proteins in G1-arrested cells, suggesting that the newly discovered link between Ufd1 and cell cycle control serves to optimize ERAD.

Results

Prolonged treatment with tunicamycin downregulates Ufd1 expression

To investigate the role of Ufd1 in the UPR of mammalian cells, we first examined expression of endogenous Ufd1 protein in HeLa cells treated with tunicamycin (TM), a glycosylation inhibitor. To our surprise, we found that Ufd1 expression was reduced 20h after treatment with 0.5μg/ml of TM, concomitant with the accumulation of GRP78/BiP, a known marker of the UPR (Figure 2-1A). Downregulation of Ufd1 in mammalian cells exposed to prolonged treatment of TM may accommodate a novel function of Ufd1 in the UPR, distinct from its direct role in retrotranslocation of misfolded proteins.

Ufd1 regulates the Cdh1-Skp2-p27 axis

To understand the significance of ER stress-dependent downregulation of Ufd1, we first sought to examine the effect of Ufd1 downregulation under non-stressed conditions by depleting Ufd1 from HeLa cells. Knockdown of Ufd1 (~75% reduction) was achieved in a stable Ufd1-

deficient cell line (Ufd1-KD) and validated at both mRNA and protein levels (Figure 2-6, drug-selected pool #2).

Given the link between Ufd1 and the cell cycle, we asked whether Ufd1 knockdown would affect cell cycle progression. By examining the levels of major cell cycle markers in Ufd1-KD cells synchronized in G1/S by double-thymidine block and release, we observed an overall downregulation of Skp2 accompanied by an upregulation of p27, a major substrate of SCF^{Skp2} (12) (Figure 2-1B). Accordingly, we found that although the order of activation of cyclin-dependent kinase 1 (CDK1) and CDK2 was preserved in Ufd1-KD cells, their activation was delayed (Figure 2-1C). Expression of exogenous Ufd1 in Ufd1-KD cells restored Skp2 and p27 levels to those seen in control cells (Figure 2-1D). The effect of Ufd1 on Skp2 was confirmed in an independently established stable Ufd1-KD clone as well as in cells with transient knockdown of Ufd1 by siRNA (Figure 2-7A).

Downregulation of Skp2 in Ufd1-KD cells may occur at the level of transcription, translation, or protein stability. While qRT-PCR analysis revealed a twofold increase in Skp2 transcription in Ufd1-KD cells compared to control (Figure 2-2A), kinetics performed with cycloheximide showed reduced protein stability of endogenous Skp2 in Ufd1-KD cells (Figure 2-7B). Using *Xenopus laevis* egg extracts supplemented with exogenous Ufd1 in the presence of recombinant Cdh1 –the adaptor of the APC/C ubiquitin ligase responsible for Skp2 degradation in the cell cycle (13-17), we confirmed that Ufd1 is a negative regulator of Skp2 degradation (Figure 2-2B). Accordingly, the stability of endogenous Skp2 upon exit from mitosis, when APC/C^{Cdh1} is active in the cell cycle, was increased in cells overexpressing Ufd1 (Figure 2-2C).

As Skp2 ubiquitination is required for its proteasomal degradation, its downregulation in Ufd1-KD cells may result from enhanced activation of APC/C^{Cdh1}. To test this, we compared the levels of Skp2 ubiquitination in control and Ufd1-KD cells. We found enhanced ubiquitination of Skp2 in Ufd1-KD cells (Figure 2-2D), which could be rescued by re-expression of the full-length Ufd1 (Figure 2-2E) or depletion of Cdh1 from Ufd1-KD cells (Figure 2-7C). These results suggest that Ufd1 stabilizes Skp2 by antagonizing its ubiquitination by APC/C^{Cdh1}.

Ufd1 acts as a scaffold for Skp2-USP13 interaction

We explored whether Ufd1 protects Skp2 from ubiquitin-dependent degradation through recruitment of a deubiquitinating enzyme that counteracts Skp2 ubiquitination. Consistent with data from a recent proteomic survey of interaction partners of human deubiquitinating enzymes (18), we observed robust *in vivo* binding between Ufd1 and USP13 (Figure 2-3A, lane 2). Using a series of Ufd1 truncation mutants, we found that amino acids 261-280 of Ufd1 were necessary for its *in vivo* binding to USP13 (Figure 2-3A, lanes 2-8), which was further confirmed by the inability of the Ufd1 mutant harboring the internal deletion Δ261-280 to interact with USP13 *in vivo* (Figure 2-8A). Notably, the N241-Ufd1 mutant containing the p97 binding site (19) interacts with p97 but not with USP13, indicating that Ufd1 has distinct binding sites for both proteins (Figure 2-3A, lane 5). We then sought to determine whether interaction with USP13 enables Ufd1 to protect Skp2 from ubiquitination by testing the ability of the mutant Ufd1-Δ261-280 to rescue the low protein expression and enhanced ubiquitination of Skp2 in Ufd1-KD cells. Unlike wildtype Ufd1, Ufd1-Δ261-280 did not rescue the reduced levels of endogenous Skp2 (Figure 2-3B) or the enhanced ubiquitination of Skp2 in Ufd1-KD cells (Figure 2-3C), indicating that Ufd1-USP13 interaction is important in controlling Skp2 stability.

If Ufd1 facilitates interaction between USP13 and Skp2, it should be able to bind Skp2. Indeed, such interaction was observed *in vivo* (Figure 2-3D, lane 2). In our efforts to map the domain of Ufd1 required for its binding to Skp2, we again identified amino acids 261-280, which are also required for Ufd1's binding to USP13 (Figure 2-3D, lanes 2-8). A schematic summarizing the ability of the Ufd1 variants to bind USP13, Skp2, and p97 is presented in Figure 2-8B. Additionally, Ufd1 interacts with free Skp2 proteins (i.e., not in complex with Skp1-Cul1), as we did not detect endogenous Cul1 in complex with Ufd1-Skp2 *in vivo* (Figure 2-8C, left panel) and that Ufd1 binds with equal affinity to both wildtype Skp2 and the Skp2ΔF-box mutant that cannot be incorporated into SCF complexes(12) (Figure 2-8C, right panel). In support of our hypothesis that Ufd1-dependent regulation of Skp2 is mediated by USP13, we also observed *in vivo*

interaction between USP13 and Skp2 (Figure 2-3E) and among these three proteins (Figure 2-3F and Figure 2-8D), suggesting the formation of a functional ternary complex in cells. Indeed, we confirmed the existence of a complex containing Ufd1, Skp2, and USP13 *in vivo* by sequential immunoprecipitations (Figure 2-3G).

Next, to assess the role of Ufd1 as a mediator of Skp2-USP13 interaction, we compared the binding of USP13 to Skp2 in control and Ufd1-KD cells. A decrease in the amount of Skp2-bound USP13 was found in Ufd1-KD cells (Figure 2-3H, middle panels). Moreover, while exogenous Ufd1 can restore the interaction between Skp2 and USP13 in Ufd1-KD cells, the ability of the mutant Ufd1-Δ261-280 to do so was attenuated (Figure 2-3H, right panels). Taken together, our data suggest that Ufd1 acts as a scaffolding protein that enables a functional interaction between USP13 and Skp2.

USP13 deubiquitinates Skp2

USP13 shares sequence and structural homology with the ubiquitin protease USP5 and yet has only been reported as an ISG15-reactive protease (20). To directly assess whether USP13 possesses deubiquitinating (DUB) activity, we performed DUB assays using K48-linked di-ubiquitins as substrates. Immunopurified USP13 (Figure 2-9A) elicited a steady cleavage of K48-linked di-ubiquitins (Figure 2-9B).

Next we evaluated the effect of USP13 on Skp2. We found that USP13 overexpression increased the levels of endogenous Skp2 protein (Figure 2-4A). In agreement, USP13 knockdown reduced the levels of endogenous Skp2 and consequently increased p27 expression (Figure 2-9C and Figure 2-4B), supporting a positive role of USP13 in the regulation of Skp2 protein levels. To directly test whether USP13 exhibits DUB activity towards Skp2, we incubated FLAG-USP13 with ubiquitinated-Skp2, both immunopurified from cells. The amount of ubiquitin conjugates on Skp2 was reduced in the presence of USP13 (Figure 2-4C). Taken together, our data show that USP13 has DUB activity towards both K48-linked di-ubiquitin and ubiquitinated Skp2.

ER-Stress regulates the Ufd1-Skp2-p27 axis and G1 cell cycle progression

The observation that Ufd1-knockdown induced Skp2 downregulation and consequently p27 upregulation under non-stressed conditions (Figure 2-1B and Figure 2-1D) led us to examine whether ER stress-dependent Ufd1 downregulation (Figure 2-1A) would result in similar biochemical changes that modulate cell cycle progression. Indeed, we observed that tunicamycin (TM) triggered Ufd1 downregulation in a dose-dependent manner, which correlated with Skp2 clearance and p27 accumulation after 20h of treatment (Figure 2-5A). ER stress-dependent regulation of Ufd1-Skp2-p27 was also observed in other cell lines, such as HeLa-S3, HEK-293T, and HFF-1 (Figure 2-10A), although the degree of response differed among different cell lines subjected to the same TM treatment. Thapsigargin, an inhibitor of ER Ca^{2+} ATPase that also induces ER stress, elicited similar responses (Figure 2-10B). Remarkably, the extent of the G1 delay correlated with the dose- and time-dependent regulation of Ufd1, Skp2, and p27 levels following TM treatment (Figure 2-5B and Figure 2-10C).

ER stress-dependent Ufd1 downregulation is a response to prolonged UPR activation (Figure 2-1A, Figure 2-5A-B). Notably, changes in the expression of Ufd1 and Skp2 largely occur in the nuclear fraction (Figure 2-10D), suggesting that the pool of Ufd1 contributing to cell cycle control is distinct from that involved in retrotranslocation of misfolded proteins in the cytosol. Consistent with this idea are the observations that both USP13 (20) and Skp2 (Figure 2-10D) are mainly localized in the nucleus.

The Cdh1-Skp2-p27 axis contributes to ER-induced G1 delay

Under non-stressed conditions, Ufd1-knockdown destabilized the Skp2 protein. To examine whether Skp2 is also regulated at the level of protein stability under ER stress conditions that downregulate Ufd1, we first treated cells with TM and the proteasome inhibitor MG-132. Addition of MG-132 prevented TM-induced downregulation of Skp2, indicating that ER stress accelerates proteasomal degradation of Skp2 (Figure 2-5C). Interestingly, treatment with a low dose of MG-132 (2μM) for 12h stabilized Skp2 and abolished p27 accumulation following TM treatment, suggesting that ER stress-dependent p27 accumulation is a consequence of Skp2

destabilization and that the co-regulation of Skp2 and p27 in response to TM occurs at the level of protein stability (Figure 2-5C, left panels, lane 3 and Figure 2-11A; Figure 2-5C, right panels, lanes 3 and 7). Of note, as we increased MG-132 concentration, both Skp2 and p27 were stabilized (Figure 2-5C, right panels).

We observed that while MG-132 attenuated TM-induced Skp2 downregulation, the effect was nevertheless incomplete. Indeed, analysis of Skp2 and p27 transcript levels following TM treatment revealed a 30% decrease in Skp2 mRNA and a 1.6 fold increase in p27 mRNA (Figure 2-11B). These data suggest ER stress-dependent transcriptional regulation of Skp2 and p27. In contrast, Ufd1 mRNA levels were comparable before and after TM treatment (Figure 2-11B). Further, we observed that TM-dependent Ufd1 downregulation was not restored by treatment with MG-132 (Figure 2-5C, left panels), suggesting that ER stress-dependent repression of Ufd1 may occur at the level of translation or proteasome-independent degradation.

Next, to determine whether APC/C^{Cdh1} targets Skp2 for ubiquitin-mediated degradation upon ER stress induction, we knocked down Cdh1 by RNAi, followed by treatment with TM. Notably, Cdh1-RNAi alone attenuated TM-induced proteasomal degradation of Skp2 and diminished TM-induced upregulation of p27 (Figure 2-11A, lane 10), demonstrating that APC/C^{Cdh1} targets Skp2 for degradation upon ER stress, which in turn leads to p27 accumulation. Cdh1-knockdown incompletely prevented TM-induced Skp2 downregulation (Figure 2-5C and Figure 2-11A) because TM treatment also transcriptionally repressed Skp2 (Figure 2-11B). Interestingly, compared to the addition of MG-132 alone, the combination of Cdh1-RNAi and MG-132 did not further stabilize Skp2 under ER stress, indicating that APC/C^{Cdh1} is the primary E3 ligase responsible for targeting Skp2 for degradation under such conditions (Figure 2-5C; right panels, lanes 11-15). Taken together, our data show that ER stress directly regulates the Cdh1-Skp2-p27 axis through Ufd1 to delay cell cycle progression. Finally, the ability of Ufd1 overexpression or p27-knockdown to overcome TM-induced G1 delay, although partial, further supports a role of these proteins in the regulation of the UPR-induced cell cycle response (Figure 2-5D-E and Figure 2-11C).

Because it was previously reported that cyclin D1 downregulation can also mediate TM-dependent G1 delay in NIH-3T3 cells (21), we sought to analyze the contribution of cyclin D1 downregulation and p27 upregulation in ER stress-induced cell cycle arrest. Interestingly in HeLa cells, overexpression of cyclin D1 could not overcome TM-induced G1 delay (Figure 2-12). Of note, Skp2 expression was still reduced regardless of cyclin D1 overexpression, indicating that Skp2 and cyclin D1 downregulation following TM treatment are independent. This points to the existence of complementing mechanisms to achieve ER stress-dependent cell cycle arrest, which may be cell type-specific. Our data suggest that in the absence of cyclin D1-driven arrest, Ufd1-Skp2-p27 contributes, at least in part, to cell cycle delay.

G1 cell cycle phase facilitates clearance of ERAD substrates

Given the link between ER stress and cell cycle, we asked whether ER stress-induced G1 delay affects ERAD. To this end, we examined the efficiency of ERAD in different phases of the cell cycle by comparing the rate of degradation of two classic ERAD substrates –the cystic fibrosis transmembrane conductance regulator (CFTR) and the ER luminal protein null Hong-Kong α1-antitrypsin (NHK)– in G1/S or G2/M-arrested cells. Notably, accelerated degradation of both proteins was observed in G1/S-arrested cells, compared to the G2/M-synchronized populations (Figure 2-5F and Figure 2-13A-B). The impaired clearance of ERAD substrates observed in G2/M-arrested cells did not result from nocodazole-induced toxicity, as the degradation of NHK was still slower in the G2/M population obtained by a 7-hour release from G1 arrest (Figure 2-5G and Figure 2-13C-D). These data suggest that ER stress-induced G1 delay serves to facilitate degradation of misfolded proteins.

This hypothesis prompted us to examine the cell cycle status of fibroblasts bearing 2 alleles of mutant CFTR gene (CFTR-ΔF508) isolated from a cystic fibrosis-affected individual. If G1 phase of the cell cycle is more conducive to ERAD, then the constitutive expression of endogenous mutant CFTR targeted to ERAD in these cells may render them more prone to G1 delay. We found that these cells not only had a slightly higher basal G1 population compared to

normal human fibroblasts (Figure 2-14A), they also had a greater increase in G1 when treated with TM (Figure 2-14B). These observations strengthens the physiological relevance of ER stress-induced cell cycle arrest.

Discussion

Our study offers new insight into cell cycle control in response to ER stress. We demonstrate that ER stress-dependent control of Ufd1 modulates Skp2 protein expression and consequently p27, to delay progression through G1 that facilitates clearance of misfolded proteins. Mechanistically, Ufd1 promotes the interaction between USP13 and Skp2 to maintain Skp2 steady-state levels (see Figure 2-5H for proposed model).

In support of our findings, TM treatment reportedly triggers G1 cell cycle arrest by inhibition of cyclin D1 translation through activation of PERK (22). Our study discloses a new mechanism to attain G1 delay following protein misfolding, through regulation of the Cdh1-Skp2-p27 axis at the level of protein stability. We began to examine the efficiency of ERAD in the context of the cell cycle, an area underexplored thus far. Our data raise the intriguing possibility that cell cycle arrest may not simply be a passive response that provides cells time to restore homeostasis, but creates conditions conducive to the degradation of misfolded proteins. Considering that CFTR and NHK are characterized ERAD substrates subjected to degradation by the ER resident ubiquitin ligases GP78, RNF5/RMA1, and Hrd1(23, 24), the cell cycle-dependent degradation of ERAD substrates we observed may be the result of cell cycle-regulated expression or activity of these ligases and other ERAD components.

We also present an initial characterization of USP13 as a DUB able to process K48-linked ubiquitins and antagonize APC/C^{Cdh1}-mediated ubiquitination of Skp2 in an Ufd1-dependent manner. Our mapping of Ufd1-USP13 interaction sites revealed that Ufd1 binds p97 and USP13 through distinct domains. Our observation that Ufd1 binds Skp2 proteins not in complex with Skp1-Cul1 suggests that Ufd1 positively regulates the abundance of free Skp2 proteins to control the formation of SCF^{Skp2} complexes.

Based on our findings, we propose a model in which the functions of Ufd1 are regulated temporally and spatially under conditions activating the UPR. In the immediate phase, Ufd1 in cooperation with p97 and Npl4 in the cytosol contribute to the retrotranslocation of misfolded proteins from the ER, whereas in a delayed response, downregulation of nuclear Ufd1 mediates G1 cell cycle delay. Both the former and latter responses serve to clear misfolded proteins. Such temporal and spatial modulation of Ufd1 expression shown here could not have been revealed in previous yeast studies using loss of function mutants that yielded all-or-none phenotypes (3, 5).

In conclusion, the identification of Ufd1-dependent recruitment of USP13 to control Skp2 stability and G1 delay provides new mechanistic insights into the regulation of the cell cycle under ER stress while also pointing to the implication of a cell cycle-dependent control of ERAD.

Figures

Figure 2-1: Prolonged ER stress downregulates Ufd1 and depletion of Ufd1 by RNAi affects cell cycle progression.

(A) Protein levels of endogenous Ufd1 were compared in HeLa cells treated with DMSO (-) or 0.5μg/ml tunicamycin (TM) (+) for 20h by immunoblotting. GRP78 was used as a marker of UPR and β-actin as a loading control. (B) Immunoblot analysis of cell cycle markers in control and Ufd1-KD cells released from G1/S arrest after double-thymidine block. Control refers to cells infected with an empty shRNA plasmid. Levels of Ufd1 were quantified and are shown in arbitrary units (AU). (C) *Top* panels, comparison of CDK1 and CDK2 kinase activities in control and Ufd1-KD cells released from G1/S arrest. *Bottom* panels, Protein levels of Skp2 in control and Ufd1-KD cells. (D) Analysis of cell cycle markers in control and Ufd1-KD cells expressing FLAG-Ufd1. The melanoma cell line CHL1 expressing high levels of p27 was used solely as a positive control for p27 immunodetection.

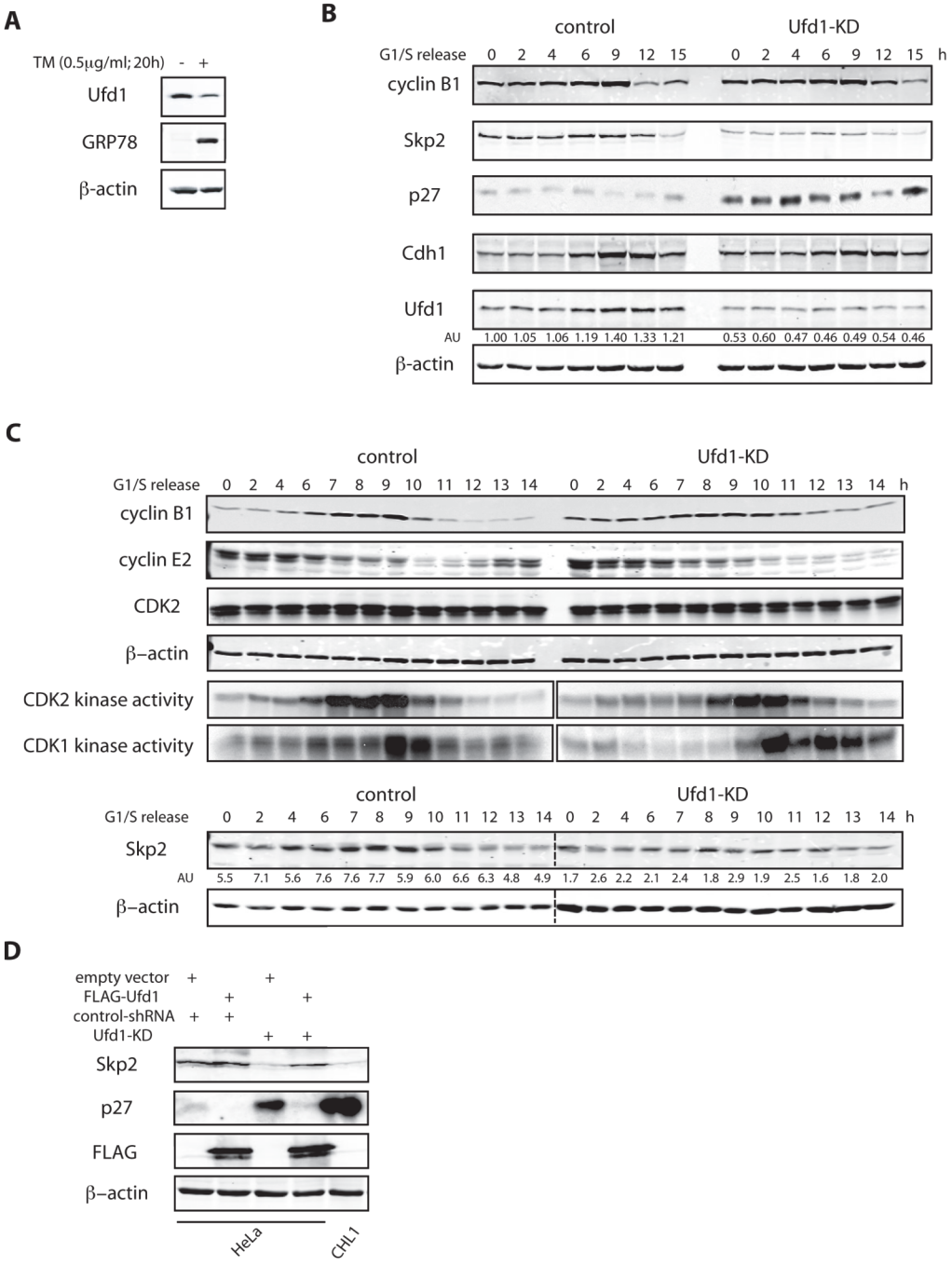
A
TM (0.5μg/ml; 20h) - +
Ufd1
GRP78
β-actin
B
control
Ufd1-KD
G1/S release 0 2 4 6 9 12 15 0 2 4 6 9 12 15 h
cyclin B1
Skp2
p27
Cdh1
Ufd1
AU 1.00 1.05 1.06 1.19 1.40 1.33 1.21 0.53 0.60 0.47 0.46 0.49 0.54 0.46
β-actin
C
control
Ufd1-KD
G1/S release 0 2 4 6 7 8 9 10 11 12 13 14 0 2 4 6 7 8 9 10 11 12 13 14 h
cyclin B1
cyclin E2
CDK2
β–actin
CDK2 kinase activity
CDK1 kinase activity
control
Ufd1-KD
G1/S release 0 2 4 6 7 8 9 10 11 12 13 14 0 2 4 6 7 8 9 10 11 12 13 14 h
Skp2
AU 5.5 7.1 5.6 7.6 7.6 7.7 5.9 6.0 6.6 6.3 4.8 4.9 1.7 2.6 2.2 2.1 2.4 1.8 2.9 1.9 2.5 1.6 1.8 2.0
β–actin
D
empty vector + +
FLAG-Ufd1 + +
control-shRNA + +
Ufd1-KD + +
Skp2
p27
FLAG
β–actin
HeLa
CHL1

Figure 2-2: Ufd1 interferes with the ubiquitination of Skp2 in vivo.

(A) Quantification of Skp2 mRNA levels in control and Ufd1-KD cells by SYBR-green qRT-PCR. (B) Skp2 degradation assays in interphase *Xenopus laevis* egg extracts supplemented with recombinant Cdh1, in the presence of the indicated amount of bacterially purified recombinant GST-Ufd1. Samples were taken at the indicated times after addition of ^{35}S-Skp2 to the extract. (C) *Top*, half-life analysis of endogenous Skp2 protein with cycloheximide (CHX) treatment in empty vector- or FLAG-Ufd1-transfected HeLa cells released from nocodazole (noco) arrest. Total lysates were immunoblotted for Skp2 or FLAG. Quantification is shown below the immunoblots. (D) *In vivo* ubiquitination of Skp2. myc-Skp2 and HA-Ub were expressed in control and Ufd1-KD cells. Immunoprecipitates obtained with c-myc antibodies were immunoblotted for either ubiquitin (Ub) or c-myc to detect polyubiquitinated Skp2, marked as $(Ub)_n$-Skp2. Control refers to cells infected with empty shRNA plasmid. (E) *In vivo* ubiquitination of Skp2. myc-Skp2 and HA-Ub were coexpressed with either empty vector or FLAG-Ufd1. Immunoprecipitates obtained with c-myc antibodies were immunoblotted for Ub. Expression of FLAG-Ufd1 in total cell extracts is shown in the bottom panel.

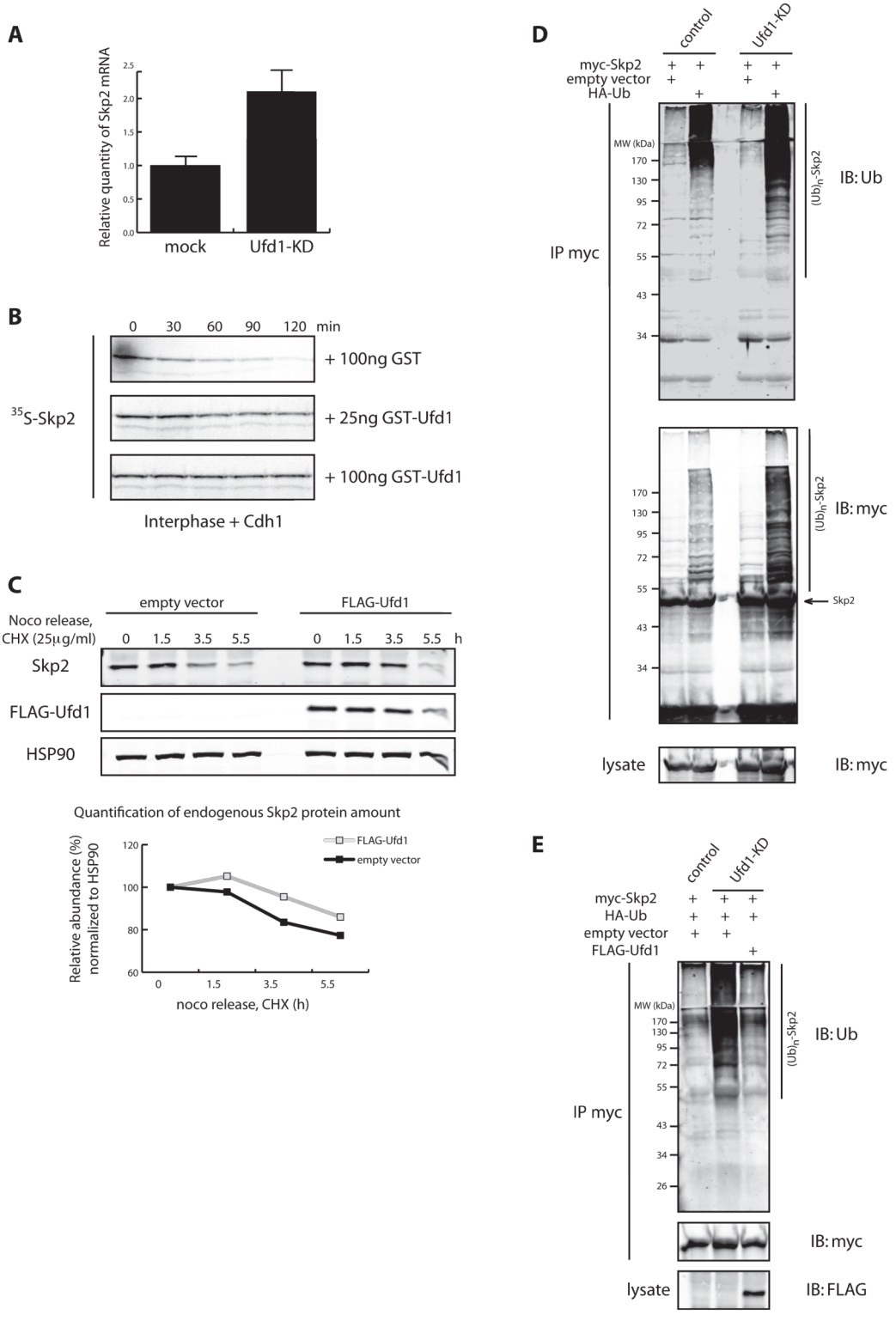
A
Relative quantity of Skp2 mRNA
2.5
2.0
1.5
1.0
0.5
0.0
mock
Ufd1-KD
B
0 30 60 90 120 min
35S-Skp2
+ 100ng GST
+ 25ng GST-Ufd1
+ 100ng GST-Ufd1
Interphase + Cdh1
C
empty vector
FLAG-Ufd1
Noco release,
CHX (25μg/ml)
0 1.5 3.5 5.5 0 1.5 3.5 5.5 h
Skp2
FLAG-Ufd1
HSP90
Quantification of endogenous Skp2 protein amount
Relative abundance (%)
normalized to HSP90
120
100
80
60
FLAG-Ufd1
empty vector
0 1.5 3.5 5.5
noco release, CHX (h)
D
control
Ufd1-KD
myc-Skp2 + + + +
empty vector + + +
HA-Ub + +
MW (kDa)
170
130
95
72
55
43
34
IP myc
(Ub)n-Skp2
IB: Ub
IB: myc
Skp2
lysate
IB: myc
E
control
Ufd1-KD
myc-Skp2 + + +
HA-Ub + + +
empty vector + +
FLAG-Ufd1 +
MW (kDa)
170
130
95
72
55
43
34
26
IP myc
(Ub)n-Skp2
IB: Ub
IB: myc
lysate
IB: FLAG

Figure 2-3: Ufd1 interferes with the ubiquitination of Skp2 by recruiting the deubiquitinating enzyme USP13.

(A) Mapping of Ufd1's binding site to USP13 *in vivo*. USP13 was expressed with empty vector (lane 1) or the indicated FLAG-Ufd1 C-terminal truncation mutants in HEK-293T cells (lanes 2-8). Ufd1-N215 denotes an Ufd1 truncation mutant containing the N-terminal amino acids 1-215, and so on. FLAG-Ufd1 immunoprecipitates were immunoblotted for USP13, p97, and FLAG. (B) Western blots of endogenous Skp2 in control (cont) and Ufd1-KD cells transfected with empty vector, FLAG-Ufd1, or mutant FLAG-Ufd1Δ261-280. (C) *In vivo* ubiquitination of Skp2 in control and Ufd1-KD cells overexpressing myc-Skp2 and HA-Ub with empty vector, FLAG-Ufd1, or FLAG-Ufd1Δ261-280. c-myc immunoprecipitates were immunoblotted for Ub. Levels of ubiquitination were quantified and shown as arbitrary units (AU). (D) Mapping of Ufd1's binding site to Skp2 *in vivo*. myc-Skp2 was expressed in HEK-293T cells with empty vector (lane 1) or the indicated FLAG-Ufd1 C-terminal truncation mutants (lanes 2-8). FLAG immunoprecipitates were immunoblotted for Skp2 and FLAG. (E) Coimmunoprecipitation of USP13 and Skp2 *in vivo*. USP13 was expressed with empty vector (lane 1) or together with myc-Skp2 (lanes 2 and 3). c-myc immunoprecipitates were immunoblotted for USP13 or Skp2. (F) Semi-endogenous coimmunoprecipitation. HeLa cells were transfected with FLAG-Skp2. FLAG immunoprecipitates were immunoblotted for endogenous USP13 and Ufd1. *short exposure and **long exposure of the same image. (G) Evidence of ternary complex formation among USP13, Ufd1, and Skp2 by sequential immunoprecipitations. HeLa cells were transfected with FLAG-Ufd1, myc-Skp2, and USP13. FLAG immunoprecipitates were eluted with FLAG-peptide. Eluates were then used for c-myc immunoprecipitation. 10% of FLAG-IP, 10% of eluate, and all of myc-IP were immunoblotted for USP13, Skp2, and Ufd1. (H) *Left* panel, immunoblots of endogenous Ufd1 in control and Ufd1-KD cells. *Middle* panel, USP13 and myc-Skp2 were coexpressed in control (lanes 1 and 2) or Ufd1-KD cells (lane 3). Control cells were transfected with either half (*) or equal amount (**) of DNA used for transfection in Ufd1-KD cells. c-myc immunoprecipitates were immunoblotted for USP13. *Right* panel, control and Ufd1-KD cells were transfected with USP13 and myc-Skp2 together with empty vector (ev), FLAG-Ufd1, or the mutant FLAG-Ufd1Δ261-280. c-myc immunoprecipitates were immunoblotted for USP13 and Skp2.

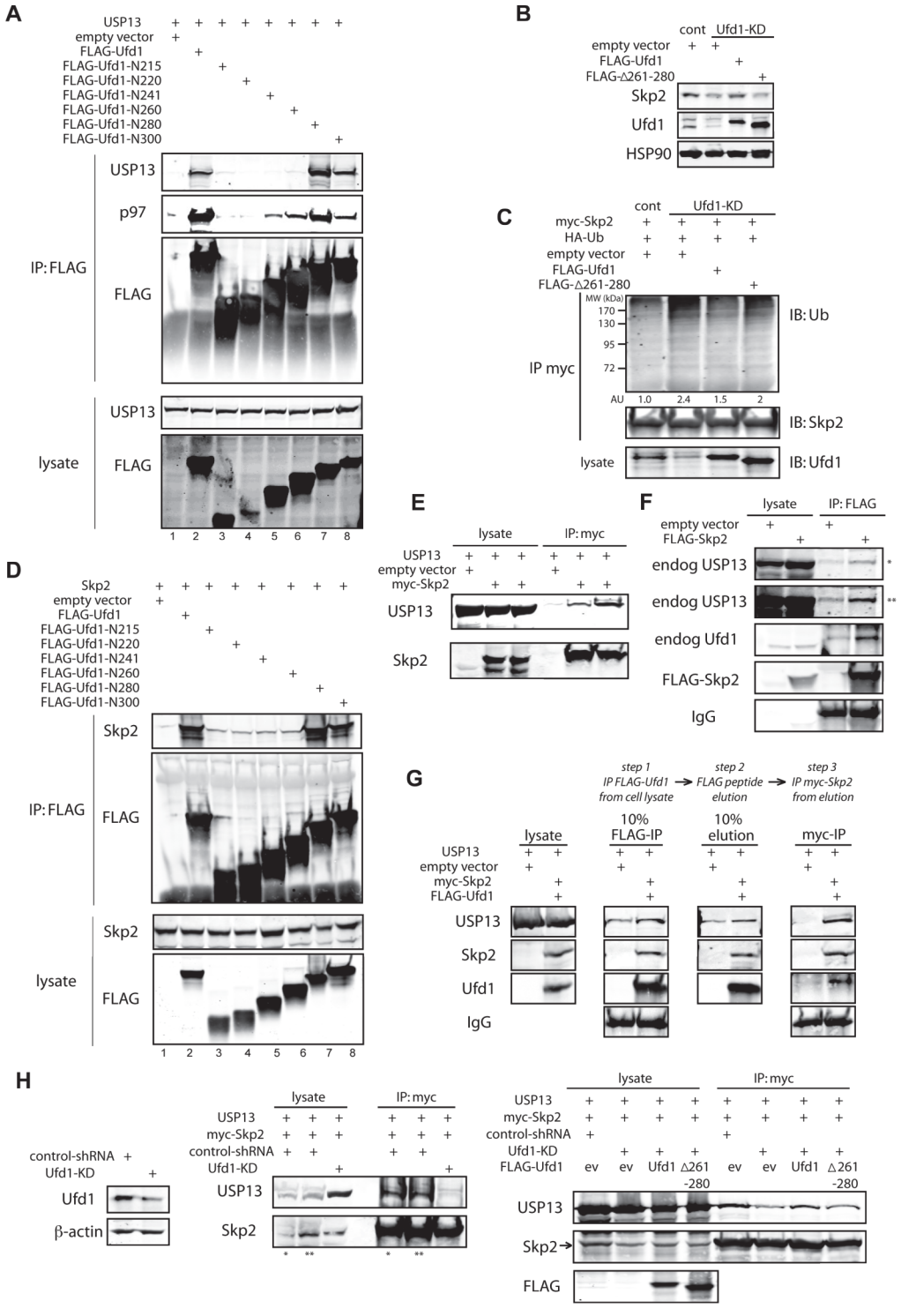
A
USP13
empty vector
FLAG-Ufd1
FLAG-Ufd1-N215
FLAG-Ufd1-N220
FLAG-Ufd1-N241
FLAG-Ufd1-N260
FLAG-Ufd1-N280
FLAG-Ufd1-N300
IP: FLAG
USP13
p97
FLAG
lysate
USP13
FLAG
1 2 3 4 5 6 7 8
B
cont
Ufd1-KD
empty vector
FLAG-Ufd1
FLAG-Δ261-280
Skp2
Ufd1
HSP90
C
cont
Ufd1-KD
myc-Skp2
HA-Ub
empty vector
FLAG-Ufd1
FLAG-Δ261-280
MW (kDa)
170
130
95
72
IP myc
IB: Ub
AU 1.0 2.4 1.5 2
IB: Skp2
lysate
IB: Ufd1
D
Skp2
empty vector
FLAG-Ufd1
FLAG-Ufd1-N215
FLAG-Ufd1-N220
FLAG-Ufd1-N241
FLAG-Ufd1-N260
FLAG-Ufd1-N280
FLAG-Ufd1-N300
IP: FLAG
Skp2
FLAG
lysate
Skp2
FLAG
1 2 3 4 5 6 7 8
E
lysate
IP: myc
USP13
empty vector
myc-Skp2
USP13
Skp2
F
lysate
IP: FLAG
empty vector
FLAG-Skp2
endog USP13
endog USP13
endog Ufd1
FLAG-Skp2
IgG
G
step 1
IP FLAG-Ufd1
from cell lysate
step 2
FLAG peptide
elution
step 3
IP myc-Skp2
from elution
lysate
10%
FLAG-IP
10%
elution
myc-IP
USP13
empty vector
myc-Skp2
FLAG-Ufd1
USP13
Skp2
Ufd1
IgG
H
control-shRNA
Ufd1-KD
Ufd1
β-actin
lysate
IP: myc
USP13
myc-Skp2
control-shRNA
Ufd1-KD
USP13
Skp2
lysate
IP: myc
USP13
myc-Skp2
control-shRNA
Ufd1-KD
FLAG-Ufd1
ev
ev
Ufd1
Δ261
-280
ev
ev
Ufd1
Δ261
-280
USP13
Skp2
FLAG

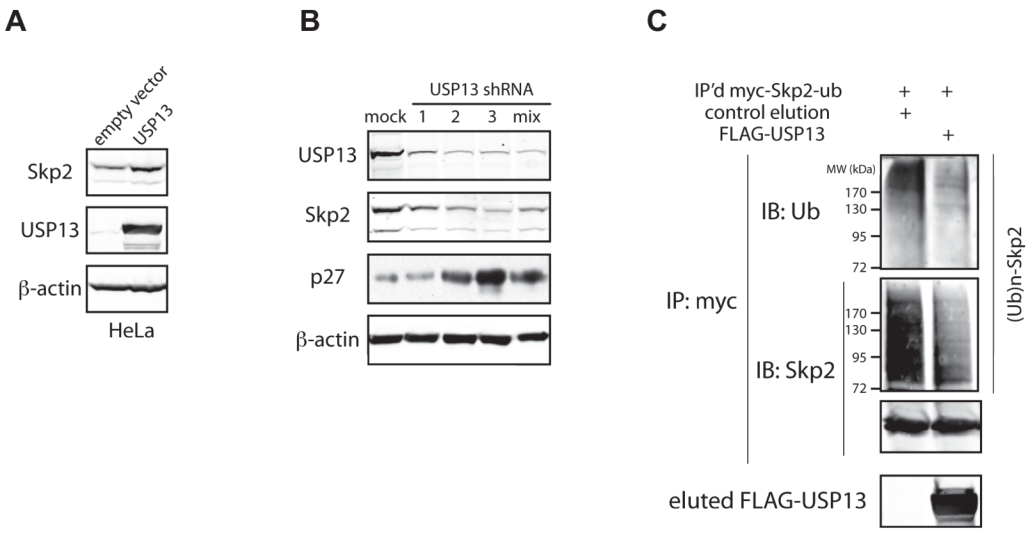

Figure 2-4: USP13 controls Skp2 levels via deubiquitination.

(A) Immunoblots of endogenous Skp2 and exogenous USP13 in HeLa cells transfected with empty vector or untagged USP13. (B) Knockdown of USP13 in HeLa cells infected with lentivirus packaged with either empty vector (mock) or one of three individual USP13-specific shRNA vectors as indicated. Immunoblots of endogenous USP13, Skp2, and p27 are shown. (C) *In vitro* deubiquitination of Skp2 by USP13 as described in Materials and Methods. Immunopurified FLAG-USP13 and immunoprecipitated myc-Skp2 were obtained from HeLa cells. Reactions were immunoblotted for Ub and Skp2. "IP'd myc-Skp2-ub" denotes ubiquitinated myc-tagged Skp2 immunoprecipitated from cells.

Figure 2-5: ER stress regulates the Ufd1-Cdh1-Skp2-p27 axis to delay progression through G1.

(A) HeLa cells were treated with DMSO or increasing concentrations of tunicamycin (TM) (0.05; 0.1; 0.25; and 0.5μg/ml) for 20h. Lysates were immunoblotted for Ufd1, Skp2, p27, and GRP78 (marker of UPR). (B) Cells were treated with DMSO, 0.5μg/ml or 2.5μg/ml of TM over a 24h time course. At the indicated timepoints, samples were collected for immunoblotting and FACS (see Figure S5C for the corresponding quantification of G1 delay based on FACS analysis). (C) *Left*, HeLa cells were treated with DMSO, 2.5μg/ml of TM alone or together with MG-132 (2 or 5μM) for 12h, and collected for immunoblotting for the indicated proteins. *Right*, HeLa cells transfected with control or Cdh1-specific shRNA (for 24h) were treated with DMSO, 2.5μg/ml of TM alone or together with MG-132 (5, 10, or 15μM) for 12h. Total cell extracts were immunoblotted for the indicated proteins. (D) HeLa cells transfected with empty vector or FLAG-Ufd1 were treated with DMSO or TM (1ug/ml for 8h). *Top*, Western blot of Ufd1. *Bottom*, graph shows increase in G1 at 8h after TM addition compared to DMSO treatment (see Figure S6C for FACS histograms). (E) HeLa cells were transfected with either control or two different p27-specific shRNAs as indicated for 24h. *Top*, Western blot of p27 in control and p27-KD cells treated with TM (2.5μg/ml for 8h). *Bottom*, graph shows percent increase in G1 at 4h and 8h after TM addition relative to 0h (percent of cells in G1 at 0h is set as baseline, with 0% increase in G1). (F) Half-life analyses of GFP-CFTR and NHK proteins with cycloheximide (CHX) treatment in double thymidine-arrested (G1/S) or nocodazole-arrested (G2/M) HeLa cells. Total lysates were immunoblotted for GFP or α1-antitrypsin/NHK (see Figure S8A for verification of cell cycle synchronization by FACS and Figure S8B for quantification of protein half-lives). (G) Half-life of NHK protein in double thymidine-arrested (G1/S) HeLa cells or cells released from double thymine arrest for 7h (approximately corresponding to G2/M). Total lysates were immunoblotted for α1-antitrypsin/NHK (see Figure S8C for verification of cell cycle synchronization by FACS and Figure S8D for quantification of NHK half-life). (H) Proposed model, downregulation of Ufd1 following prolonged ER stress reduces recruitment of USP13 to Skp2, thereby resulting in ubiquitin-dependent degradation of Skp2 by APC/C^{Cdh1}. Consequently, levels of p27 increase, contributing to G1 arrest that supports degradation of misfolded proteins.

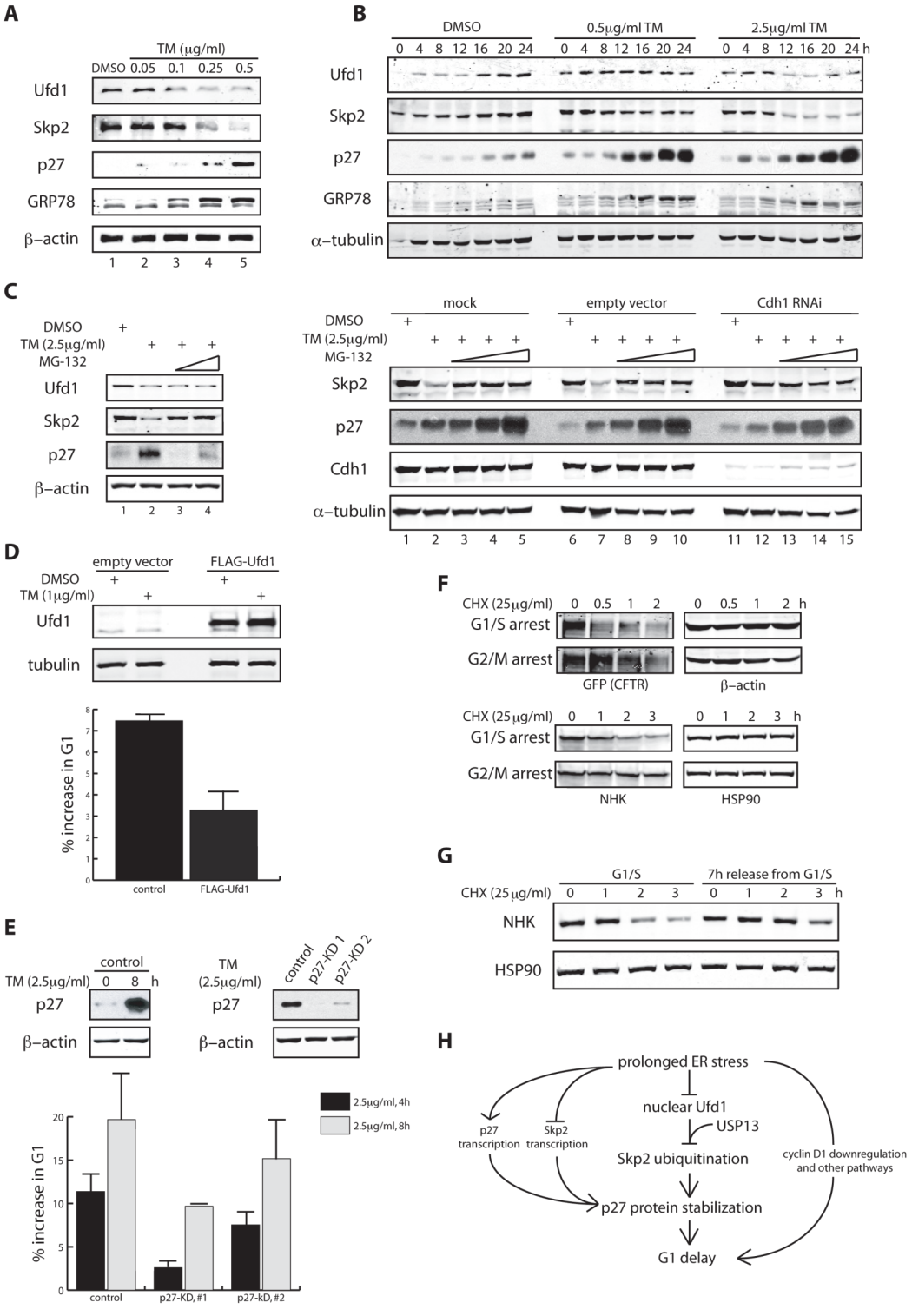
A
TM (μg/ml)
DMSO 0.05 0.1 0.25 0.5
Ufd1
Skp2
p27
GRP78
β–actin
1 2 3 4 5
B
DMSO
0.5μg/ml TM
2.5μg/ml TM
0 4 8 12 16 20 24 0 4 8 12 16 20 24 0 4 8 12 16 20 24 h
Ufd1
Skp2
p27
GRP78
α–tubulin
C
DMSO
TM (2.5μg/ml)
MG-132
Ufd1
Skp2
p27
β–actin
1 2 3 4
mock
empty vector
Cdh1 RNAi
DMSO
TM (2.5μg/ml)
MG-132
Skp2
p27
Cdh1
α–tubulin
1 2 3 4 5 6 7 8 9 10 11 12 13 14 15
D
empty vector
FLAG-Ufd1
DMSO
TM (1μg/ml)
Ufd1
tubulin
% increase in G1
control
FLAG-Ufd1
E
control
TM (2.5μg/ml) 0 8 h
p27
β–actin
TM (2.5μg/ml)
control
p27-KD 1
p27-KD 2
p27
β–actin
2.5μg/ml, 4h
2.5μg/ml, 8h
% increase in G1
control
p27-KD, #1
p27-KD, #2
F
CHX (25μg/ml) 0 0.5 1 2 0 0.5 1 2 h
G1/S arrest
G2/M arrest
GFP (CFTR)
β–actin
CHX (25μg/ml) 0 1 2 3 0 1 2 3 h
G1/S arrest
G2/M arrest
NHK
HSP90
G
G1/S
7h release from G1/S
CHX (25μg/ml) 0 1 2 3 0 1 2 3 h
NHK
HSP90
H
prolonged ER stress
nuclear Ufd1
USP13
p27 transcription
Skp2 transcription
Skp2 ubiquitination
cyclin D1 downregulation and other pathways
p27 protein stabilization
G1 delay

Figure 2-6: Validation of Ufd1-knockdown in HeLa cells by qRT-PCR and immunoblotting.

(A) By SYBR-green qRT-PCR, four different Ufd1-specific primer pairs were used to quantify Ufd1 transcripts in drug-selected pools of HeLa cells infected with lentivirus packaged with empty shRNA vector (control) or Ufd1-shRNA. Amount of Ufd1 transcript was normalized against GAPDH and is presented as a percentage of the Ufd1 transcript in control cells (set as 100%). (B) *Top*, protein levels of Ufd1 in each drug-selected pool infected with Ufd1-shRNA were analyzed by immunoblotting. *Bottom*, quantification of Ufd1 levels, detected by immunoblotting, using the Odyssey software (LiCOR) presented as a percentage of Ufd1 levels in the control (set as 100%). Asterisks (*) mark drug-resistant pools with a statistically significant difference in the amount of Ufd1 transcript compared to the control. Pool #2 with a significant downregulation of Ufd1 was employed throughout our study and referred to as Ufd1-KD cells. TM corresponds to tunicamycin treatment (2.5μg/ml for 8h).

A

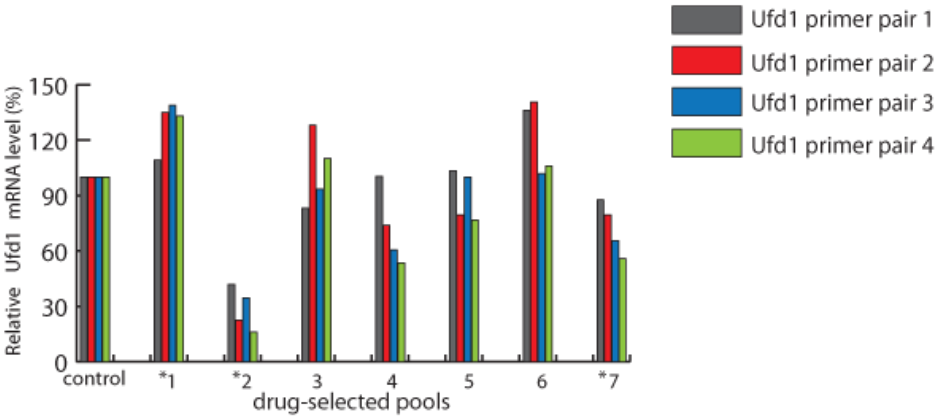
Ufd1 primer pair 1
Ufd1 primer pair 2
Ufd1 primer pair 3
Ufd1 primer pair 4
Relative Ufd1 mRNA level (%)
150
120
90
60
30
0
control
*1
*2
3
4
5
6
*7
drug-selected pools

B

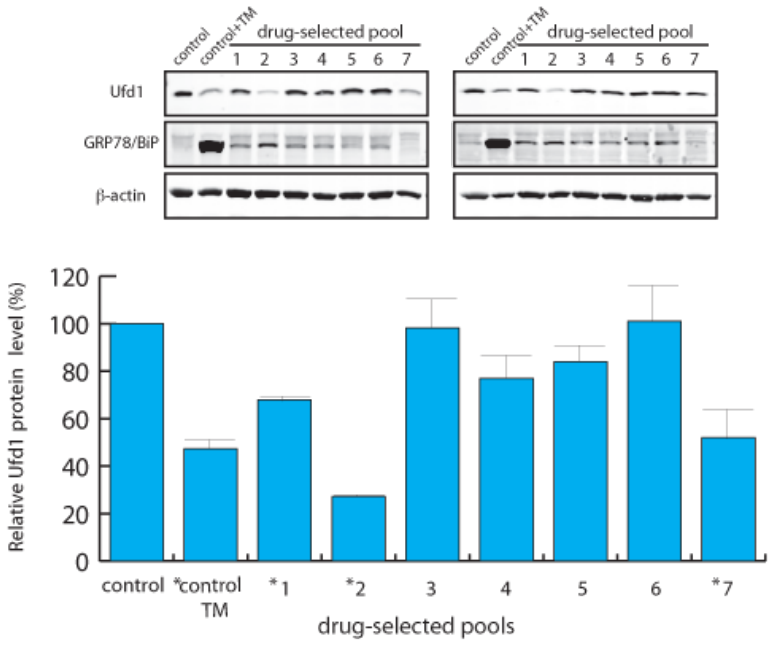
control
control+TM
drug-selected pool
1 2 3 4 5 6 7
Ufd1
GRP78/BiP
β-actin
Relative Ufd1 protein level (%)
120
100
80
60
40
20
0
control
*control TM
*1
*2
3
4
5
6
*7
drug-selected pools

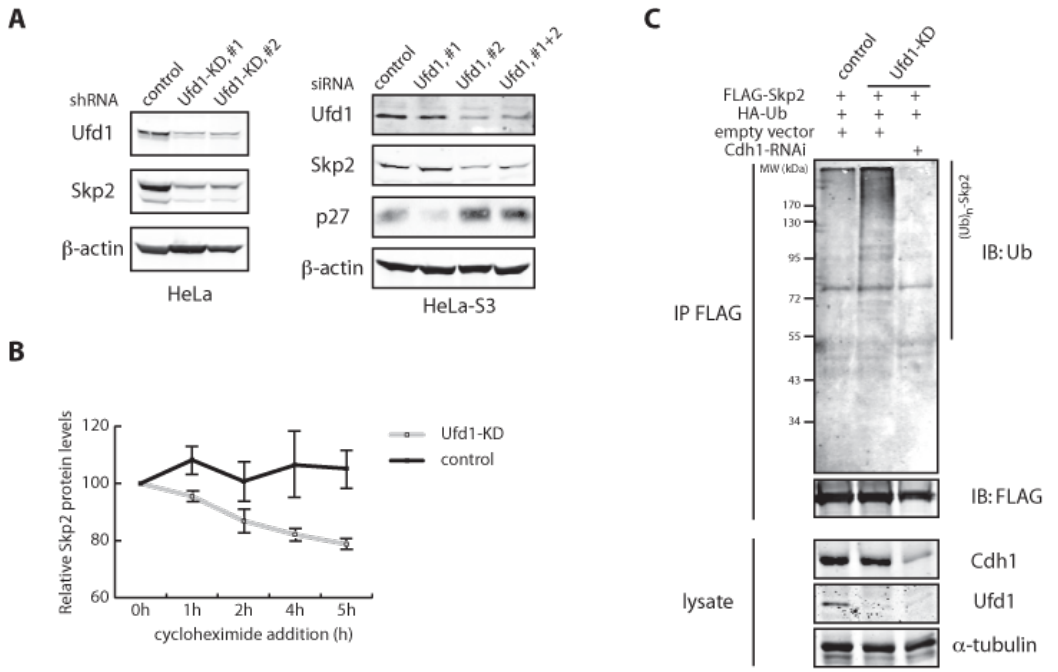

Figure 2-7: Ufd1 affects Skp2 protein levels and ubiquitination.

(A) Downregulation of Skp2 in cells with stable Ufd1 knockdown by shRNA or with transient Ufd1 knockdown by siRNA. Left, immunoblots of endogenous Ufd1 and Skp2 from two independently-derived puromycin-resistant pools of stable Ufd1-KD cells. *Right*, immunoblots of endogenous Ufd1, Skp2, and p27 from HeLa-S3 cells transfected with control siRNA or two individual Ufd1-specific siRNAs. (B) Quantification of endogenous Skp2 protein levels, normalized to β-actin, in control and Ufd1-KD cells collected at the indicated times after addition of 25μg/ml cycloheximide. Relative values are presented as percentages of the amount of Skp2/β-actin at time 0h of cycloheximide addition (set as 100%). (C) APC/C^{Cdh1} mediates ubiquitination of Skp2 in Ufd1-KD cells. *In vivo* ubiquitination of Skp2. FLAG-Skp2 and HA-Ub were expressed in control, Ufd1-KD, or Ufd1 and Cdh1 double knockdown cells. Immunoprecipitates obtained with FLAG antibodies were immunoblotted for either Ub to detect polyubiquitinated Skp2, marked as (Ub)n-Skp2. Control refers to cells infected with empty shRNA plasmid. Lysates were immunoblotted for Cdh1 and Ufd1 to confirm knockdown.

Figure 2-8: Ufd1 with internal deletion of amino acids 261-280 does not bind USP13 *in vivo*.

(A) HEK-293T cells were transfected with USP13 together with each of the following: empty vector, FLAG-Ufd1, the C-terminal truncation Ufd1 mutants FLAG-N260 and FLAG-N280 that have amino acids 1-260 and 1-280 respectively, and the internal deletion Ufd1 mutant of FLAG-Δ261-280 that lacks amino acids 261-280. FLAG immunoprecipitates were immunoblotted for USP13, p97, and FLAG. (B) Schematic depicting the binding capacity of the various Ufd1 C-terminal deletion mutants to USP13, Skp2, and p97 based on Figures 3A, 3D, and S3A. 'nd' means not determined. (C) Ufd1 targets free Skp2 proteins. *Left*, sequential immunoprecipitation of FLAG-Ufd1 and myc-Skp2 from HEK-293T cells followed by immunoblotting of endogenous Cul1. *marks the position of Cul1. *Right*, HA-Ufd1 was expressed with either FLAG-Skp2 or FLAG-Skp2ΔF-box in HEK-293T cells. FLAG-immunoprecipitates were immunoblotted for Ufd1. (D) Exogenous-endogenous coimmunoprecipitations. HeLa cells were transfected with empty vector, FLAG-Ufd1, or FLAG-USP13. FLAG immunoprecipitates were immunoblotted for endogenous Skp2.

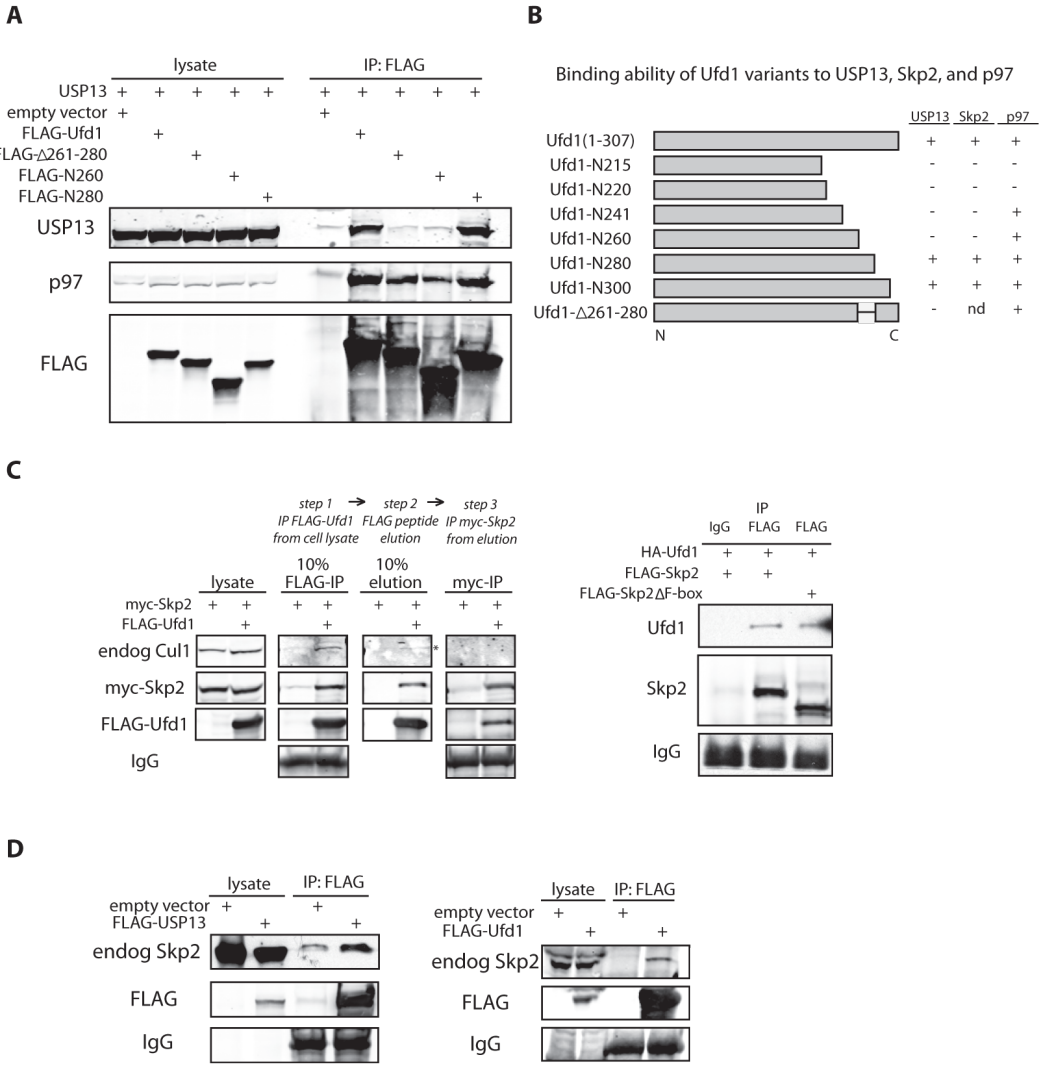
A
lysate
IP: FLAG
USP13
empty vector
FLAG-Ufd1
FLAG-Δ261-280
FLAG-N260
FLAG-N280
USP13
p97
FLAG
B
Binding ability of Ufd1 variants to USP13, Skp2, and p97
USP13 Skp2 p97
Ufd1(1-307) + + +
Ufd1-N215 - - -
Ufd1-N220 - - -
Ufd1-N241 - - +
Ufd1-N260 - - +
Ufd1-N280 + + +
Ufd1-N300 + + +
Ufd1-Δ261-280 - nd +
N
C
C
step 1 → IP FLAG-Ufd1 from cell lysate
step 2 → FLAG peptide elution
step 3 IP myc-Skp2 from elution
lysate
10% FLAG-IP
10% elution
myc-IP
myc-Skp2
FLAG-Ufd1
endog Cul1
myc-Skp2
FLAG-Ufd1
IgG
IP
IgG FLAG FLAG
HA-Ufd1
FLAG-Skp2
FLAG-Skp2ΔF-box
Ufd1
Skp2
IgG
D
lysate
IP: FLAG
empty vector
FLAG-USP13
endog Skp2
FLAG
IgG
lysate
IP: FLAG
empty vector
FLAG-Ufd1
endog Skp2
FLAG
IgG

Figure 2-9: USP13 exhibits DUB acitivity towards K48-linked di-ubiquitins.

(A) FLAG-USP13, immunopurified from HeLa cells and used in *in vitro* deubiquitination assays, was quantified against BSA standards by Coomassie staining. An estimated 20-30nM of FLAG-USP13 was used in each deubiquitination reaction (see Materials and Methods for details). (B) Deubiquitination of K48-linked di-ubiqutin substrates with internally-quenched fluorescence by USP13. 20-30nM of FLAG-USP13 immunopurified from HeLa cells were used per reaction with 200nM of substrate. Buffer only and FLAG immunoprecipitates from empty vector-transfected cells serve as controls. DUB activity was monitored over 60min by release of fluorescence (RFU). (C) USP13 was knocked-down by three individual shRNAs in HeLa cells (see Figure 4B for protein quantification of the same samples). USP13 transcripts were quantified by SYBR-green qRT-PCR. Amount of USP13 mRNA was normalized to cyclophilin and set as 100% in control cells.

A

Quantification of immunopurified FLAG-USP13 by signal intensity comparison using Coomassie stain

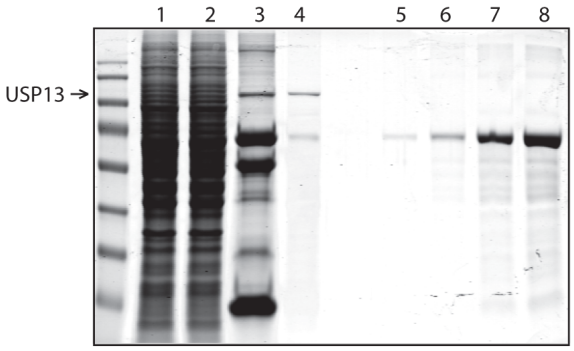

1: 60μg lysate, before IP
2: 60μg lysate, after IP
3: all FLAG-beads, after elution
4: 5% of total elution
(30% elution used per reaction)

5: BSA, 0.01μg
6: BSA, 0.1μg
7: BSA, 1μg
8: BSA, 3μg

An estimated 20-30nM of FLAG-USP13 were used in each deubiquitination reaction

B

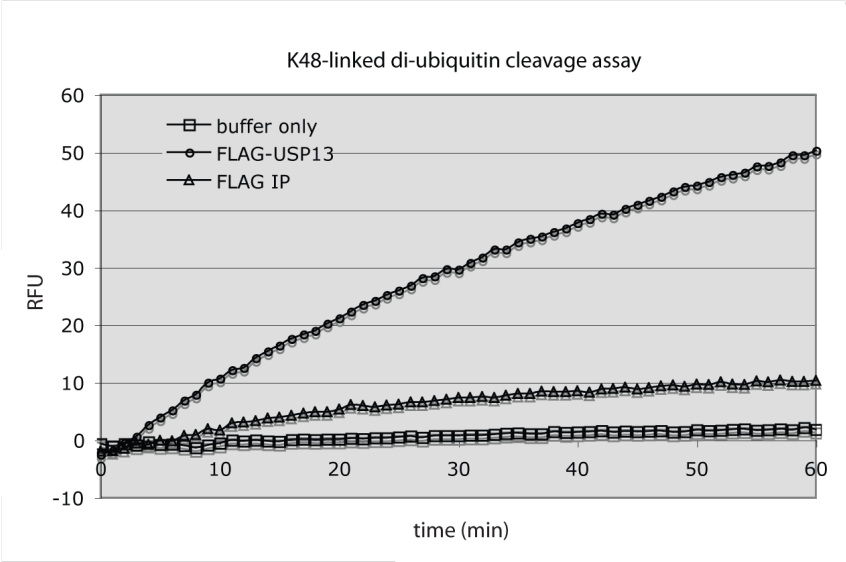

C

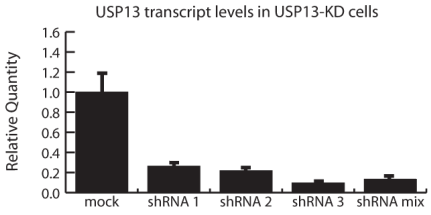

Figure 2-10: ER stress-dependent regulation of Ufd1-Skp2 and G1 cell cycle progression.

(A) Regulation of Ufd1-Skp2 by tunicamycin in different cell types. HeLa-S3, HeLa, HFF-1, and HEK-293T cells were treated with either DMSO (lane 1 of each panel) or tunicamycin (TM) (0.5, 1, or 2μg/ml) for 20h. *Top*, immunoblots of endogenous Ufd1, Skp2, and p27. *Bottom*, FACS analysis showing TM-induced G1 delay. In each pair of superimposed histograms, cell cycle profile of DMSO-treated cells is in red; cell cycle profile of 1μg/ml TM-treated cells is in blue. TM-induced G1 delay (blue histograms) is better visualized as a decrease in the S and G2/M populations. (B) Thapsigargin also regulates Ufd1-Skp2 and cell cycle. HeLa cells were treated with DMSO, increasing doses of tunicamycin (TM) (0.5, 1, 2.5, and 5μg/ml) or thapsigargin (TG) (0.5, 1, 2.5, and 5μM) for 16h. Total cell lysates were immunoblotted for the indicated proteins. *Bottom*, FACS histograms comparing G1 delay in cells treated with DMSO, 1μg/ml TM, or 1μM TG for 16h. (C) G1 cell cycle delay in response to tunicamycin is dose- and time-dependent. Control cells were treated with DMSO, 0.5μg/ml, or 2.5μg/ml of tunicamycin (TM) over a 24h time course. Samples were collected every 4h for immunoblotting (see Figure 5B) and cell cycle analysis by FACS. Graph quantifies percent increase in G1 under each condition. (D) Nuclear Ufd1 is targeted by prolonged ER stress. HeLa cells were treated with DMSO or 0.5μg/ml of tunicamycin (TM) and collected at the 0h, 24h, and 48h for cytoplasmic (cyto) and nuclear (nuc) fractionation. Fractions were immunoblotted for Ufd1 and Skp2. HSP90 served as a cytoplasmic marker and Lamin A/C served as a nuclear marker.

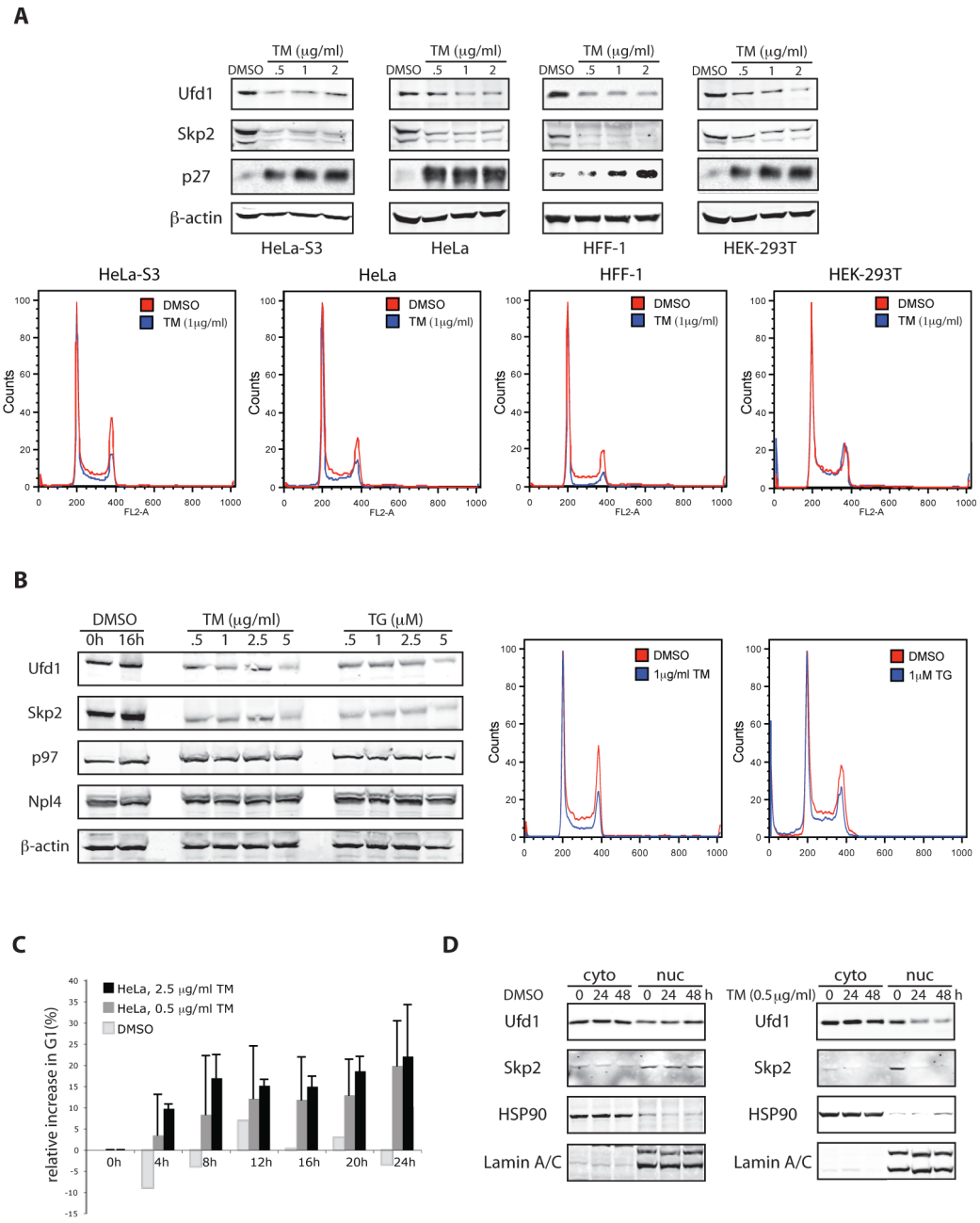
A
TM (μg/ml)
DMSO .5 1 2
Ufd1
Skp2
p27
β-actin
HeLa-S3
HeLa
HFF-1
HEK-293T
DMSO
TM (1μg/ml)
Counts
FL2-A
B
DMSO
0h 16h
TM (μg/ml)
.5 1 2.5 5
TG (μM)
Ufd1
Skp2
p97
Npl4
β-actin
1μg/ml TM
1μM TG
C
HeLa, 2.5 μg/ml TM
HeLa, 0.5 μg/ml TM
DMSO
relative increase in G1(%)
0h 4h 8h 12h 16h 20h 24h
D
cyto
nuc
DMSO
TM (0.5μg/ml)
0 24 48 0 24 48 h
Ufd1
Skp2
HSP90
Lamin A/C

Figure 2-11: APC/C^{Cdh1} mediates ER stress-dependent Skp2 degradation and subsequent p27 stabilization.

(A) HeLa cells transfected with empty shRNA vector or Cdh1-specific shRNA (for 24h) were treated with DMSO or 2.5μg/ml of tunicamycin (TM) alone or together with MG-132 (2 or 5μM) for 12h. Total cell extracts were immunoblotted for the indicated proteins. (B) Tunicamycin regulates the transcription of Skp2 and p27. Transcript levels of Ufd1, Skp2, and p27 in HeLa cells treated with either DMSO or 0.5μg/ml tunicamycin (TM) for 20h were quantified by SYBR-green qRT-PCR. Amount of each transcript was normalized to cyclophilin. (C) Ufd1 overexpression partially overcomes tunicamycin-induced G1 cell cycle delay. HeLa cells overexpressing empty vector or FLAG-Ufd1 were treated with DMSO or 1μg/ml of tunicamycin (TM) for 8h. Cell cycle profiles of DMSO- and TM-treated cells under each transfection condition were compared by FACS analysis. See figure 5D for quantification of the difference in the percentage of cells in G1 between DMSO- and TM-treated cells.

A

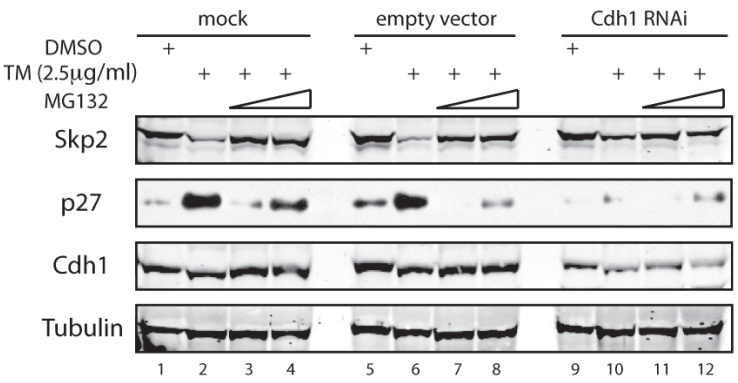
mock
empty vector
Cdh1 RNAi
DMSO
TM (2.5μg/ml)
MG132
Skp2
p27
Cdh1
Tubulin
1 2 3 4 5 6 7 8 9 10 11 12

B

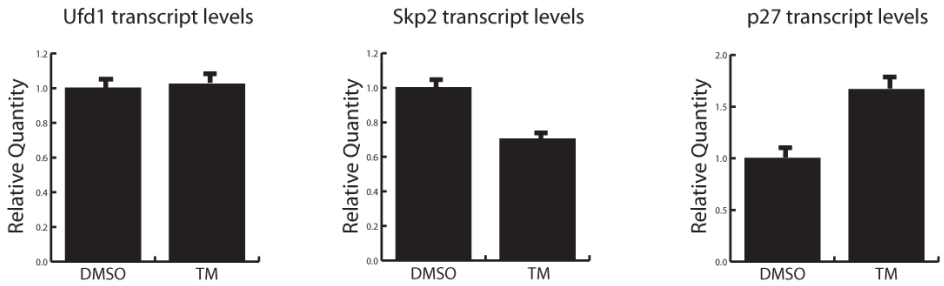
Ufd1 transcript levels
Skp2 transcript levels
p27 transcript levels
Relative Quantity
DMSO
TM

C

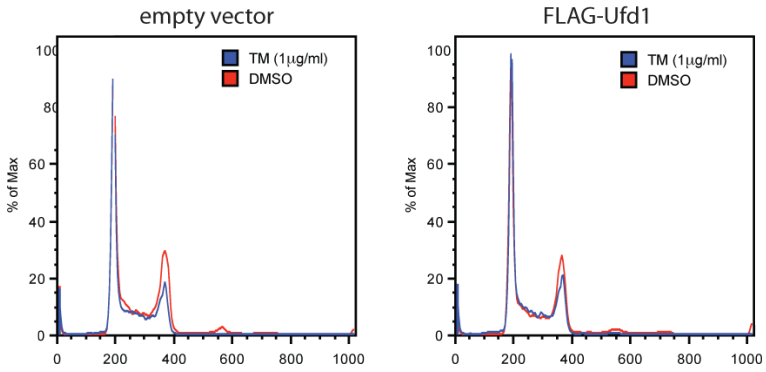
empty vector
FLAG-Ufd1
TM (1μg/ml)
DMSO
% of Max

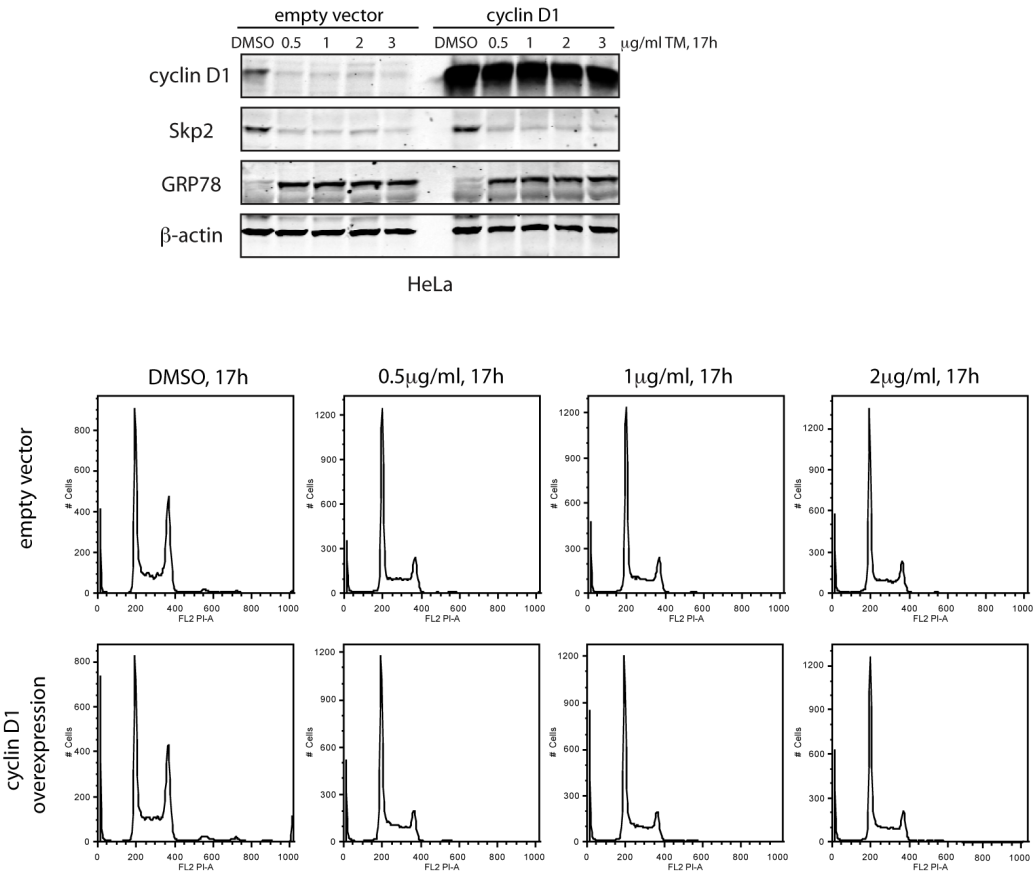

Figure 2-12: Cyclin D1 overexpression does not overcome tunicamycin-induced G1 cell cycle delay in HeLa cells.

HeLa cells transfected with empty vector or cyclin D1 were treated with DMSO or increasing concentrations of tunicamycin (TM) (0.5, 1, 2, and 3μg/ml) for 17h. Cells were collected for immunoblots of the indicated proteins and cell cycle analysis by FACS.

Figure 2-13: Enhanced clearance of NHK and CFTR in G1.

(A) Verification of cell cycle synchronization by FACS for Figure 5F. (B) Protein levels of GFP-CFTR and NHK detected by immunoblotting (Figure 5F) were quantified with the Odyssey software (LiCOR), normalized to loading controls, and presented as a percentage of the amount of corresponding proteins at time 0h of cycloheximide (CHX) treatment (set as 100%). (C) Verification of cell cycle synchronization by FACS for Figure 5G. (D) Protein levels of NHK detected by immunoblotting (Figure 5G) were quantified with the Odyssey software (LiCOR), normalized to HSP90, and presented as a percentage of the amount of NHK protein at time 0h of cycloheximide (CHX) treatment (set as 100%).

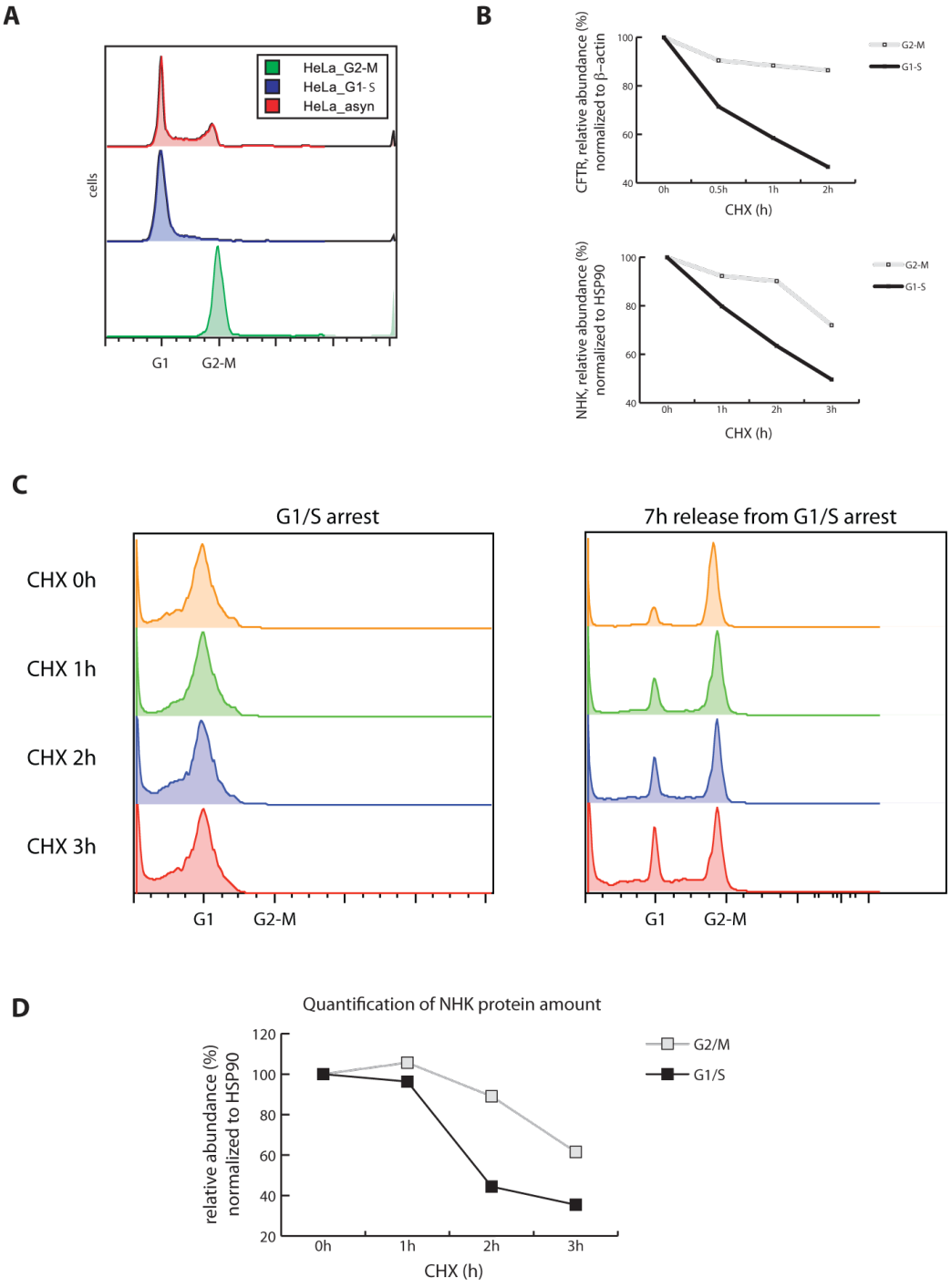
A
HeLa_G2-M
HeLa_G1-S
HeLa_asyn
cells
G1
G2-M
B
CFTR, relative abundance (%) normalized to β–actin
100
80
60
40
0h
0.5h
1h
2h
CHX (h)
G2-M
G1-S
NHK, relative abundance (%) normalized to HSP90
100
80
60
40
0h
1h
2h
3h
CHX (h)
G2-M
G1-S
C
G1/S arrest
7h release from G1/S arrest
CHX 0h
CHX 1h
CHX 2h
CHX 3h
G1
G2-M
G1
G2-M
D
Quantification of NHK protein amount
relative abundance (%) normalized to HSP90
120
100
80
60
40
20
0h
1h
2h
3h
CHX (h)
G2/M
G1/S

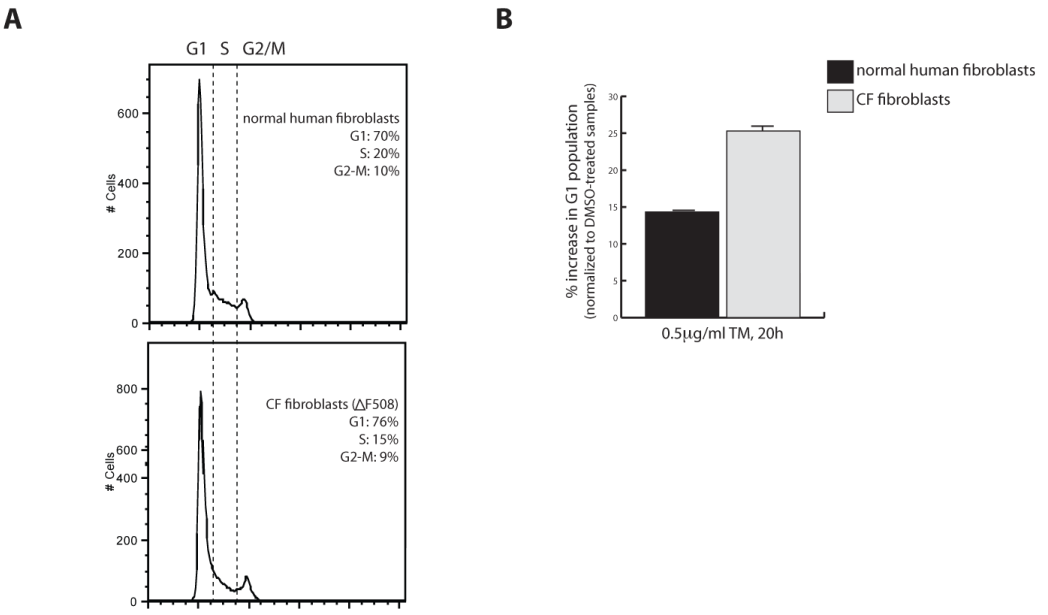

Figure 2-14: Increased G1 and hypersensitivity to tunicamycin in cells from cystic fibrosis-affected individual.

(A) FACS analysis of steady state cell cycle profiles of normal human fibroblasts (BJT) and fibroblasts from cystic fibrosis (CF)-affected individual homozygous for CFTR-ΔF508 mutation (CF fibroblasts). (B) Graph quantification of percent increase in G1 in normal human and CF fibroblasts treated with DMSO or 0.5µg/ml tunicamycin (TM) for 20h. Values shown were normalized to the percentage of cells in G1 in DMSO-treated samples.

Materials and Methods

Sequential immunoprecipitations

HeLa cells were transfected with FLAG-Ufd1, myc-Skp2, and USP13 or USP13 alone (negative control). FLAG-Ufd1 was immunoprecipitated from 8mg of total lysate by incubation with anti-FLAG M2 beads for 2h at 4°C, washed three times in IP buffer and twice in TBS, then eluted with 500µg/ml of 3xFLAG peptide. Eluate was subsequently used for IP of myc-Skp2 for 8h at 4°C. Beads were washed three times in IP buffer, run on SDS-PAGE, and immunoblotted for USP13, Skp2, and Ufd1.

Cell culture and transfection

HeLa, HeLa-S3, HEK-293T, and melanoma CHL1 cells were grown in DMEM with 10% bovine serum at 37°C with 5% CO2. HFF-1, BJT, and cystic fibrosis fibroblasts (purchased from Coriell Cell Repositories –GM01348) were grown in DMEM with 10% fetal bovine serum. HeLa cells stably expressing Ufd1-specific or USP13-specific shRNAs (Sigma MISSION pLKO.1-Puro[3] shRNA bacterial glycerol stock) were prepared by lentiviral infection (lentiviral particles packaged with the shRNA vectors were generated in HEK-293T cells) and selected with 1µg/ml of puromycin. Drug-selected pools were isolated and the efficiency of knockdown was validated by qRT-PCR and immunoblotting for expression of Ufd1 or USP13. HeLa cells infected with empty pLKO.1-Puro[3] vector served as control. Analysis of individual drug-resistant Ufd1-KD pools confirmed the major biochemical phenotypes shown in Figure 1B (see Figure S2).

For transient transfection of plasmids in HeLa cells, 80%-confluent cells grown in 10cm dishes were transfected with 5µg of each of the indicated plasmids, using Lipofectamine 2000 (Invitrogen) following manufacturer's protocols. Cells were harvested within 24-36h after transfection. For transient transfection of siRNA, 60%-confluent cells grown in 60mm-plates were transfected with 100nM of siRNA with RNAiMAX (Invitrogen) according to vendor's specification. Non-specific siRNA served as a control. For transient transfection in HEK-293T

cells, 50%-confluent cells grown in 10cm dishes were transfected with 10μg of DNA-calcium phosphate complexes, generated by bubbling the DNA, $CaCl_2$, and HEPES-buffered saline mixture. Cells were analyzed 24h after transfection.

Expression plasmids

Ufd1 was subcloned from pET26-Ufd1-His, a generous gift from Dr. Hemmo Meyer (Institute of Biochemistry, Zurich, Switzerland), into pGEX4T3. Ufd1 (a 940bp insert including restriction sites for BamH1 on the 5' end and EcoRV on the 3' end) was sub-cloned into the BamH1-EcoRV sites of either the pEF-FLAG vector or the pEF-HA vector for mammalian expression. C-terminal truncation variants of pEF-FLAG-Ufd1 (N215, N220, N241, N260, N280, and N300) were generated by insertion of 2 stop codons after the indicated amino acid from the N-terminus using site-directed mutagenesis; pEF-FLAG-ΔUfd1-261-280 was generated by site-directed mutagenesis (Stratagene, QuikChange Site-Directed Mutagenesis Kit). Integrity of all constructs was confirmed by sequencing. pCDNA3-FLAG-Skp2 and pCDNA3-FLAG-Skp2ΔF-box were a generous gift from Dr. Michele Pagano (New York University, NY, USA). pCDNA-myc-Skp2 was a generous gift from Dr. Dieter Wolf (Sanford-Burnham Medical Research Institute, La Jolla, USA). pEF-HA-Ubiquitin vector has been previously described [24]. pCMV6-XL-USP13 was obtained from OriGene (SC117705) and cloned into pEF-FLAG vector using the restriction enzymes SmaI (5') and NotI (3'). pSUPER-Cdh1-shRNA was a generous gift from Dr. Reuven Agami (The Netherlands Cancer Institute, Amsterdam, Netherlands). pLKO.1-USP13-shRNAs were purchased from Open Biosystems (RHS4533). pRS-p27-shRNA and control pRS-shRNAs were purchased from OriGene (TR314022). GFP-CFTR and pCDNA3-NHK constructs were generous gifts from Dr. Ron Kopito (Stanford University, Stanford, USA). pPL8-cyclin D1 (from mouse) was a generous gift from Dr. Per Hydbring (Dana Farber Cancer Institute, Boston, USA).

siRNA/shRNA target sequences

CDKN1B/p27-shRNAs

CGGCTAACTCTGAGGACACGCATTTGGTG

AAGGAAGCGACCTGCAACCGACGATTCTT

Ufd1-shRNAs

CTGGCAATAGACTGGATGGAA

TGGGCTACAAAGAACCCGAAA

CAGCCGACTTAACATTACCTA

CCCAATCAAGCCTGGAGATAT

Ufd1-3'UTR-siRNAs

CAGCAGGAGCAATTCTGCATCCCTA CCTATGAAGGTGACTAAATTGTCTA

USP13-shRNAs

CGCCTGATGAACCAATTGATA

CGATTTAAATAGCGACGATTA

CCGGTGAAATCTGAACTCATT

Cdh1-shRNA (previously published by Brummelkamp TR *et al*, Science, 2002).

Antibodies

Commercially available antibodies used were as follows: Ufd1L (19– BD Transduction Laboratories, used at 1:2000 dilution), Skp2 (H-435– Santa Cruz at 1:500), p27 (57– BD Transduction Laboratories at 1:500), Cdh1 (DCS-266– Abcam at 1:1000), cyclin B1 (GNS1– Santa Cruz at 1:1000), cyclin E2 (1142-1– Epitomics at 1:1000), Cdk2 (M2– Santa Cruz at 1:500), GRP78 (N-20– Santa Cruz at 1:1000), FLAG (M2– Sigma at 1:5000), GFP (mouse– Zymed at

1:1000), α1-antitrypsin/NHK (mouse– US Biological at 1000), Ubiquitin (FL-76– Santa Cruz at 1:1000), c-myc (9E10– Santa Cruz at 1:2000), USP13 (HPA004827– Sigma at 1:1000 and 2141C– Abgent at 1:500), HSP90 (F-8– Santa Cruz at 1:1000), Lamin A/C (636– Santa Cruz at 1:1000), cyclin D1 (2922– Cell Signaling at 1:1000), Npl4 (H-300– Santa Cruz at1:1000), p97 (ab19444– Abcam at 1:1000), and tubulin (TU-02– Santa Cruz at 1:2000).

Immunoblotting and immunoprecipitation

For western-blots of total cell lysates, cells were detached from plates with 0.05% trypsin-EDTA, washed with cold PBS, and lysed on ice for 20min after resuspension in IP buffer (50mM Tris-HCl [pH=7.5], 150mM NaCl, 0.5% NP-40, 5mM EDTA, 5mM EGTA, 20mM NaF, 100µM sodium-orthovanadate, 2mM β-glycerophosphate, 1mM DTT, 1mM PMSF, 4mg/ml aprotinin, 100µM leupeptin, and 2mg/ml pepstatin A). After 20min centrifugation (13200rpm, 4ºC), supernatants were saved and protein concentration was performed using Coomassie Plus protein assay reagent (Thermo).

For co-immunoprecipitation *in vivo*, cells expressing the proteins of interest for 24h were washed with cold PBS and lysed with IP buffer. Target protein was immunoprecipitated from total cell lysates containing 2mg of protein with 1µg of target-specific antibody overnight at 4ºC in a rotating wheel, followed by incubation with 30µl of a 50% slurry of protein G-agarose for 2h at 4°C with rotation. Immunoprecipitates were washed 4 times with IP buffer, resuspended in loading buffer and analyzed by SDS-PAGE and western-blotting.

Cell cycle synchronization and fluorescence-activated cell sorting (FACS)

For G1/S synchronization of HeLa cells by double thymidine block: cells were incubated with 2mM thymidine for 18h, released into fresh media for 12h and then incubated with 2mM thymidine again for 16h. Cells were then washed twice with PBS and given fresh media to release from the arrest. For G2/M synchronization by thymidine-nocodazole block: HeLa cells were

incubated with 40ng/ml of nocodazole for 16h following release from the first thymidine block as detailed above.

For cell cycle analysis by FACS, cells were washed with cold PBS, fixed with 70% ethanol in PBS for 1h at -20°C, and washed again with cold PBS. Cells were then incubated with PBS with 50µg/ml propidium iodide and 100µg/ml RNase A for 1h at room temperature. DNA content was analyzed by 3 color-FACS and quantification of G1, S, and G2/M populations was performed with the help of FlowJo software.

SYBR-green qRT-PCR

Total RNA was extracted from cells grown in 10cm plates (Sigma, RTN70-1KT). Up to 2µg of total RNA was used per 20µl cDNA reverse transcription (Applied Biosystems, High-Capacity cDNA Reverse Transcription Kit). 5µl of 20% v/v diluted cDNA was used per 25µl qRT-PCR with SYBR GreenER qPCR SuperMix Universal (Invitrogen) and target gene-specific primers. 40 cycles of qPCR and analysis were performed using Stratagene Mx3000p. Human cyclophilin or GAPDH was used as a control to normalize transcript levels of experimental samples. Specificity of all primer sets were validated by dissociation curve. qPCR primer sequences are as follows:

Ufd1

Forward 1-GAGGGAAGATAATTATGCCAC

Reverse 1-CTTCCAAGAGTAAGTTCTGC

Forward 2-GAGGGAAGAGCCGACTTAAC

Reverse 2-CTCTGAGGTTGGAATTTGGAG

Forward 3-GACATGAACGTGGACTTTG

Reverse 3-GGAATTCCTCTTTTAATATC

Forward 4-GGGCCTAATGACAGGTCAG

Reverse 4-CTTGAAGGTTGACGCTCTCC

Skp2

Forward-GCTATGCACAGGAAGCACCT

Reverse-CCCATGAAACACCTGGAAAG

p27

Forward-CGGCTAACTCTGAGGACACG

Reverse-CTTAATTCGAGCTGTTTACG

USP13

Forward-GCATGGGACAGAGAATGGGC

Reverse-CCTAACTTAGTCATCTGTGTG

Cyclophilin

Forward-GACCCAACACAAATGGTTC

Reverse-AGTCAGCAATGGTGATCTTC

GAPDH

Forward-GAAGGTGAAGGTCGGAGTC

Reverse-ATGGGATTTCCATTGATGAC

Cdk kinase assays

Cells were synchronized in G1 and released into fresh media. At the indicated time-points, cells were harvested and lysed with modified IP buffer (0.1% NP-40, 25mM Tris-HCl

[pH=7.5], 50mM NaCl, 5mM EGTA, 60mM β-glycerophosphate, 20mM NaF, 100μm sodium-orthovanadate, 1mM DTT, 1mM PMSF, 100μM leupeptin, and 4mg/ml aprotinin). Approximately 5mg of total cell lysate were used to immunoprecipitate either CDK2 or CDK1, with 0.5μg of CDK2 antibody or 0.5μg of cyclin B1 antibody, respectively. Immunoprecipitates were washed three times with histone H1 buffer (15mM MgCl2, 20mM EGTA, 80mM β-glycerophosphate [pH=7.4], 1mM DTT, 1mM PMSF, 4mg/ml aprotinin, and 100μM leupeptin). Kinase reactions were performed by incubating each pellet with 35μl of histone H1 buffer supplemented with 0.1μg histone H1, 0.2μl ^{32}P-γATP and 50μM ATP. Reactions were incubated for 30min at 30°C in a shaker at 800rpm and then stopped with sample buffer and heat-denatured. Samples were run in SDS-PAGE gel, dried, and analyzed by PhosphorImager.

APC/C^{Cdh1}-dependent degradation assay

Interphase *Xenopus laevis* egg extracts were prepared as previously described [25] and supplemented with 6xHis-Cdh1 protein purified from pelleted baculovirus-infected insect cells (a generous gift from Olivier Coux, CRBM-CNRS, Montpellier, France). Skp2 protein was *in vitro* translated with [^{35}S]-methionine and added to the extract for degradation assays as previously described [25], in the presence of bacterially purified GST-Ufd1 as indicated. A sample of this mixture was recovered at the indicated times and the levels of ^{35}S-Skp2 were analyzed by PhosphorImager.

In vivo ubiquitination assays

After co-transfecting HeLa cells with myc-Skp2 and HA-Ub plasmids for 24h, cells were treated with 5μM MG-132 for 5h, then harvested and resuspended in 50μl of cold Tris buffered saline (TBS) buffer (10mM Tris-HCl [pH=8]), followed by 60μl of 2% SDS in TBS. Suspension was heat denatured for 10min and cooled on ice for 5min. 900μl of 1% Triton X-100 in TBS supplemented with protease inhibitors were added to the mixture and sonicated. Mixture was spun down and 2mg of supernatant were incubated with 1μg of c-myc antibody rotating overnight at

4°C, followed by an additional 1h of incubation with 30µl of a 50% slurry of G-protein agarose. Precipitates were washed once with 1ml 1% Triton X-100 and 0.1% SDS in TBS, twice with 0.5M LiCl and 1% Triton X-100 in TBS, and once with 1% Triton X-100 in PBS.

Deubiquitination assays

Internally quenched fluorescence-diubiquitin (IQF-DiUb, K48-2) of K48 linkage was from LifeSensors. FLAG-USP13 was expressed and immunoprecipitated from HeLa cells using anti-FLAG M2 affinity gel (Sigma, A2220), washed three times in IP buffer and twice in TBS (25mM Tris-HCl [pH=7.6], 150mM NaCl, 1mM DTT), then eluted with 500µg/ml of 3xFLAG peptide (Sigma, F4799). Immunopurified FLAG-USP13 was quantified against BSA by Coomassie staining (Figure S4A). 20-30nM USP13 were used per reaction with 200nM K48-linked DiUb in assay buffer (50mM Tris-HCl [pH=8.0], 10mM DTT) in a 96-well plate (Greiner BioONE 655076). 60min kinetic reads were performed at 25°C using a FlexStation 3 spectrometer with 540/580nm excitation/emission and mirror cut-off of 570nm. Results were analyzed by SoftMax Pro.

For deubiquitination of Skp2 by USP13, myc-Skp2 and HA-Ubiquitin were coexpressed in HeLa cells. Cells were treated with 20µM MG-132 for 3h before lysis and IP using c-myc antibodies conjugated to agarose beads. Immunoprecipitates were washed three times in IP buffer and twice in TBS. FLAG-USP13 was immunopurified separately (see above). 20-30nM of USP13 was incubated with Skp2 for 1h at 25°C. Reactions were stopped by addition of sample buffer, ran on SDS-PAGE, and immunoblotted with Ub and Skp2 antibodies.

Cycloheximide and degradation assays

Asynchronous Hela cells were treated with 25µg/ml cycloheximide (CHX) and collected at the indicated times after addition of CHX for immunoblot analysis of proteins of interest. For analysis of half-life of NHK and GFP-CFTR in synchronized cell cultures, cells were first arrested in G1/S by double thymidine block or in G2/M by thymidine-nocodazole block, transfected with

either NHK or GFP-CFTR during the release after the first thymidine treatment, followed by addition of 25μg/ml cycloheximide to G1/S- or G2/M-arrested cells. Finally, cells were harvested at the indicated time-points after CHX addition for immunoblot analysis.

Cytosolic and nuclear fractionation

Fractionation was performed using reagents from the Nuclear Extract Kit (Active Motif, 40010). Briefly, cells were detached from plates with 0.05% trypsin-EDTA and washed with cold PBS. Cells were first lysed with a Hypotonic Buffer. Centrifugation yielded the cytosolic fraction as the supernatant and the nucleus fraction as the pellet. The nuclear pellet was further lysed with Complete Lysis Buffer to yield the nuclear extract, following manufacturer's instructions.

Acknowledgements

We thank R. Agami, O. Coux, P. Hydbring, R. Kopito, H. Meyer, M. Pagano, D. Ron, and D. Wolf for essential reagents used in this study (as detailed in Materials and Methods). We also thank Y. Altman for help with FACS analysis and members of the Ronai lab for stimulating discussions. This work was supported by NCI grants CA097105 and CA78419 to ZR. MC has been part of the Molecular Pathology Ph.D. Program at University of California, San Diego and supported in part by a Molecular Pathology Cancer Training Grant (5T32CA077109). GJG was supported in part by a Sass Foundation post-doctoral fellowship. Chapter 2, in full, has been submitted as it may appear in Proceedings of the National Academy of Sciences, 2011, Chen, Meifan; Gutierrez, Gustavo J., Ronai, Ze'ev A. The dissertation author was the primary investigator and author of this paper. Specifically, the dissertation author performed experiments and analyzed data.

References

1. Johnson ES, Ma PC, Ota IM, & Varshavsky A (1995) A proteolytic pathway that recognizes ubiquitin as a degradation signal. *J Biol Chem* 270(29):17442-17456.

2. Park S, Isaacson R, Kim HT, Silver PA, & Wagner G (2005) Ufd1 exhibits the AAA-ATPase fold with two distinct ubiquitin interaction sites. *Structure* 13(7):995-1005.

3. Ye Y, Meyer HH, & Rapoport TA (2001) The AAA ATPase Cdc48/p97 and its partners transport proteins from the ER into the cytosol. *Nature* 414(6864):652-656.

4. Cao J*, et al.* (2007) Ufd1 is a cofactor of gp78 and plays a key role in cholesterol metabolism by regulating the stability of HMG-CoA reductase. *Cell Metab* 6(2):115-128.

5. Bays NW, Wilhovsky SK, Goradia A, Hodgkiss-Harlow K, & Hampton RY (2001) HRD4/NPL4 is required for the proteasomal processing of ubiquitinated ER proteins. *Mol Biol Cell* 12(12):4114-4128.

6. Ballar P, Shen Y, Yang H, & Fang S (2006) The role of a novel p97/valosin-containing protein-interacting motif of gp78 in endoplasmic reticulum-associated degradation. *J Biol Chem* 281(46):35359-35368.

7. Lin PH, Chiang MT, & Chau LY (2008) Ubiquitin-proteasome system mediates heme oxygenase-1 degradation through endoplasmic reticulum-associated degradation pathway. *Biochim Biophys Acta* 1783(10):1826-1834.

8. McConnell E, Lass A, & Wojcik C (2007) Ufd1-Npl4 is a negative regulator of cholera toxin retrotranslocation. *Biochem Biophys Res Commun* 355(4):1087-1090.

9. Nowis D, McConnell E, & Wojcik C (2006) Destabilization of the VCP-Ufd1-Npl4 complex is associated with decreased levels of ERAD substrates. *Exp Cell Res* 312(15):2921-2932.

10. Ramadan K*, et al.* (2007) Cdc48/p97 promotes reformation of the nucleus by extracting the kinase Aurora B from chromatin. *Nature* 450(7173):1258-1262.

11. Cao K, Nakajima R, Meyer HH, & Zheng Y (2003) The AAA-ATPase Cdc48/p97 regulates spindle disassembly at the end of mitosis. *Cell* 115(3):355-367.

12. Carrano AC, Eytan E, Hershko A, & Pagano M (1999) SKP2 is required for ubiquitin-mediated degradation of the CDK inhibitor p27. *Nat Cell Biol* 1(4):193-199.

13. Pines J (2006) Mitosis: a matter of getting rid of the right protein at the right time. *Trends Cell Biol* 16(1):55-63.

14. Peters JM (2006) The anaphase promoting complex/cyclosome: a machine designed to destroy. *Nat Rev Mol Cell Biol* 7(9):644-656.

15. Gutierrez GJ & Ronai Z (2006) Ubiquitin and SUMO systems in the regulation of mitotic checkpoints. *Trends Biochem Sci* 31(6):324-332.

16. Wei W*, et al.* (2004) Degradation of the SCF component Skp2 in cell-cycle phase G1 by the anaphase-promoting complex. *Nature* 428(6979):194-198.

17. Bashir T, Dorrello NV, Amador V, Guardavaccaro D, & Pagano M (2004) Control of the SCF(Skp2-Cks1) ubiquitin ligase by the APC/C(Cdh1) ubiquitin ligase. *Nature* 428(6979):190-193.

18. Sowa ME, Bennett EJ, Gygi SP, & Harper JW (2009) Defining the human deubiquitinating enzyme interaction landscape. *Cell* 138(2):389-403.

19. Bruderer RM, Brasseur C, & Meyer HH (2004) The AAA ATPase p97/VCP interacts with its alternative co-factors, Ufd1-Npl4 and p47, through a common bipartite binding mechanism. *J Biol Chem* 279(48):49609-49616.

20. Catic A*, et al.* (2007) Screen for ISG15-crossreactive deubiquitinases. *PLoS One* 2(7):e679.

21. Brewer JW, Hendershot LM, Sherr CJ, & Diehl JA (1999) Mammalian unfolded protein response inhibits cyclin D1 translation and cell-cycle progression. *Proc Natl Acad Sci U S A* 96(15):8505-8510.

22. Brewer JW & Diehl JA (2000) PERK mediates cell-cycle exit during the mammalian unfolded protein response. *Proc Natl Acad Sci U S A* 97(23):12625-12630.

23. Christianson JC, Shaler TA, Tyler RE, & Kopito RR (2008) OS-9 and GRP94 deliver mutant alpha1-antitrypsin to the Hrd1-SEL1L ubiquitin ligase complex for ERAD. *Nat Cell Biol* 10(3):272-282.

24. Morito D*, et al.* (2008) Gp78 cooperates with RMA1 in endoplasmic reticulum-associated degradation of CFTRDeltaF508. *Mol Biol Cell* 19(4):1328-1336.

Chapter 3 : APC/C^{Cdh1} regulates ER stress-dependent G1 delay

Abstract

APC/C^{Cdh1} regulates exit from mitosis and G1 phase of the cell cycle. Although much is known about its regulation and function in unperturbed cell cycle, data supporting its role in executing stress-induced checkpoint response is scarce. Here, we provide evidence for ER stress-dependent activation of APC/C^{Cdh1} that leads to cell cycle delay in G1 independently of the p53 and cyclin D1 pathways. We demonstrate that ER stress activates APC/C^{Cdh1} both by promoting the association of the APC/C core to the coactivator Cdh1 and post-transcriptionally downregulating its inhibitor Emi1. This leads to the degradation of APC/C^{Cdh1} substrates in ER stressed-cells, concomitant with G1 cell cycle arrest that can be largely overcome by depletion of Cdh1. Our findings reveal the potential role of APC/C^{Cdh1} as a key effector of checkpoint responses activated by ER stress.

Introduction

The anaphase promoting complex or cyclosome (APC/C) is a multisubunit ubiquitin ligase that regulates the progression of mitosis and establishment of G1 in the cell cycle through sequential activation by the substrate adaptors Cdc20 and Cdh1[1]. APC/C^{Cdc20} initiates anaphase and mitotic exit by targeting securin and mitotic cyclins for ubiquitin-dependent proteasomal degradation. The switch from APC/C^{Cdc20} to APC/C^{Cdh1} in late mitosis continues the destruction of mitotic proteins including cyclin B, polo-like kinase (Plk1), and Cdc20 itself to complete mitosis and establish G1. Sequential assembly of APC/C^{Cdc20} and APC/C^{Cdh1} depends on their differential regulation by the mitotic cyclin-dependent kinases (Cdks): Cdk-dependent phosphorylation of the APC/C core promotes association with Cdc20, whereas phosphorylation of Cdh1 inhibits its binding to the APC/C core[2,3]. This renders APC/C^{Cdc20} active in mitosis when Cdk activities are high and APC/C^{Cdh1} active in telophase and Cdk activities decline. Opposing the Cdk-mediated inhibitory phosphorylation on Cdh1 is the phosphatase Cdc14[4,5]. In addition, binding of inhibitors like the early mitotic inhibitor (Emi1) keeps the activity of the APC/C in check[6]. Recently, nuclear

PTEN has been shown to positively regulate APC/C^{Cdh1} by facilitating the association between Cdh1 and APC/C in a phosphatase-independent manner[7].

Given the critical roles that the APC/C plays in cell cycle control, one would expect it to be a major target of checkpoint signaling that modulates cell cycle progression in response to internal and environmental stimuli. Surprisingly, besides the regulation of APC/C^{Cdc20} by the spindle assembly checkpoint that ensures proper chromosomal segregation only when all sister chromatids are attached to the mitotic spindle[8], evidence demonstrating the APC/C as a target of checkpoint responses to cellular stressors is lacking. A few studies point to the control of APC/C by genotoxic stress in mammalian cells. It was shown that ionizing radiation activates the APC/C to degrade cyclin D1, which triggers an immediate p53-independent G1 arrest[9]. DNA damage incurred in G2 has also been reported to activate APC/C^{Cdh1} that specifically targets Plk1 for degradation, resulting in G2 arrest through the stabilization of Claspin[5,10]. In the latter case, DNA damage-induced translocation of Cdc14B from the nucleolus to the nucleoplasm is responsible for the activation of APC/C^{Cdh1} in G2. While these findings support the role of APC/C as an effector of checkpoint responses, they reveal a limitation in our understanding of stress-induced regulation of the APC/C that is currently confined to the context of DNA damage.

In this study, we explored APC/C-dependent regulation of the ER stress checkpoint. ER stress occurs when there is an imbalance between the demand for protein folding and ER capacity. This disequilibrium in ER homeostasis can result from physiological fluctuations in protein synthesis or pathological accumulation of misfolded proteins. ER stress activates an adaptive program coordinated by ATF6, IRE1, and PERK aimed to restore homeostasis by upregulation of chaperones to facilitate protein folding, global inhibition of translation to reduce protein synthesis, activation of ER-associated degradation to remove misfolded proteins, and induction of apoptosis when perturbations in the ER cannot be resolved[11]. It is becoming clear that ER stress also causes cell cycle arrest that is suggested to provide time for repair. It has been shown that the mammalian ER stress checkpoint delays cell cycle progression through G1 via the following pathways: donwregulation of cyclin D1 by PERK-mediated translational repression and proteolysis[12] and

transcriptional induction of p21 via PERK-dependent stabilization of p53[13]. Both the p53- and cyclin D1-dependent checkpoint responses converge at the inactivation of Cdk2 complexes by the Cdk inhibitor p21 to delay progression through G1 phase.

Intriguingly, p53-deficient HeLa cells still exhibit G1 arrest in response to ER stress that cannot be overcome by the overexpression of cyclin D1 (unpublished data, Chapter 2 of dissertation), indicating the presence of p53- and cyclin D1-independent pathways in the control of the ER stress checkpoint. We previously identified one such pathway involving the accumulation of p27, also an inhibitor of the Cdk2 complexes, as a result of reduced deubiquitination and transcriptional downregulation of Skp2. This pathway, however, only partially contributes to ER stress-induced cell cycle arrest in HeLa cells, suggesting that the ER stress checkpoint in these cells engages additional cell cycle regulators.

Here, we identify activation of APC/C^{Cdh1} as a key component of the p53- and cyclin D1-independent ER stress checkpoint response that delays cell cycle progression through G1. Our study provides evidence for ER stress-dependent regulation of APC/C^{Cdh1}, which is required to establish cell cycle delay. Our findings also reveal the potential of the APC/C to mediate a range of stress-induced checkpoint responses wider than previously anticipated.

Results

ER stress activates APC/C^{Cdh1}

To identify the cell cycle effectors responsible for establishing ER stress-induced G1 arrest independently of p53 and cyclin D1, we first looked for cell cycle proteins whose expression change in response to ER stress in HeLa cells. When cells were treated with tunicamycin (TM), an ER stress inducer that inhibits glycosylation of newly synthesized glycoproteins, we observed a marked decrease in the protein levels of endogenous cyclin B1 and Plk1, both of which are substrates of APC/C^{Cdh1} (Figure 3-1A). This suggests ER stress-induced activation of APC/C^{Cdh1}. Notably, the protein level of Cdh1 itself was also reduced under ER stress, likely because of the ability of APC/C^{Cdh1} to target itself for proteasomal degradation[14]. The

steady downregulation of exogenous myc-Cdh1 in HeLa cells upon TM treatment demonstrates that ER stress destabilizes Cdh1 protein (Figure 3-1B, *Left*), as opposed to decreasing its transcription, which was found to be constant before and after TM treatment (Figure 3-1B, *Right*). Taken together, these results suggest ER stress-dependent activation of APC/C^{Cdh1} that leads to the downregulation of its substrates, including its adaptor/activator Cdh1.

Depletion of Cdh1 overcomes ER stress-induced G1 delay

To test whether ER stress activates APC/C^{Cdh1} to target its substrates for proteasome-mediated degradation, we compared the protein level of Plk1 and Cdh1 in cells treated with TM alone and cells co-treated with both TM and MG-132, a proteasome inhibitor. TM downregulated both Plk1 and Cdh1, which could be prevented by co-treatment with MG-132 (Figure 3-2A, compare lanes 1-4), indicating accelerated degradation of Plk1 and Cdh1 by proteasomes under ER stress conditions. In addition, depletion of Cdh1 by RNA interference (RNAi) alone reduced the loss of Plk1 in TM-treated cells (Figure 3-2A, compare lanes 6 and 10), supporting our hypothesis that ER stress activates APC/C^{Cdh1}.

Given our observations that Cdh1 depletion can biochemically rescue the effects of TM on the cell cycle, we proceeded to determine the extend to which Cdh1 depletion can overcome ER stress-dependent G1 arrest. We treated asynchronous control-transfected or Cdh1-shRNA-transfected cells with TM for either 8 hours or 16 hours (Figure 3-2B and Figure 3-2C, immunoblots), followed by analysis of cell cycle distribution by fluorescence activated cell sorting (FACS). As previously shown (unpublished data, Chapter 2), ER stress induces cell cycle arrest in a time-dependent manner (Figure 3-2B and Figure 3-2C, *Bottom* FACS histograms and quantification showing TM-dependent G1 increase in empty vector-transfected cells). Regardless of the length of TM treatment, depletion of Cdh1 almost completely overcame TM-induced G1 arrest (Figure 3-2B and Figure 3-2C, *Bottom* FACS histograms and quantification showing TM-dependent G1 increase in Cdh1-RNAi cells). These findings identify APC/C^{Cdh1} as a key regulator of ER stress-dependent G1 arrest.

ER stress promotes binding of Cdh1 to the APC/C core

ER stress-dependent activation of APC/C^{Cdh1} is not a result of Cdh1 upregulation, because not only does ER stress have no effect on the transcription of Cdh1, but it accelerates the destruction of the Cdh1 protein via self-ubiquitination (Figure 3-1A, Figure 3-1B, Figure 3-2A). This points to post-translational regulation of APC/C^{Cdh1} activity under ER stress conditions.

Because complex formation between the APC/C core and Cdh1 is a prerequisite to APC/C^{Cdh1} activation, we tested whether ER stress promotes the assembly of APC/C^{Cdh1}. Strikingly, although TM treatment reduced the protein level of Cdh1, it enhanced the association between endogenous Cdh1 and the APC/C core subunit Cdc27 (Figure 3-3A, compare lanes 4 and 5). In contrast, co-treatment with TM and MG-132 reversed the positive effect of TM alone on the complex formation of APC/C^{Cdh1} (Figure 3-3A, compare lanes 4-6), despite the stabilization of Cdh1 protein by MG-132 (Figure 3-2A, Figure 3-3A). We noticed that proteasomal inhibition led to a cell cycle arrest in G2/M in those cells (Figure 3-3, *Bottom Right* FACS histogram and quantification). Likely, high mitotic Cdk activities block binding of Cdh1 to the APC/C core in the presence of TM and MG-132. This observation shows that the protein level of Cdh1 is not always positively correlated with the abundance of active APC/C^{Cdh1} complexes. Taken together, our findings suggest that ER stress activates APC/C^{Cdh1} at least in part by promoting Cdh1 recruitment to an active ubiquitin ligase complex.

ER stress downregulates the APC/C inhibitor Emi1

The assembly of APC/C^{Cdh1} is necessary but not sufficient to activate the ligase, which also requires removal of the inhibitor. Emi1 is an APC/C inhibitor that acts by competitive binding to APC/C^{Cdh1} as a pseudosubstrate[6]. Its transcriptional induction at the G1-S transition by the transcription factor E2F leads to the inhibition of APC/C^{Cdh1} that promotes G1 exit[15]. In response to TM treatment, the protein level of Emi1 is drastically decreased (Figure 3-4A, *Left* and Figure 3-4B). This is not a result of transcriptional repression (Figure 3-4A, *Right*), but rather a result of

proteasomal degradation that can be rescued by MG-132 (Figure 3-2A, lanes 1-4). To test the possibility that ER stress conditions may convert Emi1 from a pseudosubstrate into a true substrate of APC/C^{Cdh1}, we examined the effect of TM on the protein expression of Emi1 in cells depleted of Cdh1 by RNAi. We observed no difference in the degree of ER stress-dependent Emi1 downregulation between control- and Cdh1-shRNA-transfected cells (Figure 3-4B), arguing against the involvement of APC/C^{Cdh1} as the ligase responsible for targeting Emi1 for degradation under ER stress. Finally, we found that overexpression of Emi1 biochemically overcame the downregulation of APC/C^{Cdh1} substrates in response to TM treatment (Figure 3-4C), suggesting that ER stress activates APC/C^{Cdh1} by dowregulating Emi1 in addition to promoting recruitment of Cdh1 to the APC/C core.

Discussion

Our study provides the first evidence on ER stress-dependent activation of APC/C^{Cdh1} that is critical in coordinating the consequent delay in progression through G1. Under ER stress conditions, activation of APC/C^{Cdh1} alters the cell cycle independently of p53 and cyclin D1, but reinforces the Ufd1-USP13-Skp2-p27 axis –as the decline of Ufd1 reduces the deubiquitination of Skp2, APC/C^{Cdh1} is activated to ubiquitinate Skp2. The contribution of APC/C^{Cdh1} to cell cycle arrest in response to TM treatment is greater than that of the Ufd1-USP13-Skp2-p27 pathway, because inactivation of APC/C^{Cdh1} results in an almost complete rescue of ER stress-induced G1 delay, in contrast to the partial rescue by Ufd1 overexpression or p27 depletion.

We show here that ER stress activates APC/C^{Cdh1} by a dual mechanism that promotes the association of the APC/C core and the coactivator Cdh1, as well as downregulating its inhibitor Emi1. This leads to degradation of its substrates including Cdh1 itself. The observation that cyclin B1 and Plk1, both of which promote the inhibitory phosphorylation of Cdh1, are reduced under TM treatment suggests that the enhanced complex formation of APC/C^{Cdh1} could be a result of decreased inhibitory phosphorylation on Cdh1. Also worthy of examination is the subcellular localization of Cdc14B, which was shown to activate Cdh1 under genotoxic stress by translocation

from the nucleolus to the nucleoplasm[5]. A third interesting possibility is ER stress-dependent regulation of nuclear PTEN that was suggested to facilitate the binding of Cdh1 to the APC/C core. Our finding that Emi1 is downregulated post-transcriptionally by ER stress raises the question of what mediates its degradation under such conditions. At the present, we cannot exclude the possibility that ER stress translationally represses Emi1.

The implications of identifying the APC/C^{Cdh1} as a regulator of the ER stress checkpoint are severalfold. First, the repertoire of stress conditions that engage APC/C^{Cdh1} to execute cell cycle arrest is no longer limited to genotoxic stress. Based on our findings, any condition that disrupts ER homeostasis such as alterations in metabolic conditions, redox states, calcium concentrations may regulate APC/C^{Cdh1} [16]. Second, in addition to arresting the cells in G1, a cell cycle phase shown to be conducive to the degradation of misfolded proteins (unpublished data, Chapter 2 of dissertation), the activation of APC/C^{Cdh1} may exert a pro-survival function by directly targeting the ER stress-induced pro-apoptotic proteins c-Jun amino terminal kinase (JNK) and tribbles-related protein 3 (TRB3) for ubiquitin-proteasome degradation[17]. APC/C^{Cdh1} may thereby act as a switch that determines cell fate when sustained ER stress causes irreparable cellular damage. Third, our current finding points to APC/C^{Cdh1} as a possible effector in the pathogenesis of human diseases characterized by ER stress. Exploration of whether and how APC/C^{Cdh1} contributes to diseases caused by misfolded proteins may identify cell cycle regulators as novel therapeutic targets for protein folding diseases.

Figures

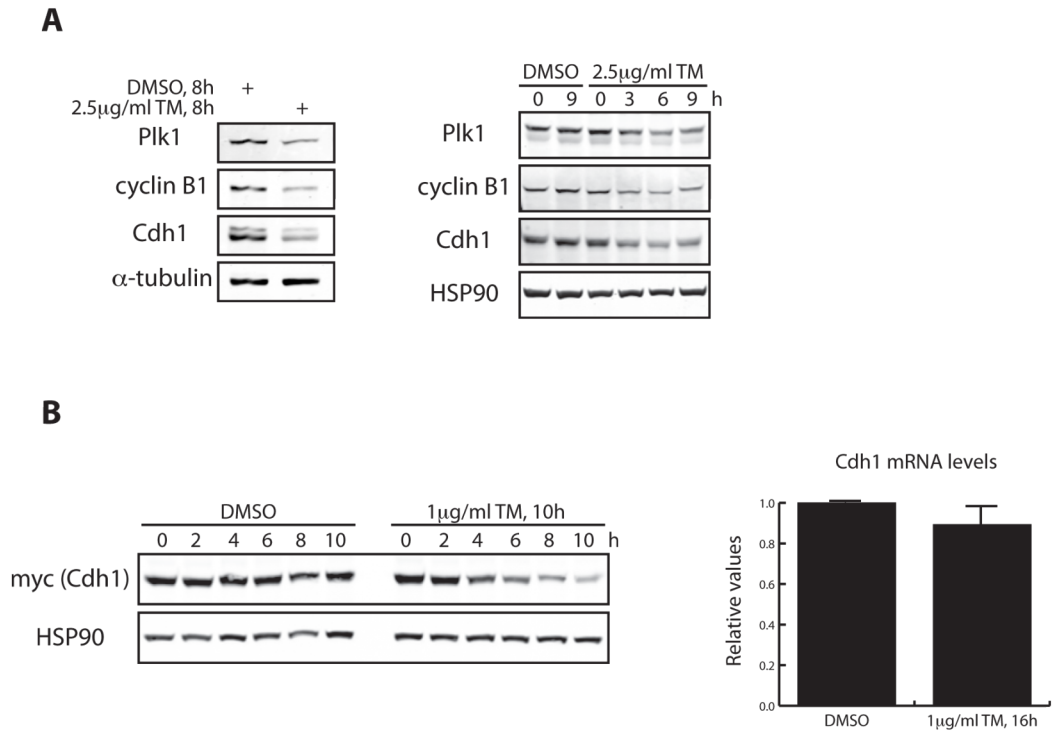

Figure 3-1: ER stress activates APC/C^{Cdh1}

(A) *Left*, HeLa cells were treated with DMSO or 2.5μg/ml of tunicamycin (TM) for 8h. Total cell lysates were immunoblotted for endogenous Plk1, cyclin B1, and Cdh1. *Right*, DMSO or 2.5μg/ml of TM was added to HeLa cells and collected at the indicated times after addition of the drug. Total lysates were immunoblotted for the indicated proteins. (B) *Left*, DMSO or 1μg/ml of TM was added to HeLa cells transfected with myc-Cdh1. Cells were collected at the indicated times after addition of the drug and total cell lysates were immunoblotted for myc. HSP90 served as a loading control. *Right*, Quantification of Cdh1 mRNA levels in HeLa cells treated with DMSO or 1μg/ml of TM for 16h by SYBR-green qRT-PCR.

Figure 3-2: Depletion of Cdh1 overcomes ER stress-induced G1 delay.

(A) HeLa cells transfected with empty vector or Cdh1-specific shRNA (for 24h) were treated with DMSO, 1.5μg/ml of TM alone or together with MG-132 (2 or 5μM) for 16h. Total cell extracts were immunoblotted for the indicated proteins. (B) HeLa cells transfected with empty vector or Cdh1-specific shRNA (for 24h) were treated with DMSO or 2.5μg/ml of TM for 8h. *Top*, Cells were collected for immunoblotting of endogenous Cdh1 for verification of transfection efficiency and GRP78 (marker of unfolded protein response). *Bottom*, Cells were also collected for FACS analysis of cell cycle distribution; representative FACS histograms are shown. Graph shows quantification of increase in G1 as a percentage of cells based on FACS analysis. (C) HeLa cells transfected with empty vector or Cdh1-specific shRNA (for 24h) were treated with DMSO or 1μg/ml of TM for 16h. *Top*, Cells were collected for immunoblotting. *Bottom*, FACS analysis of cell cycle distribution. Graph shows quantification of increase in G1 as a percentage of cells based on FACS analysis.

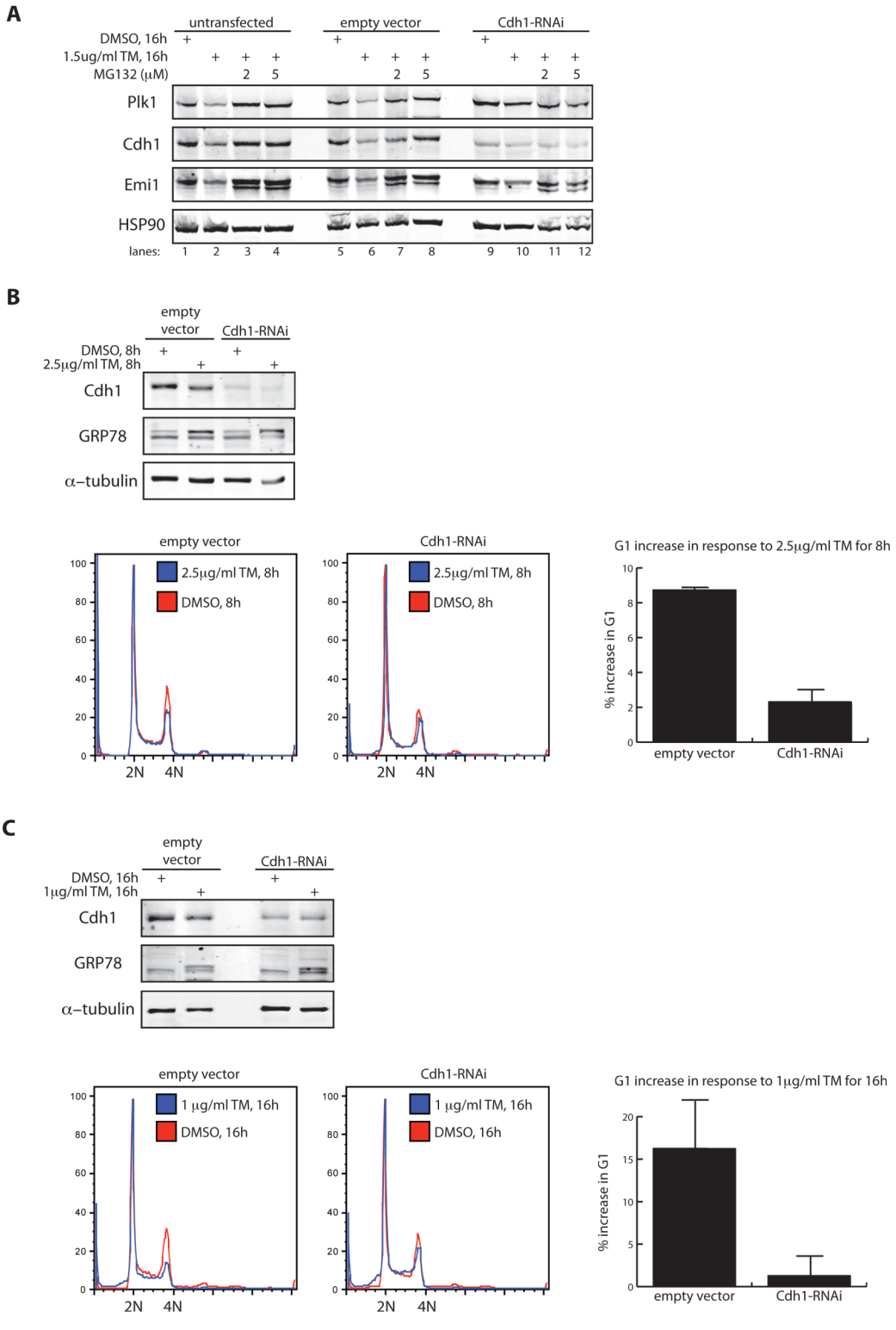
A
untransfected
empty vector
Cdh1-RNAi
DMSO, 16h
1.5ug/ml TM, 16h
MG132 (μM)
Plk1
Cdh1
Emi1
HSP90
lanes: 1 2 3 4 5 6 7 8 9 10 11 12
B
empty vector
Cdh1-RNAi
DMSO, 8h
2.5μg/ml TM, 8h
Cdh1
GRP78
α–tubulin
empty vector
Cdh1-RNAi
2.5μg/ml TM, 8h
DMSO, 8h
2N 4N
G1 increase in response to 2.5μg/ml TM for 8h
% increase in G1
empty vector
Cdh1-RNAi
C
empty vector
Cdh1-RNAi
DMSO, 16h
1μg/ml TM, 16h
Cdh1
GRP78
α–tubulin
empty vector
Cdh1-RNAi
1 μg/ml TM, 16h
DMSO, 16h
2N 4N
G1 increase in response to 1μg/ml TM for 16h
% increase in G1
empty vector
Cdh1-RNAi

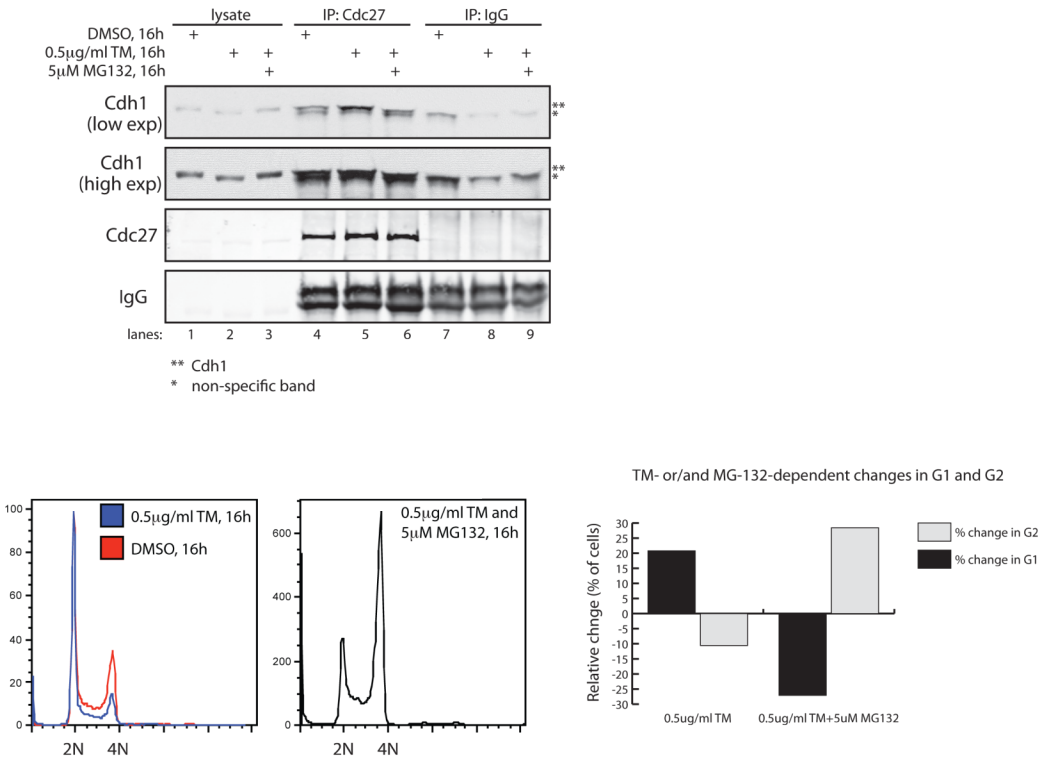

Figure 3-3: ER stress promotes binding of Cdh1 to the APC/C core.

(A) *Top*, HeLa cells were treated with DMSO, 0.5µg/ml of TM alone or together with 5µM of MG-132 for 16h. Immunoprecipitates of endogenous Cdc27 and IgG controls were immunoblotted for endogenous Cdh1. *Bottom*, FACS analysis of cell cycle distribution of cells treated as mentioned above. Quantification of cell cycle distribution based on these FACS analyses is shown in the graph on bottom right.

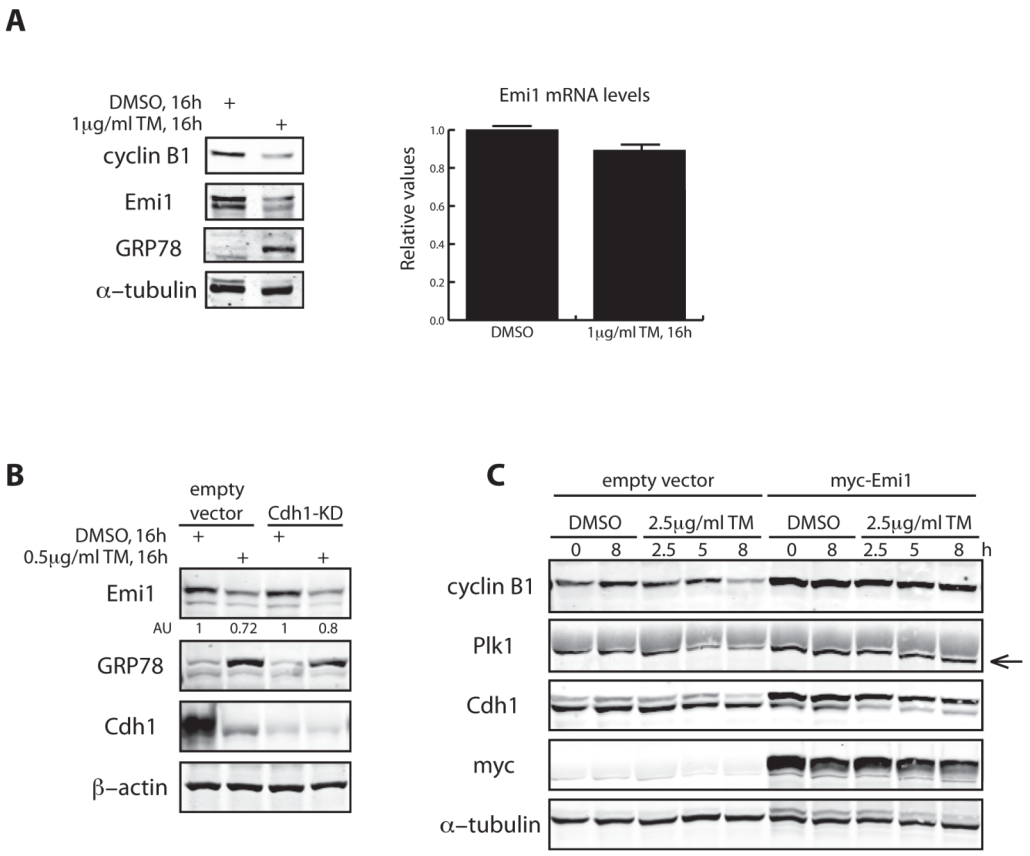

Figure 3-4: ER stress downregulates the APC/C inhibitor Emi1.

(A) *Left*, Total cell lysates from HeLa cells treated with DMSO or 1μg/ml of TM for 16h were immunoblotted for the indicated endogenous proteins. *Right*, Quantification of Emi1 mRNA levels in HeLa cells treated with DMSO or 1μg/ml of TM for 16h by SYBR-green qRT-PCR. (B) HeLa cells transfected with empty vector or Cdh1-specific shRNA (for 24h) were treated with DMSO or 0.5μg/ml of TM for 16h. Total cell lysates were immunoblotted with the indicated antibodies. Signal intensity of Emi1 immunoblot was normalized to that of β-actin and presented as arbitrary units (AU). (C) HeLa cells transfected with empty vector or Cdh1-specific shRNA (for 24h) were treated with DMSO or 2.5μg/ml of TM for the indicated times. Total cell lysates were immunoblotted with the indicated antibodies.

Materials and Methods

Cell culture and transfection

HeLa cells were grown in DMEM with 10% bovine serum at 37°C with 5% CO2. For transient transfection of plasmids in HeLa cells, 80%-confluent cells grown in 10cm dishes were transfected with 5μg of each of the indicated plasmids, using Lipofectamine 2000 (Invitrogen) following manufacturer's protocols. Cells were harvested within 24-36h after transfection.

Expression plasmids

Both pSUPER-empty vector and pSUPER-Cdh1-shRNA were generous gifts from Dr. Reuven Agami (The Netherlands Cancer Institute, Amsterdam, Netherlands). Both $pCS2^{+}$-myc empty vector and $pCS2^{+}$-myc-Emi1 were generous gifts from Dr. Peter Jackson (Genentech, San Francisco, USA). pCMV-myc-Cdh1 was used to overexpress Cdh1 in HeLa cells.

shRNA target sequence

pSUPER-Cdh1-shRNA: TGAGAAGTCTCCCAGTCAG (previously published by Brummelkamp TR *et al*, Science, 2002)

Antibodies

Commercially available antibodies used were as follows: Cdh1 (DCS-266– Abcam at 1:1000), cyclin B1 (GNS1– Santa Cruz at 1:1000), GRP78 (N-20– Santa Cruz at 1:1000), c-myc (9E10– Santa Cruz at 1:2000), Plk1 (F-8– Santa Cruz at 1:1000), Emi1 (37-6600– Invitrogen at 1:500), Cdc27 (AF3.1– Santa Cruz at 1:1000), HSP90 (F-8– Santa Cruz at 1:1000), α-tubulin (TU-02– Santa Cruz at 1:2000).

Immunoblotting and immunoprecipitation

For western-blots of total cell lysates, cells were detached from plates with 0.05% trypsin-EDTA, washed with cold PBS, and lysed on ice for 20min after resuspension in IP buffer (50mM Tris-HCl [pH=7.5], 150mM NaCl, 0.5% NP-40, 5mM EDTA, 5mM EGTA, 20mM NaF, 100µM sodium-orthovanadate, 2mM β-glycerophosphate, 1mM DTT, 1mM PMSF, 4mg/ml aprotinin, 100µM leupeptin, and 2mg/ml pepstatin A). After 20min centrifugation (13200rpm, 4ºC), supernatants were saved and protein concentration was performed using Coomassie Plus protein assay reagent (Thermo).

For co-immunoprecipitation *in vivo*, untransfected cells or cells expressing the proteins of interest for 24h were washed with cold PBS and lysed with IP buffer. Target protein was immunoprecipitated from total cell lysates containing 2mg of protein with 1µg of target-specific antibody overnight at 4ºC in a rotating wheel, followed by incubation with 30µl of a 50% slurry of protein G-agarose for 2h at 4°C with rotation. Immunoprecipitates were washed 4 times with IP buffer, resuspended in loading buffer and analyzed by SDS-PAGE and western-blotting.

Cell cycle synchronization and fluorescence-activated cell sorting (FACS)

Cells were washed with cold PBS, fixed with 70% ethanol in PBS for 1h at -20°C, and washed again with cold PBS. Cells were then incubated with PBS with 50µg/ml propidium iodide and 100µg/ml RNase A for 1h at room temperature. DNA content was analyzed by 3 color-FACS and quantification of G1, S, and G2/M populations was performed with the help of FlowJo software.

SYBR-green qRT-PCR

Total RNA was extracted from cells grown in 10cm plates (Sigma, RTN70-1KT). Up to 2µg of total RNA was used per 20µl cDNA reverse transcription (Applied Biosystems, High-Capacity cDNA Reverse Transcription Kit). 5µl of 20% v/v diluted cDNA was used per 25µl qRT-PCR with SYBR GreenER qPCR SuperMix Universal (Invitrogen) and target gene-specific

primers. 40 cycles of qPCR and analysis were performed using Stratagene Mx3000p. Human cyclophilin or GAPDH was used as a control to normalize transcript levels of experimental samples. Specificity of all primer sets were validated by dissociation curve. qPCR primer sequences are as follows:

Cdh1

Forward - GCAACAAGAGCCAGAAGCTGC

Reverse - CCAGGTTCCCCCGCTCAGACC

Emi1

Forward - GGACTTAATCAATGTGTCTAAAG

Reverse - CTTGGCAACCTCAGAGAATTC

Cyclophilin

Forward-GACCCAACACAAATGGTTC

Reverse-AGTCAGCAATGGTGATCTTC

Acknowledgements

We thank R. Agami and P. Jackson for the essential reagents used in this study. We also thank the Ronai lab members for discussions. This work was supported by NCI grant CA18143 to ZR. Chapter 3, in part, is currently being prepared for submission for publication. Chen, Meifan; Gutierrez, Gustavo J.; Ronai, Ze'ev A. The dissertation author was involved in designing and performing the experiments, as well as analyzing the data.

References

[1] Pines, J., Mitosis: a matter of getting rid of the right protein at the right time. *Trends Cell Biol* **16** (1), 55 (2006).

[2] Kramer, E. R. et al., Mitotic regulation of the APC activator proteins CDC20 and CDH1. *Mol Biol Cell* **11** (5), 1555 (2000).

[3] Crasta, K. et al., Inactivation of Cdh1 by synergistic action of Cdk1 and polo kinase is necessary for proper assembly of the mitotic spindle. *Nat Cell Biol* **10** (6), 665 (2008).

[4] Jaspersen, S. L., Charles, J. F., and Morgan, D. O., Inhibitory phosphorylation of the APC regulator Hct1 is controlled by the kinase Cdc28 and the phosphatase Cdc14. *Curr Biol* **9** (5), 227 (1999).

[5] Bassermann, F. et al., The Cdc14B-Cdh1-Plk1 axis controls the G2 DNA-damage-response checkpoint. *Cell* **134** (2), 256 (2008).

[6] Miller, J. J. et al., Emi1 stably binds and inhibits the anaphase-promoting complex/cyclosome as a pseudosubstrate inhibitor. *Genes Dev* **20** (17), 2410 (2006); Reimann, J. D., Gardner, B. E., Margottin-Goguet, F., and Jackson, P. K., Emi1 regulates the anaphase-promoting complex by a different mechanism than Mad2 proteins. *Genes Dev* **15** (24), 3278 (2001).

[7] Song, M. S. et al., Nuclear PTEN regulates the APC-CDH1 tumor-suppressive complex in a phosphatase-independent manner. *Cell* **144** (2), 187.

[8] Musacchio, A. and Salmon, E. D., The spindle-assembly checkpoint in space and time. *Nat Rev Mol Cell Biol* **8** (5), 379 (2007).

[9] Agami, R. and Bernards, R., Distinct initiation and maintenance mechanisms cooperate to induce G1 cell cycle arrest in response to DNA damage. *Cell* **102** (1), 55 (2000).

[10] Sudo, T. et al., Activation of Cdh1-dependent APC is required for G1 cell cycle arrest and DNA damage-induced G2 checkpoint in vertebrate cells. *EMBO J* **20** (22), 6499 (2001).

[11] Schroder, M. and Kaufman, R. J., The mammalian unfolded protein response. *Annu Rev Biochem* **74**, 739 (2005).

[12] Brewer, J. W., Hendershot, L. M., Sherr, C. J., and Diehl, J. A., Mammalian unfolded protein response inhibits cyclin D1 translation and cell-cycle progression. *Proc Natl Acad Sci U S A* **96** (15), 8505 (1999); Brewer, J. W. and Diehl, J. A., PERK mediates cell-cycle exit during the mammalian unfolded protein response. *Proc Natl Acad Sci U S A* **97** (23), 12625 (2000); Raven, J. F. et al., PKR and PKR-like endoplasmic reticulum kinase induce the proteasome-dependent degradation of cyclin D1 via a mechanism requiring eukaryotic initiation factor 2alpha phosphorylation. *J Biol Chem* **283** (6), 3097 (2008).

[13] Zhang, F. et al., Ribosomal stress couples the unfolded protein response to p53-dependent cell cycle arrest. *J Biol Chem* **281** (40), 30036 (2006).

[14] Listovsky, T. et al., Mammalian Cdh1/Fzr mediates its own degradation. *EMBO J* **23** (7), 1619 (2004).

[15] Hsu, J. Y. et al., E2F-dependent accumulation of hEmi1 regulates S phase entry by inhibiting APC(Cdh1). *Nat Cell Biol* **4** (5), 358 (2002).

[16] Rutkowski, D. T. and Kaufman, R. J., A trip to the ER: coping with stress. *Trends Cell Biol* **14** (1), 20 (2004).

[17] Ohoka, N. et al., TRB3, a novel ER stress-inducible gene, is induced via ATF4-CHOP pathway and is involved in cell death. *EMBO J* **24** (6), 1243 (2005); Ohoka, N. et al., Anaphase-promoting complex/cyclosome-cdh1 mediates the ubiquitination and degradation of TRB3. *Biochem Biophys Res Commun* **392** (3), 289; Nishitoh, H. et al., ASK1 is essential for endoplasmic reticulum stress-induced neuronal cell death triggered by expanded polyglutamine repeats. *Genes Dev* **16** (11), 1345 (2002); Gutierrez, G. J. et al., Interplay between Cdh1 and JNK activity during the cell cycle. *Nat Cell Biol* **12** (7), 686.

Chapter 4 : Conclusions and implication

Our work identified two cooperating pathways involving the ubiquitin proteasome system that coordinate G1 cell cycle delay in response to ER stress independently of cyclin D1 and p53. In the first pathway, ER stress conditions downregulate Ufd1, a protein that antagonizes the ubiquitination of Skp2 through its ability to recruit USP13. This leads to the stabilization of the Cdk2 inhibitor p27 that partially contributes to G1 delay. ER stress-dependent induction of Skp2 and p27 also occurs at the transcriptional level, pointing to the involvement of ER stress-responsive transcriptional machinery in cell cycle control. In the second pathway, ER stress selectively activates the ligase activity of APC/C^{Cdh1}, the inhibition of which largely overcomes ER stress-induced G1 arrest, indicating its central role in coordinating the ER stress checkpoint.

These findings suggest a regulatory role of the above-mentioned cell cycle proteins in checkpoint responses to physiological conditions that perturb ER function, such as glucose deprivation and changes in redox states. The ER stress checkpoint may also be activated in pathological conditions that overwhelm the ER with misfolded proteins, such as in the case of conformational diseases. In support of this, we observed an increase in G1 population in fibroblasts from a cystic fibrosis carrier in the steady state as well as in response to treatment with ER stress inducer. This suggests a basal level of ER stress checkpoint activation in cells constitutively expressing misfolded proteins and points to the interesting phenomenon of adaptation to prolonged ER stress that allows cell growth under such conditions. There may be a threshold of extended ER stress below which the cells can evolve to survive and above which leads to cell death.

On the other hand, ER stress-dependent alterations in the cell cycle may contribute to the pathogenesis of diseases characterized by ER stress, like diabetes[1], cancer[2], and neurodegenerative disorders[3]. For example, in postmitotic neurons, APC/C^{Cdh1} controls various aspects of neuronal development including axon growth and patterning[4]. Our finding that ER stress activates APC/C^{Cdh1} raises the intriguing possibility that ER stress leads to neuronal degeneration through deregulation of APC/C^{Cdh1}. Elucidation of the molecular basis of ER stress-dependent control may provide new insights to the pathogenesis of ER stress-related diseases.

As important as the identification of ER stress checkpoint regulators is an understanding of its functional significance. Data from yeast and mammalian cells suggest that it is a prosurvival mechanism that prevents the inheritance of stressed ER that would otherwise have a deleterious effect on the daughter cells[5] and promotes the clearance of misfolded proteins (unpublished data, Chapter 2 of dissertation). Our finding that the ER stress checkpoint requires the activation of APC/C^{Cdh1}, which could target the pro-apoptotic proteins JNK and TRB3 for degradation, further supports a pro-survival function of cell cycle arrest in ER-stressed cells. Knowing the outcome of the ER stress checkpoint would help devise potential therapeutic strategies against diseases caused by ER stress-induced cell death.

ER stress also induces autophagy, an alternative for degradation of protein aggregates and organelles by lysosomes[6]. Our observation that G1 phase of the cell cycle presents an environment favorable for removal of ERAD substrates raises the possibility that autophagy may contribute to the clearance of misfolded proteins in G1. Supporting this idea is the report that the induction of autophagy is cell cycle-dependent. In particular, increased autophagy was observed in the G1 and S phases[7]. It would be of interest to test whether the cell cycle machinery mediates the crosstalk between ER stress checkpoint and autophagy.

The discovery that ER stress inhibits cytokinesis in yeast raises the question of whether an analogous ER stress surveillance pathway exists in mammalian cells. One supporting observation is that similar to the UPR-deficient yeast mutants that exhibit a polyploidy phenotype[8], the depletion of Ufd1 leads to polyploidy in mammalian cells [9] (unpublished data from our lab). Definite answers will require further investigation.

Finally, complementing our finding that ER stress-dependent downregulation of Ufd1 leads to G1 cell cycle delay in mammalian cells is the report that heat shock, which causes protein aggregation, induces G1 delay in the temperature sensitive mutants of Ufd1, Cdc48/p97, and Npl4 in budding yeast[10]. This suggests a conserved role of Cdc48-Ufd1-Npl4 in the regulation of cell cycle progression through G1 under ER stress in eukaryotes, although the involvement of Cdc48/p97 and Npl4 in the mammalian ER stress checkpoint remains to be elucidated.

References

[1] Harding, H. P. and Ron, D., Endoplasmic reticulum stress and the development of diabetes: a review. *Diabetes* **51 Suppl 3**, S455 (2002).

[2] Ma, Y. and Hendershot, L. M., The role of the unfolded protein response in tumour development: friend or foe? *Nat Rev Cancer* **4** (12), 966 (2004).

[3] Lindholm, D., Wootz, H., and Korhonen, L., ER stress and neurodegenerative diseases. *Cell Death Differ* **13** (3), 385 (2006).

[4] Huynh, M. A., Stegmuller, J., Litterman, N., and Bonni, A., Regulation of Cdh1-APC function in axon growth by Cdh1 phosphorylation. *J Neurosci* **29** (13), 4322 (2009).

[5] Babour, A., Bicknell, A. A., Tourtellotte, J., and Niwa, M., A surveillance pathway monitors the fitness of the endoplasmic reticulum to control its inheritance. *Cell* **142** (2), 256.

[6] Ding, W. X. et al., Differential effects of endoplasmic reticulum stress-induced autophagy on cell survival. *J Biol Chem* **282** (7), 4702 (2007).

[7] Tasdemir, E. et al., Cell cycle-dependent induction of autophagy, mitophagy and reticulophagy. *Cell Cycle* **6** (18), 2263 (2007).

[8] Bicknell, A. A., Babour, A., Federovitch, C. M., and Niwa, M., A novel role in cytokinesis reveals a housekeeping function for the unfolded protein response. *J Cell Biol* **177** (6), 1017 (2007).

[9] Dobrynin, G. et al., Cdc48/p97-Ufd1-Npl4 antagonizes Aurora B during chromosome segregation in HeLa cells. *J Cell Sci* **124** (Pt 9), 1571.

[10] Hsieh, M. T. and Chen, R. H., Cdc48 and Cofactors Npl4-Ufd1 Are Important for G1 Progression during Heat Stress by Maintaining Cell Wall Integrity in Saccharomyces cerevisiae. *PLoS One* **6** (4), e18988.